CHARLES UNIVERSITY

Faculty of Science

Department of Analytical chemistry

Martina Rombaldová, M.Sc.

Metabolipidomic profiling of white adipose tissue by UPLC-MS/MS

Metabolipidomická analýza bílé tukové tkáně pomocí UPLC-MS/MS

Doctoral thesis

Supervisor: RNDr. Ondřej Kuda, Ph.D.

Prague, 2019

I hereby declare that this thesis is my own work and effort and that it has not been submitted anywhere with the intention to acquire any other academic degree. I am aware that any use of the results obtained in this work, beyond the Charles University and Institute of Physiology the Czech Academy of Sciences is possible only with a written consent of these institutions.

In Prague, June 2019

…..……..……...

Martina Rombaldová, M.Sc.

Supervisor: RNDr. Ondřej Kuda, Ph.D.
Metabolism of bioactive lipids
Institute of Physiology
The Czech Academy of Sciences

Supervisor-consultant: prof. RNDr. Pavel Coufal, Ph.D.
Department of Analytical Chemistry
Faculty of Science
Charles University

I would primarily thank to my supervisor RNDr. Ondřej Kuda, Ph.D. for professional and patient guidance my work. He has been always very helpful, given me a lot of experience and valuable advice. Also, he was very supportive with writing my thesis. Likewise I would like to thank prof. RNDr. Pavel Coufal, Ph.D. for comments and advice to my doctoral thesis.

I am very grateful to my collaborators from Institute of Physiology for many professional counsels and friendly environment. Also, many thanks belong to my family, especially to my husband and my mother, without which I would never finish my studies. I would like to thank Hanka for great support as well.

Abstract

Obesity is a serious problem in society today [1,2]. It might seems to have been caused simply by excess consumption of food compared to energy expenditure but obesity is actually a complex metabolic disorder centred on adipose lipid metabolism and cellular signalling systems linked to it [3]. Understanding the biology of adipose tissue (AT) is very important for the identification of novel and potential therapeutic targets in order to prevent and treat obesity-related disorders [4]. We utilized analytical approach liquid chromatography coupled to mass spectrometry (LC-MS) to study adipose tissue metabolism. Also, we were especially interested in the effect of omega-3 polyunsaturated fatty acids (PUFA) on that metabolism. Rodent and cell line experiments were performed and analyses were done of white adipose tissue (WAT), serum/plasma samples or cells as well as milk samples from mothers.

At first, we established several ultra performance liquid chromatography-tandem mass spectrometry (UPLC-MS/MS) methods for analysis of acylcarnitines (AC), amino acids (AmA) and other metabolites. Importantly, these methods were able to distinguish isobaric species of AC which is not usually possible. Using these approaches we uncovered several acylcarnitines, i.e. long chain AC, carnitine, acylcarnitine C4 and C6, C4DC, as well as amino acids tyrosine, alanine, ornithine and threonine that could serve as complex, gender-specific biomarkers of propensity to obesity and partially as a biomarker of obesity-associated insulin resistance. It was discovered that maternal intake of a cafeteria diet during lactation in rats alters in the plasma profile of AC and AmA. Specifically, it was noticeable in acetylcarnitine and medium- and long-chain AC, as well as glycine, alanine, isoleucine, serine and proline, in the offspring.

Second, we focused on mutual interaction between two main cell types of adipose tissue, adipocytes and adipose tissue macrophages. Our results showed that macrophages modulate lipolysis and fatty acid re-esterification in adipocytes while their modulation depends on polarization states of macrophages and responses to dietary omega-3 PUFA supplementation. Then UPLC-MS/MS metabolomic method revealed that inflammatory M1 and anti-inflammatory M2 macrophages act differently. This thesis also explores lipid mediators synthesized in adipose tissue. As a result, the origin of lipid mediator protectin D1 was discovered. Also, levels of several lipid mediators in different cell types of WAT were determined and showed interplay between them. Moreover, we documented the omega-3 PUFA´s ability to lower the inflammation in WAT.

Later on, we concentrated on branched fatty acid hydroxy fatty acids (FAHFA) lipid molecules that influence WAT metabolism as well. We identified a novel compound of FAHFA lipid class, docosahexaenoic acid hydroxylinoleic acid (DHAHLA), by its fragmentation scheme and detected several DHAHLA´s isomers in murine serum. We then demonstrated that adipocytes and macrophages are able to synthetize 13-DHAHLA and we proved its anti-inflammatory and pro-resolving properties. Subsequently, we found 13-DHAHLA in human breast milk for the first time but only in samples from mothers who were supplemented with omega-3 PUFA during pregnancy. It is also important to indicate that FAHFA from breast milk reach a newborn's circulation and thus potentially positively influence its metabolism.

In summary, we used very sensitive UPLC-MS/MS methodology to broaden our knowledge on adipose tissue metabolism. Specifically, we focused on mutual interaction between main components of adipose tissue and we analysed different metabolites (e.g. acylcarnitines, lipid mediators, FAHFA compounds) that influence adipose tissue metabolism in various samples.

Abstrakt

V současné době je obezita vážný problém [1,2]. Ačkoliv by se mohlo zdát, že jde pouze o vyšší příjem potravy oproti energetickému výdeji, jde o složitou metabolickou chorobu, která se váže na lipidový metabolismus v tukové tkáni a buněčnou signalizaci s ním spojenou [3]. Je velmi důležité porozumět biologii tukové tkáně, abychom mohli rozpoznat nové a potencionální terapeutické cíle, které by nám pomohly předcházet a léčit choroby spojené s obezitou [4]. V našem výzkumu jsme využili především analytickou techniku kapalinové chromatografie s hmotnostní spektrometrií (LC-MS) ke studiu metabolismu tukové tkáně a rovněž jsme se zaměřili na vliv omega-3 polynenasycených mastných kyselin (PUFA) na tento metabolismus. Prováděli jsme pokusy na hlodavcích a buněčných liniích a analyzovali jsme bílou tukovou tkáň, vzorky séra/plasmy, buněk a mateřského mléka.

Nejprve jsme zavedli několik metod ultraúčinné kapalinové chromatografie s tandemovou hmotnostní detekcí (UPLC-MS/MS) k analýze acylkarnitinů (AC), aminokyselin (AmA) a dalších metabolitů. Tyto metody nám umožnily rozdělit isobarické acylkarnitiny, ačkoliv to není obvykle možné. Použití těchto metod také odhalilo několik acylkarnitinů, t.j. AC s dlouhým řetězcem, karnitin, acylkarnitiny C4 a C6, C4DC stejně tak jako aminokyseliny tyrosin, alanin, ornithin a threonin, které by mohly sloužit jako komplexní pohlavně specifické biomarkery náchylnosti k obezitě a k obezitou podmíněné inzulínové rezistenci. Navíc jsme odhalili, že příjem vysokotukové diety kojících krysích samic vede ke změnám v profilu AC a AmA v plasmě mláďat. Konkrétně jde o acetylkarnitin, AC se středně dlouhými a dlouhými řetězci a glycin, alanine, isoleucine, serin a prolin.

Poté jsme se zaměřili na vzájemné interakce dvou hlavních typů buněk v tukové tkáni, adipocytů a makrofágů tukové tkáně. Naše výsledky ukázaly, že makrofágy specificky mění lipolýzu a re-esterifikaci mastných kyselin v adipocytech, přičemž tyto změny závisí na polarizačním stavu makrofágů a jsou odpovědí na suplementaci omega-3 PUFA v dietě. Dále jsme s využitím UPLC-MS/MS metabolomické metody odhalili, že se prozánětlivé M1 a protizánětlivé M2 makrofágy chovají rozdílně. V další části dizertační práce jsme zkoumali lipidové mediátory, které vznikají v tukové tkáni. Zjistili jsme původ lipidového mediátoru protektinu D1. Také jsme stanovili hladiny několika dalších lipidových mediátorů v různých buněčných typech tukové tkáně a ukázali jsme jejich vzájemné působení. Navíc jsme doložili schopnost omega-3 PUFA snížit zánět v tukové tkáni.

Následně jsem se zaměřili na větvené estery oxidovaných mastných kyselin (FAHFA) lipidové molekuly, které rovněž ovlivňují metabolismus tukové tkáně. Popsali jsme novou sloučeninu z této lipidové třídy, t.j. ester kyseliny dokosahexaenové a hydroxylinolové (DHAHLA), pomocí fragmentačních schémat a detekovali jsme několik jejích izomerů v myší plasmě. Poté jsme ukázali, že jsou adipocyty a makrofágy schopné vytvořit 13-DHAHLA a dokázali jsme její protizánětlivé účinky. Následně jsme jako první odhalili výskyt 13-DHAHLA v mateřském mléce, ale pouze ve vzorcích od matek, které během těhotenství užívaly omega-3 PUFA suplementaci. Naše výsledky rovněž naznačují, že se molekuly FAHFA z mateřského mléka mohou dostat do oběhu novorozence a tak pozitivně ovlivnit jeho metabolismus.

Závěrem lze říci, že jsme s využitím velmi citlivé techniky UPLC-MS/MS rozšířili naše znalosti o metabolismu tukové tkáně. Konkrétně jsme se zabývali vzájemnou interakcí mezi hlavními složkami tukové tkáně a analyzovali jsme různé metabolity (např. acylkarnitiny, lipidové mediatory, FAHFA sloučeniny) v různorodých vzorcích, které tento metabolismus ovlivňují.

TABLE OF CONTENT

LIST OF ABBREVIATIONS

(QQ)Q	(triple) quadrupole mass analyser
2-AG	2-arachidonoylglycerol
AA	arachidonic acid (20:4, omega-6)
AC	acylcarnitines
Acylcarnitine C4	butyrylcarnitine
Acylcarnitine C6	hexanoylcarnitine
AEA	anandamide
ALA	alpha-linolenic acid (18:3, omega-3)
AmA	amino acids
APCI	atmospheric pressure chemical ionization
AT	adipose tissue
ATGL	adipocyte triglyceride lipase
ATM	adipose tissue macrophages
BAT	brown adipose tissue
BDMD	bone marrow-derived macrophages
BMI	body mass index
BUME	butanol/methanol
C18 column	octadecyl reversed phase column
COX	cyclooxygenase
CYP	cytochrome P450
DC	direct current

DG	diacylglycerol
DGAT	diacylglycerol acyltransferase
DHA	docosahexaenoic acid (22:6, omega-3)
DHAHDHA	docosahexaenoic acid hydroxydocosahexaenoic acid
DHAHLA	docosahexaenoic acid hydroxylinoleic acid
DHEA	docosahexaenoylethanolamine
DNL	*de novo* fatty acid synthesis
EPA	eicosapentaenoic acid (20:5, omega-3)
EPI	product ion scan mass spectrometry mode
ESI	electrospray ionization source
FA	fatty acids
FAHFA	branched fatty acid hydroxy fatty acids
HF(D)	corn oil-based high-fat (diet)
HFF	corn oil-based high-fat diet with omega-3 PUFA
HILIC	hydrophilic interaction liquid chromatography
hMADS	human multipotent adipose-derived stem cells
HPLC	high performance liquid chromatography
HSL	hormone-sensitive lipase
IDO	indoleamine 2,3-dioxygenase
IS	internal standard
LC-MS	chromatographic separation coupled to mass spectrometry
LLE	liquid liquid extraction
LOX	lipoxygenase

LPS	lipopolysaccharide
m/z	mass-to-charge ratio
MALDI	matrix assisted laser desorption/ionization
MG	monoacylglycerol
MGL	monoacylglycerol lipase
MRM	multiple reaction monitoring mode
MS	mass spectrometry
MS/MS	tandem mass spectrometry
MS^n	tandem mass spectrometry
MTBE	methyl-tert-butyl ether
NLS	neutral loss scan mass spectrometry mode
NP	normal phase chromatography
O-CAF	offspring of dams fed a cafeteria diet during lactation
O-PCaf	offspring of diet-induced obese dams submitted to a dietary normalization before gestation
PAHSA	palmitic acid hydroxystearic acid
PBMCs	human peripheral blood mononuclear cell
PD1	protectin D1
PIS	precursor ion scan mass spectrometry mode
PLS-DA	partial least squares discriminant analysis
PUFA	polyunsaturated fatty acids
qPCR	quantitative polymerase chain reaction
RF	radio frequency

RP	reversed phase chromatography
SIM	selected ion monitoring mass spectrometry mode
SMR	selected reaction monitoring mode
SPE	solid phase extraction
ST(D)	standard low caloric diet
SVF	stromal vascular fraction
T2D	type 2 diabetes
TG	triacylglycerol
TOF	time-of-flight mass analyser
UCP1	uncoupling protein 1
UPLC	ultra performance liquid chromatography
VLDL	very low-density lipoproteins
WAT	white adipose tissue

1. THEORY

1.1. BIOLOGY

1.1.1. Obesity

Nowadays the obesity is a serious problem even in childhood and in adolescence. Obesity is defined as a body mass index (BMI) of 30 and higher [2] while BMI represents an index of an individual's fatness [5]. BMI is calculated as weight divided by height squared [6] and it is used for classifying (categorizing) adults into groups (see **Figure 1**) [5]. Unfortunately, there is a positive association between the body mass index and the risk of type 2 diabetes (T2D) [1]. Up to 51.6% of adults people were over-weight in 2014 in EU (35.7% pre-obese and 15.9% obese). The lowest level of obesity among the adult population was in Romania (9.4%) and Italy (10.7%) while Malta was at the opposite side of the scale (26.0%) in the same year. The Czech Republic belongs to states with relatively high number of obese people, as there are 19.3 % of obese men. Interestingly, it has been shown that obesity is closely connected with the age of population and their education level because the older and lower the education level in population, the more cases of obesity were found [2].

Categories	BMI
Underweight	15-19.9
Normal weight	20-24.9
Overweight	25-29.9
Preobesity	
Class I obesity	30-34.9
Class II obesity	35-39.9
Class III obesity	≥40

Figure 1. *Categories of body mass index (BMI). Adapted from [5].*

It might seem to have been caused simply by excess consumption of food compared to energy expenditure but obesity is actually a complex metabolic disorder centred on adipose lipid metabolism and cellular signalling systems linked to it [3]. Obesity results in ectopic

accumulation of lipids, release of pro-inflammatory molecules from white adipose tissue into circulation [7] and it is accompanied by low-grade inflammation [8] and activation of adipose tissue macrophages [9,10]. Another serious health condition connected to obesity is metabolic syndrome. It includes a group of risk factors for metabolic diseases, e.g. large waistline, high triacylglycerol level, low high-density lipoprotein cholesterol level, high blood pressure and high fasting blood glucose. Due to the rise of obesity, the metabolic syndrome is becoming a problem in nowadays society [11].

1.1.2. Adipose tissue

Adipose tissue (AT) has been increasingly recognized as a major player in systemic metabolic regulation [4] because it has a fundamental role in energy balance and overall body homeostasis [12]. Adipose tissue stores energy in form of lipid when energy intake exceeds expenditure [13] and then it can be utilized by the organism to fulfil subsequent metabolic requirements during times of little or no consumption [12]. It also acts as an endocrine organ and produces numerous bioactive factors which communicate with other organs and modulate a range of metabolic pathways (e.g. adipokines) [4]. Further, AT together with liver form a functional metabolic unit that is important for thermoregulation under the cold exposure [14]. Conversely, adipose tissue dysfunction plays a prominent role in the development of obesity and is related to disorders such as insulin resistance, cardiovascular diseases, diabetes, depression and cancer. Therefore, understanding its biology and pathology is of great importance for the identification of novel and potential therapeutic targets in order to prevent and treat of obesity-related disorders [4].

Adipose tissue is extremely plastic organ [7] which is distributed similar in mice and men [15] in various anatomical locations around body (**Figure 2**). Accumulation of visceral white adipose tissue (WAT) is in correlation with metabolic syndrome [7] whereas subcutaneous WAT is protective in the development of obesity and related metabolic diseases in rodents [16,17]. Also, it has been shown that subcutaneous fat improves glucose tolerance and insulin sensitivity in rodents. Unfortunately, metabolic function of subcutaneous and visceral fat in humans is still not clear today but it seems that fat distribution, rather than total fat mass, most likely plays an important role in the development of obesity and its associated diseases [4].

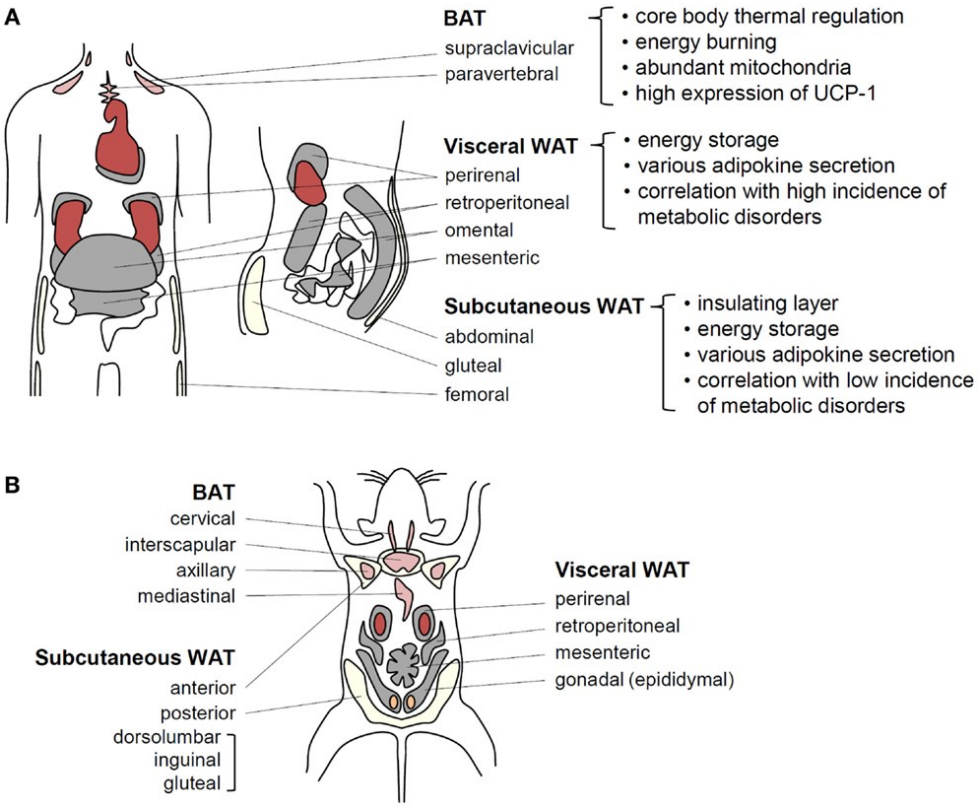

Figure 2. *Adipose tissue functions in energy homeostasis and thermal regulation. (A) In humans, BAT localized around the shoulders and ribs contributes to heat generation. Brown adipocytes exhibit abundant mitochondria and UCP-1 expression related to thermogenesis. It has been speculated recently that BAT efficiency for fat-burning could be harnessed to reduce obesity. Visceral WAT (VAT) and subcutaneous WAT (SAT) possesses considerable capacities for energy storage. VAT surrounds intra-abdominal organs, whereas SAT spreads throughout the body beneath the skin. These fat tissues secrete various adipokines to regulate energy homeostasis. VAT is more strongly associated with obesity-induced metabolic disorders than SAT. (B) In adult mice, BAT is well developed and easily observed compared with that in adult humans. Among WAT depots within the abdominal cavity, the paired gonadal depots located around the ovaries in females and the testes in males are studied as a model of VAT. However, these depots do not exist in humans. The paired inguinal depots in the anterior to the upper part of the hind limbs are representative SATs in mice. Adapted from [18].*

Adipocytes are the predominant cell type in adipose tissue [4] while the remainder are called stromal vascular fraction (SVF). SVF includes blood and endothelial cells, adipose precursor cells of varying degrees of differentiation, adipose-derived stem/stromal cells, smooth muscle cells, lymphocytes, pericytes, and fibroblasts [3,19]. Adipose precursors differentiate in three types of adipocytes, i.e. white, brown and beige (for details see below). They can coexist in one depot and their phenotype can be reversed. Interestingly, number of adipocyte is set in childhood and adolescence and it is independent on body weight fluctuation [7].

White adipocytes are mainly present in white adipose tissue [20]. They have a unilocular lipid droplet, few mitochondria, low oxidative rate [21] and do not have uncoupling protein1 (UCP1) [7]. UCP1 is an unique protein that disconnects oxidative phosphorylation from ATP [22]. In line with this, white adipocytes have high capacity of storing energy in the form of triacylglycerols, and protect organs such as muscle and liver from lipotoxicity [4] that is associated with metabolic syndrome and T2D [23,24]. It has been known for several years that there is another type of WAT called beige or brite (brown-like-in-white) fat, in which UCP1 expression can be stimulated by cold stress or β3-adrenoceptor agonists [25]. Beige adipocytes that are predominant in beige fat can be also derived from white adipocytes in a process known as browning or beiging of WAT [26]. Conversely, brown adipocytes, located in brown adipose tissue (BAT), are specialized cells with multilocular morphology, abundant mitochondria and enrichment of UCP1 [4]. Typical depots of BAT are in **Figure 2**. Both brown and beige adipocytes generate heat on demand through UCP1-dependent uncoupling [14] and offer a new way to battle obesity and other metabolic disorders [26–30].

1.1.2.1. Metabolism of adipose tissue

Adipose tissue, as an energy storage organ, stores triacylglycerols (TG) and releases fatty acids through lipogenesis and lipolysis, respectively [4]. Systemically, feeding stimulates the lipogenic pathway where excess of carbohydrate is converted into fatty acids in process *de novo* fatty acid synthesis (DNL). Then fatty acids are esterified to storage TG in the process called triacylglycerols biosynthesis [4][31]. Lipogenesis is primary active in the liver [31] where it is more efficient [32] than in adipose tissue. Conversely, fasting induces the activation of lipolytic pathway that promotes the breakdown of TG and release of fatty acids from adipose tissue. The balance between lipogenesis and lipolysis is critical for maintaining systemic energy homeostasis and insulin sensitivity [4].

De novo fatty acid synthesis specifically, glucose is converted into pyruvate in glycolytic pathway. Then pyruvate enters tricarboxylic acid cycle in mitochondria and citrate is produced by this pathway. Later, citrate is converted into acetyl-CoA, malonyl-CoA and finally palmitate that is further metabolised into various fatty acids (**Figure 3**). Therefore, the main product of DNL is palmitate but stearate and shorter fatty acids are also generated [31]. High DNL is observed in the presence of high fatty acid oxidation while it may be related to

refilling of triglyceride stores and/or futile cycling [14]. Deregulation of DNL is associated with obesity or metabolic syndrome [31] because cells fail to respond to the normal action of insulin [33]. Of note, the plasma glucose levels, as well as insulin levels [4] associated with glucose intake, can stimulate lipogenesis whereas polyunsaturated fatty acids (PUFA) decrease lipogenesis by suppressing gene expression in murine liver [31].

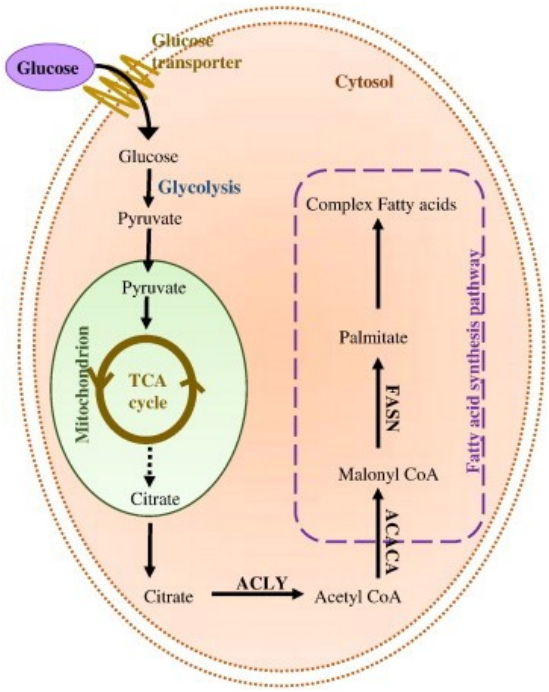

***Figure 3**. De novo lipogenesis: Glucose, taken up by the glucose transporter, enters the glycolytic pathway and generates pyruvate. This pyruvate is converted into acetyl-CoA that feeds the tricarboxylic acid (TCA) cycle. The citrate produced exits the mitochondrion and is converted back into acetyl-CoA by the enzyme ATP-citrate lyase (ACLY). Acetyl-CoA carboxylase (ACACA) acts on this acetyl-CoA yielding malonyl-CoA which is then utilized as a substrate for the production of 16-carbon saturated palmitate by the main biosynthetic enzyme fatty acid synthase (FASN). Adapted from [31].*

Triacylglycerol synthesis occurs in multiple tissues, e.g. in the liver where very low-density lipoproteins (VLDL) are formed or in adipose tissue, and it is summarized in **Figure 4** [34]. Briefly, TG synthesis combines the products of glycolysis, i.e. glycerol-3-phosphate or dihydroxyacetone phosphate with acyl-CoAs [12] to synthetize lysophosphatidic acid (1-acylglycerol-3-phosphate). Lysophosphatidic acid is further esterified and converted into phosphatidic acid (1,2-diacylglycerol-3-phosphate) that is shunted into the synthesis of various phospholipids or into the synthesis of TG. Entry into TG synthesis involves the conversion of phosphatidic acid to the intermediate 1,2-diacylglycerol (1,2-DG) that is subsequently converted to TG [34]. Diacylglycerol acyltransferase (DGAT) catalyses the final and critical step in the TG synthesis pathway, and plays an important role

in lipid deposition in adipocytes [35]. Of note, the storage of neutral TG in adipocytes increases the lipid droplet size, which results in adipose expansion and subsequent obesity [4] but on the other hand it avoids lipotoxicity [23].

Opposite to lipogenesis, lipolysis is the catabolic process [4] leading to hydrolysis of the primary and secondary ester bonds between long chain fatty acids (FA) and the glycerol backbone in TG [23,36]. As a result, WAT releases free fatty acids and glycerol (**Figure 4**) [23,36] that can be transported in blood and subsequently taken up into muscles, liver and other organs while it drives lipid distribution and modulates the whole-body energy balance [4]. WAT-derived FA can be used as energy substrates (specifically for β oxidation and ATP production [24]), for generation of acylcarnitines and VLDL in liver [14,37], as well as an essential precursors for lipid and membrane synthesis and mediators in cell signalling processes [24]. Also, part of liberated FA can be re-esterified back to TG by DGAT1 and DGAT2 enzymes while it results in futile TG/FA cycling which is important biochemical activity in white adipocytes [7]. Lipolysis takes place in every organ but the most abundant is in white and brown adipose tissue [24]. The activation of the pathway is triggered by energy demand (e.g. exercise, fasting, cold exposure) [7,24], sympathetic tone and β adrenergic signalling [14], or when the storage of neutral TG exceeds the capacity of adipocytes [4]. Lipolysis is catalysed by adipocyte triglyceride lipase (ATGL), hormone-sensitive lipase (HSL) or monoacylglycerol lipase (MGL) [12] and several hormones have been proved to regulate the lipolytic pathway as well, e.g. insulin, glucagon, catecholamine [4].

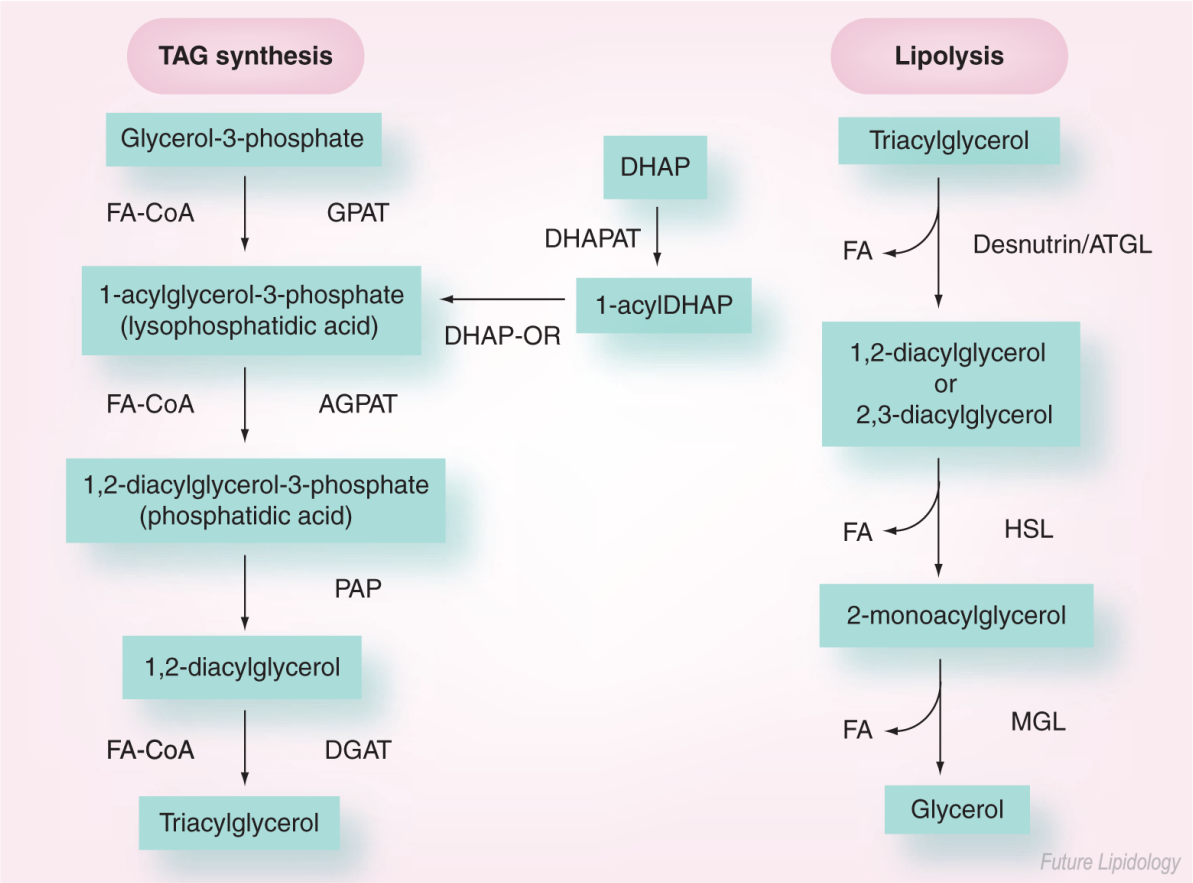

Figure 4. *The enzymes of triacylglycerol synthesis and hydrolysis AGPAT: 1-acylglycerol-3 phosphate acyltransferase; ATGL: Adipose triglyceride lipase; CoA: Coenzyme A; DGAT: Diacylglycerol acyltransferase; DHAP: Dihydroxyacetonephosphate; DHAPAT: Acyl-CoA:dihydroxyacetone-phosphate acyltransferase; DHAP-OR: Dihydroxyacetone-phosphate oxido reductase; FA: Fatty acid; GPAT: Glycerol-3-phosphate acyltransferase; HSL: Hormone-sensitive lipase; MGL: Monoglyceride lipase; PAP: Phosphatidic acid phosphatase; TAG: Triacylglycerol. Adapted from [34].*

Unique immune cell repertoire in WAT suggests that the immune cells are involved in the control of mature adipocyte metabolism. Specifically, adipose tissue macrophages (ATM) contribute to low-grade adipose tissue inflammation and insulin resistance in obesity. Negative effect of excess lipids on macrophages could be partially ameliorated by omega-3 PUFA because they promote the "healthy adipocyte" phenotype in mice and humans in epididymal but not subcutaneous WAT. "Healthy white adipocytes" are characterized by high mitochondrial content, high lipolytic activity, especially high activity of TG/FA cycling, *de novo* lipogenesis and oxidative phosphorylation while they do not contain UCP1 protein [7]. Interestingly, it may explain why 10-40 % of obese men stay metabolically healthy [38]. ATM as well as omega-3 PUFA are more discussed below.

1.1.2.2. Adipose tissue macrophages

Adipose tissue macrophages are the predominant immune cell population in the adipose tissue, especially under obese conditions [39]. They play an essential role in immune response and normal tissue development [1,40]. Also, adipose tissue macrophages are associated with changes in metabolic state of the adipose tissue [41–43] and contribute to low-grade WAT inflammation and insulin resistance [44–46]. Further, they probably buffer the local acute increase in fatty acid concentration in plasma [10] because they internalize them [1,47] and it leads to formation of macrophages "foam cells" [10]. Interestingly, ATM are the strongest predictors of T2D development in obese patients [48] and therefore there is a great effort to understand the role of ATM in metabolism at present days [1].

Macrophages express a different functional program to adapt the microenviromental challenges as they are polarized from M1 to M2 state [49]. Polarization of macrophages is well defined in *in vitro* studies but it is more dynamic *in vivo* [10,50], it is influenced by dietary lipid composition for example [10,50,51]. Specifically, omega-3 PUFA support switch from M1 to M2 phenotype via anti-inflammatory lipid mediators derived from omega-3 PUFA [8,49,52]. Obese individuals have more M1 macrophages [1]. They originate from monocytes and secrete high levels of proinflammatory cytokines [1] (e.g. IL6, TNF-α [40] and IL-1β, which can inhibit insulin signalling [39]). Also, M1 lead to the development of type 2 diabetes [1] and contribute to the formation of 'crown-like structures' that surround dying adipocytes [39]. On the other hand, M1 protect the host against different types of microbial threats [53]. Conversely, alternatively activated macrophages, called M2, are anti-inflammatory and they are predominant in lean individuals [1]. M2 are activated by IL-4 [40] and express the anti-inflammatory cytokine IL-10 [39]. Moreover, M2 contribute to a metabolic homeostasis in the lean adipose tissue [39], promote WAT remodelling and support systemic insulin sensitivity [52,54,55].

1.1.3. Metabolome

Metabolome is the global collection of all low molecular-weight metabolites that are produced by cells during metabolism, and provides a direct functional readout of cellular activity and physiological status [56]. In general, metabolites can be polar (e.g. acylcarnitines and amino acids) or nonpolar (e.g. lipids). Lipids as well as acylcarnitines and amino acids are

more discussed below. Central carbon metabolism is a major pathway from which the metabolic fluxes are distributed to different branches and it builds-up the storage pool when nutrients are in excess and balances the biosynthesis precursors and energy supplies as well. Although metabolic pathways are known for decades the regulation and quantification of metabolic network is not fully understood [57]. It is crucial to be able to determine and quantify metabolites to understand the metabolic response in health and disease state [58,59]. Simultaneously analysing of hundreds of endogenous metabolites presents a challenge because of their chemical diversity, different chemical structures and properties [60]. Also, metabolites can be present in trace levels in cellular and intracellular compartments and thus we need very sensitive technique to recover and detect as many metabolites as possible [61]. Mass spectrometer seems as an optimal platform for target metabolomics [60].

1.1.3.1. Acylcarnitines and amino acids

Acylcarnitines (AC) and amino acids (AmA) are associated with obesity and adipose tissue metabolism. Specifically, it has been shown that both AmA and AC have influence on development of insulin resistance [62] and impaired glucose tolerance in diabetes [63].

Acylcarnitines are the intermediates of fatty acid and amino acid oxidation [63], they are involved in energy metabolism and adenosine triphosphate production [11] and they are important diagnostic markers as well [63]. Specifically, their measurement in plasma is a useful tool for early diagnosis of inherited disorders of fatty acids catabolism [64] and odd-numbered AC are newly discovered as potential markers of the metabolic syndrome [65–67]. Unfortunately, the cause of changes in AC levels in disease [63] or during development of obesity state [68] is still unclear. Amino acids play central role as substrates in organ metabolism [69]. Complete oxidation of amino acid´s carbons occurs only if their carbons are ultimately converted to acetyl-CoA and then acetyl-CoA is oxidized to CO_2 and H_2O via the Krebs cycle and mitochondrial electron transport system [70].

In general, higher rate of fatty acid oxidation and augmented levels of long-chain AC were discovered in plasma during fasting [71]. Also, it has been shown that increased levels of AC with long chain can be found in serum during obesity [68]. Conversely, insulin reduces all plasma AC species in humans [66]. Acylcarnitines specifically, AC with long chain and C4-OH are linked to obesity and T2D in humans [68], metabolite C3:0, C5:0 and C4DC were

reported as biomarkers of T2D [63,65] and acylcarnitine C16-DC is related to peroxisomal fatty acid oxidation [68]. Furthermore, higher plasma levels of amino acid ornithine were found in obese mice [72].

1.1.3.2. Lipids

Cellular lipids are the major constituents of animal and plant cells and main components of lipoproteins in serum. Most of them are not soluble in water but only in non-polar solvents [73]. Lipids are composed from defined building blocks [74]. Usually they consist of polar hydrophilic head group and non-polar hydrophobic part (i.e. glycerophospholipids) but some lipids are composed of non-polar components only (i.e. triacylglycerols, diacylglycerols, cholesterolesters). The polar head group of lipids defines the individual lipid class [73]. Lipid classification into 8 classes is recommended by LIPID maps consortium and the classes are fatty acids, glycerolipids, glycerophospholipids, sphingolipids, sterol lipids, prenol lipids, saccharolipids and polyketides [74,75]. The most abundant lipid classes are triacylglycerols (TG) and phospholipids [76–78]. Triacylglycerols serve as important energy storage depots, risk predictors for cardiac diseases or diabetes [79,80] and they are main components of adipose tissue [81]. Further, fatty acids may be saturated, monounsaturated or polyunsaturated while predominant fatty acids contain 16 and 18 carbons in chain [81]. Interestingly, new lipid classes are still being discerned by target biochemical approaches [74].

Lipids have many function in organism [82–84]. Firstly, lipids are part of membranes as they create the hydrophobic barriers and separate cellular compartments in biological organism. Secondly, they are optimal matrix to facilitate specific conformations, interactions and dynamics for the activity of transmembrane proteins. Also, lipids are perfect energy reservoir (e.g. triacylglycerols) and storage depots of bioactive second messenger (e.g. eicosanoids, diacylglycerols). Messenger can propagate cellular signalling for cell growth, differentiation, death and response to stimuli [73]. Of note, lipid metabolism is crucial for energy homeostasis [81]. Levels of lipids are strictly regulated and misbalance in their levels or in lipid metabolism may lead to rise of pathologies [81], e.g. tumour development [11]. Lipid´s transportation in blood circulation has two main channels, one is for lipids that come from diet and second carry out lipids originated from liver [81]. Besides these two channels there is also reversed transportation of cholesterol [85].

Lipidomics aims to study the pathways and networks of the cellular lipids by characterization and quantification of all lipids presented in biological system [73,86]. It is a part of metabolomics [81] and was emerged in 2003 [11]. Lipidomics has two directions: target and global analysis. Target analysis of lipids focuses on known lipids and develops a specific method with a high sensitivity for quantitative analysis of these lipids. Thus, target analysis is commonly used for studying signal processing. Contrarily global analysis is an untargeted analysis that aims at detecting every lipid species presented in the sample. Therefore global analysis is useful for studying lipid metabolism, molecular mechanisms and biomarker´s discovery [11]. Determination of lipids is challenging because they have totally different polarity states [74,87] and cellular lipidome is dynamically changing at any moment by nutritional status, health conditions, etc. [73]. Lipidomics utilizes mainly principles and technological tools of analytical chemistry, particularly mass spectrometry [11]. Establishment of a powerful method for lipidomic analysis is very important [73] because it can show problems in lipid metabolism including risk factors for many diseases, e.g. cancer, atherosclerosis, diabetes [88–90]. Moreover, lipid biomarkers help to elucidate the inflammatory processes through determination of eicosanoids, leukotriens etc. [91]. Nevertheless, there are a few areas of technological progress that need further development. First, it is still impossible to determine a whole cellular lipidome. Then bioinformatics for interpreting large sets of data is limited, and finally, a definitive unravelling of the biochemical mechanisms responsible for a disease state is still rare [11].

Omega-3 polyunsaturated fatty acids

Omega-3 PUFA belong to the lipid family of polyunsaturated fatty acids (PUFA). Number 3 in the term defines the position of the double bond that is closest to the methyl terminus of fatty acid´s acyl chain, i.e. all omega-3 PUFA have double bond on carbon 3 [92]. PUFA are key components of the phospholipids in cell membranes [92] and they are precursors of many metabolites [93]. Alpha-linolenic acid (18:3, known as ALA), eicosapentaenoic acid (20:5, known as EPA) and docosahexaenoic acid (22:6, known as DHA) are common omega-3 fatty acids found within biological membranes [94]. Indeed, ALA is the major omega-3 PUFA contained in most of human´s diets because it is in plants, nuts, seed etc. [92]. Animals and humans cannot synthetize ALA unlike plants [92] but

animals can metabolize ALA to eicosatetraenoic acid (20:4, omega-3 PUFA) and further to EPA and DHA [81,95].

Marine omega-3 PUFA have anti-inflammatory properties [96–98], exert beneficial metabolic effect and counteract adverse effects of obesity [99]. Its positive impact on obesity is explained by amelioration of low-grade inflammation in WAT, liver, as well as in other tissues while it results in the preservation of the "healthy adipocyte" phenotype in WAT (for details see above). Although it was shown that omega-3 PUFA could decrease the size of fat cells in humans with diabetes weight reduction was observed only for mice not for humans [7]. We have demonstrated in our clinical trial that omega-3 PUFA could improve postprandial lipid metabolism in overweight/obese patients with type 2 diabetes but they cannot reverse type 2 diabetes [100]. Nevertheless omega-3 PUFA are invaluable in stimulating the synthesis of anti-inflammatory lipid mediators in obese WAT (the lipid mediators are discussed below) [99]. Further, omega-3 PUFA could partially improve the negative effect of excess lipids on macrophages and increase the rate of FA re-esterification and oxidation [49]. Several studies have also shown that they reduce circulating levels of triacylglycerol in both obese mice and humans but on the other hand they enhance insulin sensitivity only in obese rodents and not in humans [7]. Omega-3 PUFA are protective against coronary heart disease [7] and ischaemic stroke as well [101]. Of note, the impact of omega-3 PUFA can be augmented by combined intervention, e.g. caloric restriction, exercising in humans or administration of anti-diabetic drugs [7].

Omega-3 PUFA are present in marine fish while the seafood is a good source of them as well [92]. World health organisation recommends regular fish consumption (1-2 servings per week) while serving should provide an equivalent of 200-500 mg of eicosapentaenoic and docosahexaenoic acid [89]. A single lean fish meal (e.g. cod) could provide about 0.2 to 0.3 g of marine omega-3 PUFA. On the other hand single oily fish meal (e.g. salmon or mackerel) could provide as many as 1.5 to 3.0 g of these fatty acids. It seems that a dose of at least 2 g per day is necessary to achieve omega-3 PUFA´s anti-inflammatory effect while this would equate to about 30 mg per kg body weight and day. It means one meal of salmon or mackerel every day which is almost impossible. The most effective strategy is to add fish oil concentrate (not only fish oil capsule which is also insufficient) as a nutritional supplement [92]. Interestingly, metabolic efficacy and bioavailability of omega-3 PUFA depend on their chemical binding form [50], e.g. omega-3 PUFA in a form of phospholipids are better than in a form of triacylglycerols [102].

Lipid mediators

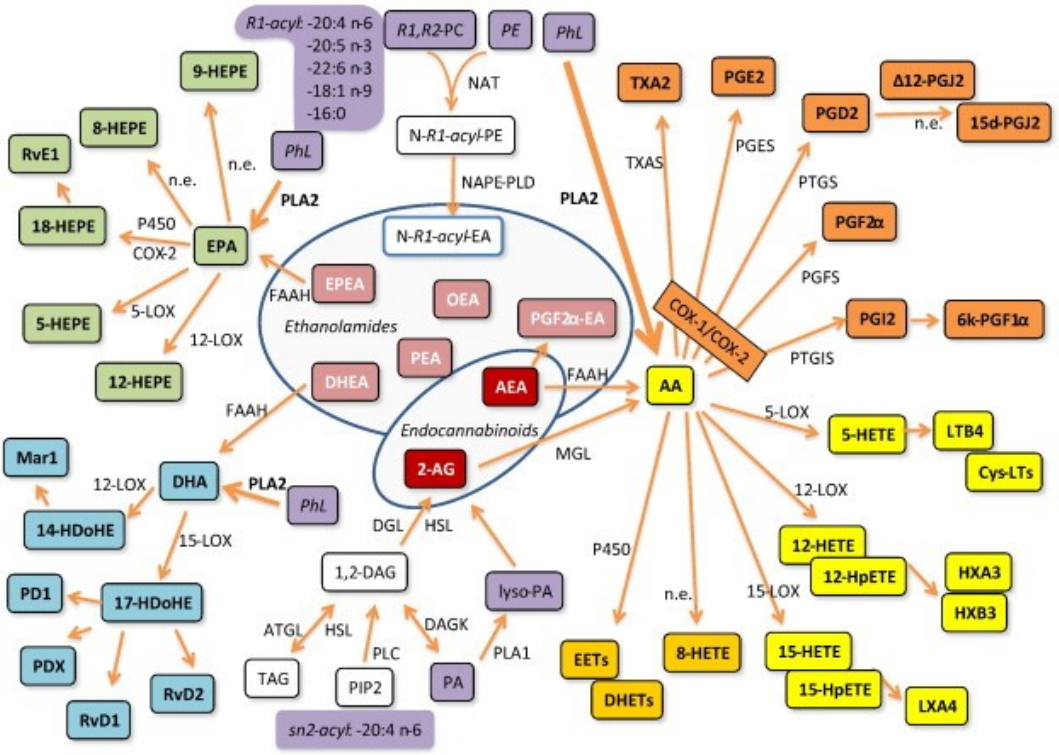

Figure 5. *Overview of lipid mediators in WAT. Production of lipid mediators begins on the plasma membrane, where phospholipids (violet) are cleaved by phospholipase A2 to yield free arachidonic (AA) , eicosapentaenoic (EPA) or docosahexaenoic (DHA) acids, which are subsequently metabolized into either eicosanoids (orange, yellow, green) or docosanoids (blue) by a variety of enzymes. Endocannabinoids (red) come either from membrane phospholipids via N-acyl-phosphatidylethanolamine intermediate or from 1,2-diacylglycerol, product of PIP2, PA or TAG metabolism, in case of 2-AG. 2-AG, 2-arachidonoyl glycerol; AA, arachidonic acid; AEA, arachidonoylethanolamide; ATGL, adipose triglyceride lipase; COX, cyclooxygenase; DAG, diacylglycerol; DAGK, diacylglycerol kinase; DGL, diacylglycerol lipase; DHEA, docosahexaenoylethanolamide; − EA, − ethanolamide; EPEA, eicosapentaenoylethanolamide; FAAH, fatty acid amide hydrolase; HSL, hormone-sensitive lipase; HX*, hepoxilin; LOX, lipoxygenase; LT*, leukotriene; MGL, monoacylglycerol lipase; n.e., non-enzymatic oxidation; NAPE-PLD, N-acyl phosphatidylethanolamine-specific phospholipase D; NAT, N-acyl transferase; OEA, oleoylethanolamide; P450, cytochrome P450; PA, phosphatidic acid; PC, phosphatidylcholine; PE, phosphatidylethanolamine; PEA, palmitoylethanolamide; PG*, prostaglandin; PIP2, phosphatidylinositol biphosphate; PLC, phospholipase C; TX*, thromboxane. For nomenclature of lipid mediators see LIPIDMAPS.org. Adapted from [50].*

Oxidation of polyunsaturated fatty acids leads to production of lipid mediators through enzymatic, i.e. cyclooxygenase (COX), lipoxygenase (LOX) and cytochrome P450 (CYP) reactions, or free radical-mediated reactions. Lipid mediators occurred in WAT are shown in **Figure 5**. They are involved in many biochemical and signalling pathways, especially in inflammatory environment [93]. High storage capacity of WAT for omega-3 PUFA indicates that this tissue is very important as a source of various types of omega-3 PUFA-derived lipid mediators [7]. Interestingly, new families of these lipid mediators have been discovered in last 10 years [92], e.g. FAHFA (for details see below). Lipid mediators derived from arachidonic acid (20:4, omega-6 PUFA, known as AA) are predominantly proinflammatory whereas EPA (20:5, omega-3 PUFA) derived mediators have opposite effect [93]. Also, it has been reported

that lipid mediator protectin D1, analyte of our interest, decreases accumulation of adipose tissue macrophages, shifts polarization of macrophages towards M2 and improves insulin sensitivity in obese mice [103–105].

Eicosanoids are lipid mediators derived from 20-carbon PUFA, especially arachidonic acid [92] or eicosapentaenoic acid [93]. They are key mediators and regulators of inflammation [106–108] and their precursors (corresponding fatty acids) are released from the membrane phospholipids due to inflammatory stimuli. Of note, EPA-derived eicosanoids are usually less biologically active than AA-derived [92]. Endocannabinoids are complex eicosanoids that are produced by cleavage of phospholipids by phospholipases [109]. They regulate food intake, energy balance as well as lipid and glucose metabolism and inflammation [110]. The two major endocannabinoids, anandamide (AEA) and 2-arachidonoylglycerol (2-AG), have pro-inflammatory properties and they are associated with obesity. Omega-3 PUFA reduce the level of arachidonic acid in membrane phospholipids and thus suppress the amount of endocannabinoids in peripheral tissues [8]. Specifically, administration of omega-3 PUFA leads to sustained decreased levels of 2-AG and AEA in WAT of obese mice. In contrast, the amount of 2-AG and AEA in patients with T2D remains unchanged despite omega-3 PUFA supplementation [7].

Branched fatty acid hydroxy fatty acids (FAHFA) are newly discovered lipid molecules first described in 2014 by Yore et al. [111]. They are members of a lipid class called estolides (intermolecular esters of hydroxy fatty acids), i.e. wax [112]. FAHFA are synthetized by adipose tissue [113] and they were detected in both human and mice WAT [99]. In general, they could improve local and whole body glucose metabolism [3]. Also, FAHFA decrease accumulation of macrophages, expression of pro-inflammatory adipokines and promote macrophages polarization toward M2 metabotype [7]. We were focused on novel member of this family, i.e. omega-3 PUFA docosahexaenoic acid esterified to 9- and 13-hydroxyoctadecadienoic acid (HLA) that is termed 9-DHAHLA and 13-DHAHLA.

1.2. ANALYTICAL CHEMISTRY

We utilized particularly very sensitive liquid chromatography and mass spectrometry detection to study adipose tissue metabolism. Here, we discuss preparation of samples, then we describe analytical techniques used in our research and finally we devote to quantitative analysis.

1.2.1. Preparation of metabolomic and lipid samples

1.2.1.1. Metabolomic samples

First, cell metabolism must be interrupted by quenching to obtain metabolomic samples. Quenching is a drastic change of temperature or pH and is necessary because levels of metabolites can be changed in any moment [81]. Then samples are separated from biomass by adding an organic solvent/solvent mixture, e.g. acetonitrile [81] or methanol [114]. Thus the high-molecular-weight species (i.e. proteins and RNA) precipitate and they can be removed by centrifugation step and we acquired metabolite-containing supernatant for analysis [114]. Lastly, the solvents are evaporated and samples are concentrated [81] while the sample solutions can be reconstituted in a high aqueous solvent for reversed-phase applications or high organic solvent for direct analysis without lyophilization in HILIC applications. Of note, internal standards can be spiked into samples for quantitative analyses where they compensate variability in sample processing and analytical platform operation [114].

1.2.1.2. Lipid samples

Lipid extraction process exploits the high solubility of lipids in organic solvent [11]. Unfortunately, it is impossible to have one extraction method for all lipid species because lipids are very divergent [86]. In general, lipid extraction helps to remove salts and protein that interfere with separation techniques or mass spectrometry detection from sample [86] and simultaneously preserves lipids for further analyses [11]. The two lipid extraction processes are liquid/liquid or solid phase extraction (for details see below).

In practice, lipids in tissue and cells are relatively protected by natural antioxidant system but they can be more prone to chemical and enzymatic modification due to sample homogenization. To avoid these modifications it is recommended to work at temperature close to 0 °C and to add a small percentage of organic solvent or the antioxidants (e.g. butylated hydroxytoluene [115]) to the homogenization buffer. Also, the extracts should be stored in glass vials, solubilized in sufficient organic solvent at -80 °C and inert gas should be kept in vials instead of air/oxygen [86]. Polyunsaturated lipids are susceptible to photodegradation and it is better not to work with them in direct sunlight [93].

Liquid/liquid extraction (LLE)

Liquid/liquid extraction (LLE) is based on the partition of an analyte between two immiscible (organic/aqueous) phases and it is used to extract groups or families of molecules [116]. Usually, lipids portion into the organic phase, water soluble molecules remain in the aqueous phase and protein are precipitated [86]. The solvent choice is based on its polarity; generally, polar solvents extract polar analytes more efficiently than the apolar analytes. The advantage of using this method is that it is both inexpensive and easy to implement. Contrarily, it has the inconvenience of being time-consuming, difficult to automate, often consuming toxic solvents and less efficient for highly polar compounds [116].

Two well established LLE platforms are methods by Folch [117] and Bligh&Dyer [118]. Bligh&Dyer extraction utilizes solution chloroform/methanol/water (1:1:0.9, v/v/v) and it is appropriate for a small amount of sample (less than 50 mg). Extraction solution for modified Folch method is chloroform/methanol (2:1, v/v) while water or 0.9% NaCl wash the solvent extract. This approach is convenient for sample size of 100 mg [11]. Both platforms as well as their modifications are widely used today [86,115]. Nevertheless they have same drawbacks, e.g. working with hazardous chloroform and quite a demanding collection of chloroform phase with lipids [11].

Other extraction approaches used in lipidomics are methyl-tert-butyl ether (MTBE) and butanol/methanol (BUME) methods. Extraction solution of MTBE approach is methyl-tert-butyl ether/methanol/water (5:1.5:1.45, v/v/v/v). Methyl-tert-butyl ether presented in the top layer [11] has lower density than water [86] and therefore it is more suitable to remove this phase after phase separation [11]. The limitation of this approach is that MTBE

phase with lipids may also contains aqueous component which may carry over the water-soluble contaminants. Finally BUME method, butanol/methanol (BUME, 3:1, v/v) are added to a small volume of aqueous phase and then equal volume of heptane/ethyl acetate (3:1, v/v) and 1% acetic acid are added there as well. This approach ensures that less water-soluble contaminants are carried over in organic phase but on the other hand it is difficult to evaporate the butanol in organic phase [11].

Solid phase extraction (SPE)

Solid phase extraction is a sample preparation technology that uses solid particle, i.e. chromatographic bed, to chemically separate different components of a sample [119]. The approach is based on the partition of a sample between a mobile liquid phase (the biological matrix and various solvents) and a solid stationary phase [116] while sample is nearly always in the liquid state [119]. It uses the same basic chromatographic principles as high performance liquid chromatography, but in a different format and for a different reason. Here, chromatography is used to better prepare a sample before it is submitted for analytical testing [119]. Since its introduction, many stationary phases have been developed, allowing more targeted extractions or adaptations for the extraction of a large number of chemicals of various types. The diversity of stationary phases allows extraction of polar compounds that were previously difficult to extract by organic phases [116]. Today, scientists find SPE very useful in solving difficult sample preparation and analytical problems [119], for example to characterize a specific compound or a family of compounds [116] and for the selective removal of interferences from sample [119].

There are many benefits of using SPE. First, it can reduce ion suppression in mass spectrometry applications and enables us to detect trace concentration of very low level compounds. Then SPE can simplify complex sample matrix along with compound purification and fractionate sample matrix. For example, different classes of compounds separated by their polarity are in **Figure 6** while then they are separately analyzed in a much more efficient way because their compounds would be more similar [119].

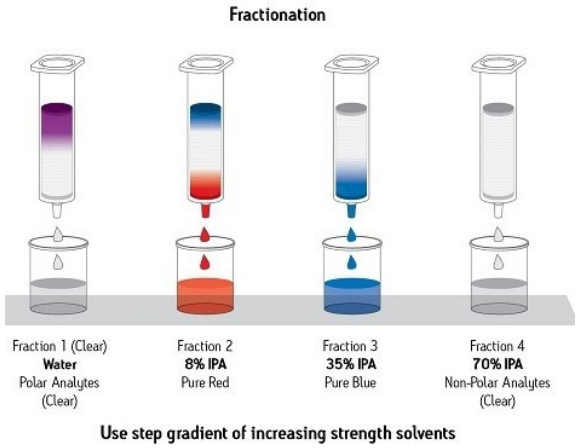

Figure 6. *Sample preparation by SPE. Adapted from [119].*

We utilized offline solid phase extraction procedure, which can be performed on SPE cartridges or 96 well plates, and consists of four main steps. First step is the conditioning of the stationary phase that regenerates retention sites involved in the molecular interactions [116]. Subsequently, the sample is loaded on the cartridge [93,116]. The flow rate during sample loading has to be appropriate because too fast a flow rate may lead to reducing the efficiency at which analytes are retained on cartridges [93]. Also, acidification of sample before the extraction helps to protonate lipid mediators and allows them to be retained on a cartridge [92]. Later on, SPE column is washed while it aims to eliminate weakly-retained molecules [116] or remove excess salts and another water-soluble impurities [92]. Then cartridges are washed by hexane to remove any water in lipid extraction processes [92]. Finally an appropriate organic solvent, e.g. methylformate for lipid mediators [92], is used to elute the analytes [116]. These extracts are dried in Speedvac or using SPE drying attachment with nitrogen supply and reconstituted in the mobile phase used in the mass spectrometry (MS) measurement. Wash volumes, used in SPE, are determined by the mass of the sorbent bed, commonly it is 1 ml of solvent per 100 mg of bed mass. Nevertheless usually larger volumes are utilized for lipid extraction in order to remove all weakly bound impurities from sorbent bed, e.g. 4x5 ml on 500 mg sorbent bed. It is important because impurities can cause ion suppression on MS and loosing MS sensitivity. Of note, extracts from solid tissue samples larger than 200 mg may potentially cause ion-suppression in mass spectrometry and contaminate the system as well [92].

1.2.2. Liquid chromatography

1.2.2.1. In general

High performance liquid chromatography (HPLC) utilizes either a solid or liquid-coated solid stationary phase and a liquid mobile phase to separate the analytes through adsorption of analyte to the stationary phase [120]. This technique is able to discover and quantify low or trace-abundance lipid species and allows separation of complex mixtures [121]. Also, HPLC offers the most flexibility for interfacing with various detection systems, e.g. mass spectrometry [115]. In general, liquid chromatography is very sensitive, robust [59] and has resolution and specificity [120].

Liquid chromatographic separation coupled to mass spectrometry (LC-MS) can simplify complex sample extracts [121] and analyse large nonvolatile polar compounds without derivatization [122]. LC-MS is appropriate for analysis of lipid extracts [121] or for distinguishing of isomeric species with the same mass (i.e. isobaric compounds) [93,115]. Also, it is popular tool for identification of metabolites [68] because it can reduce high complexities of biological samples [11]. Main advantage of LC-MS is its compatibility with commonly used solvents [122] and the option to choose different columns for separation [60]. HPLC with MS detection is fast additionally and sample preparation for that analyses is simple [60]. On the other hand, LC-MS can make high abundance lipids more concentrated and it leads to forming the aggregates and decreased ionization efficiency [121]. Moreover, only limited number of retention times can be observed in chromatogram in one run. LC-MS data include both mass spectra and chromatogram with retention time that also helps to identify the analytes [11]. Unfortunately, mass spectral libraries are not currently available because of non-reproducibility between different LC-MS systems caused by differences in liquid chromatography column chemistries and mass spectrometer designs [114].

Ultra performance liquid chromatography (UPLC) is category of HPLC that utilizes column particles smaller than 2 μm in diameter. These particles create very high operating pressures (in the range of 6000 to 15,000 psi) and it results in superior resolution, speed, and sensitivity compared with HPLC [123]. Also, UPLC substantially increases a number of detected metabolites when compared with traditional HPLC. In general, ultra performance liquid chromatography coupled to mass spectrometry provides high mass accuracy and its linear dynamic range can operate over three to five orders of magnitude [114].

1.2.2.2. Liquid chromatography modes

Most lipidomic applications use reversed-phase column chemistries although other chemistries, e.g. hydrophilic interaction chromatography or normal phase chromatography, are also utilized [114]. Typical mobile phase for lipidomic analysis is a mixture of aqueous buffer with methanol or acetonitrile but hexane or isopropanol are also used as cosolvents [115]. Metabolites can be determined by ion-pair, hydrophilic interaction liquid chromatography, ion exchange, normal phase [59] or reverse phase chromatography coupled to triple quadrupole or ion trap [87].

Reversed phase chromatography

Reversed phase (RP) chromatography has a nonpolar capped silica stationary phase and polar mobile phase [115] and it allows separation of individual lipid species due to their different hydrophobicities [121]. Usually, RP starts with a high aqueous content mobile phase (with modifiers, e.g., formic acid) and the organic phase fraction is increased, typically operating from 100% aqueous to 100% organic. The organic solvent is commonly either methanol or acetonitrile. Acetonitrile is a more non-polar (or lipophilic and hence 'stronger') organic solvent and operates at lower back-pressures, although it can present problems with elevated background and reduced sensitivity at high acetonitrile concentrations [114]. Salts (e.g. ammonium acetate, ammonium formate or acetic and formic acid [115]) in mobile phase help to retain polar compounds on RP column but their high concentration can cause the signal instability, ion suppression or contamination of MS source [122,124]. Therefore application of pH in mobile phase instead of salt gradient may allow mass spectrometry detection [125].

In practice, the same gradient elution program utilized in both positive and negative mode offers advantages in metabolite identification because single metabolite is recorded with the same retention time in both ion modes. The use of reversed-phase chemistries provides efficient retention and separation of relatively nonpolar metabolites across a large molecular weight range (50 to >1,500) and includes high-molecular-weight lipid species (e.g. phospholipids and triacylglycerols) and nonpolar amino acids (e.g., tryptophan) [114]. Also, hydrophobic molecules (lysophosphatidylcholine, lysophosphatidylethanolamine) are separated by reverse phase chromatography [125,126]. Oxygenated PUFA mediators are

usually separated on octadecyl (C18) reversed phase column with acidified methanol or acetonitrile-based mobile phase system due to their polarity [92]. Phospholipids with long fatty acyl chains are quite non-polar and thus highly organic solvents are needed to remove them from C18 column and more polar oxidized and chain-shortened forms of phospholipids elute at the beginning of analysis on butyl column with high aqueous content in mobile phase [115].

Normal phase chromatography

Normal phase (NP) chromatography involves a silica stationary phase with nonpolar mobile phase [115]. NP is able to separate complex lipid extract to individual lipid classes [121] and it is the most effective for separation of phospholipids [115]. Unfortunately the solvents are only partially soluble [127] and less well suited to generating a good electrospray of mass spectrometer [115].

Hydrophilic interaction liquid chromatography

Hydrophilic interaction liquid chromatography (HILIC) is a more robust form of a normal phase separation [115] and it utilizes a polar stationary phase in combination with a mobile phase, containing high concentration of organic solvent in water [128]. The primary function of HILIC stationary phase is to bind water at its surface (see **Figure 7**) [127]. The mechanism of separation is complicated. Although HILIC is traditionally assumed to result from the partition between the aqueous layer accumulated close to the solid surface and a highly organic bulk mobile phase the separation mechanism is obviously more complex. Differences in the chromatographic selectivity of various polar compounds indicate that adsorption on the polar centres on the solid phase surface may also contribute to the retention. Also, mixed retention mechanism (e.g. polar, hydrophobic or ion exchange interactions) potentially conduces to the retention of sample compounds. Specifically, polar interactions control the retention in acetonitrile-rich mobile phases, whereas the column may show essentially reversed-phase behaviour with the major role of hydrophobic interactions in highly aqueous mobile phase [128].

Properties of HILIC separation systems strongly depend both on the stationary phase and the composition of the mobile phase [128]. For example, high organic content in mobile phase leads to high ionization efficiency of HILIC [127,129]. Yet the technique is versatile [130] and enables faster separation compared to reverse phase chromatography because of lower viscosity of eluent [129]. Furthermore HILIC is well compatible with mass spectrometry [115,127] and it is advantageous that it can be used without ion pair reagent [131]. Of note, many new types of columns based on silica gel have appeared in the past years, e.g. organic polymers [128] or ZIC-HILIC [127]. ZIC-HILIC is a sulfoalylbetaine (zwitterionic) phase that incorporates a positive and negative charge in relatively long alkyl chain and thus it can undergo electrostatic interaction and attract polar molecules [127]. Hydrophilic interaction liquid chromatography provides an alternative approach to effective separation of polar analytes in compares to RP because these analytes elute very early [126,129] or they are not sufficiently retained [114,122,128] on conventional RP phases. Therefore HILIC is suitable for separation of strongly or moderately polar (hydrophilic) samples [126–128] and it also allows simultaneous separation of different classes of important metabolites [130].

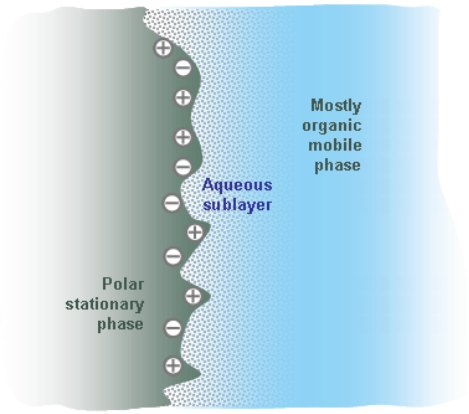

***Figure** 7. Graphical representation of the micro environment around the surface of the stationary phase in HILIC chromatography. Adapted from [132].*

1.2.3. Mass spectrometry

1.2.3.1. In general

Mass spectrometry (MS) is a powerful analytical technology that can be used to identify unknown organic or inorganic compounds, determine the structure of complex

molecules, or quantitate extremely low concentrations of known analytes. Molecules must be ionized, or electrically charged to produce individual ions and must be present in the gas phase for MS-based analysis. MS instruments analyse molecules by relating the mass of each molecule to the charge; this identifying characteristic is specific to each molecule and is referred to as the mass-to-charge ratio *(m/z*). Ions produced from small molecule analytes (1000 Da) usually possess a single charge; therefore, their *m/z* is equivalent to the mass of the ion. This is commonly designated as $[M+H]^+$ for protonated (positive) and $[M-H]^-$ for deprotonated (negative) ions. Relative ion abundance of a specific *m/z* is plotted versus time in chromatogram [133]. Mass spectrometer is able to fragment the ions and measure the *m/z* of product ion which together allow the identification of many compounds [115]. Also, multiple overlapping chromatograms can be extracted from the same analytical run, as the mass analysers are able to detect multiple ions independently within the time scale of a chromatographic peak [133].

Mass spectrometry measurement in practice, the sample is introduced into the ion source through a charged capillary or by direct infusion of the sample using a syringe pump (i.e. shotgun approach) or by coupling to a liquid chromatography system (i.e. LC-MS) [115]. Molecules are ionized in ion source and then directed [133] using electric field and mass filtres [86] to the mass analyser where individual ions are selected according to their *m/z* [133]. Of note, ion suppression is a negative effect that influences the ionization of analyte by the presence of other endogenous or exogenous molecules and must be avoided [86].

The analytical power of the mass spectrometer lies in its resolution [133]. Mass resolution is the minimum mass difference between two mass spectral peak and therefore it is a measure of the ability to distinguish two peaks of different elemental composition [134]. The higher the value the better the resolution [86], but overly high resolution can be problematic as well because of potential overlaps analytes [11]. Next characteristic of MS is mass accuracy that is defined as the mass difference detected by the analyser divided by the observed, or true mass [133]. Resolving power refers to an instrument's ability to distinguish two adjacent ions of equal intensity [135] and it is a measure of precision over a wide range of m (or *m/z*) [134]. Moreover, resolving power is useful for evaluating mass analyser performance and may be defined either for a single peak of mass or for two equal-magnitude peaks [134]. Other properties of mass spectrometry is high sensitivity [81], specificity and coupling capability to separation technologies [60,136]. Sensitivity is the amount of moles

that can be detected by instrument (usually in fentomol range) [86] whereas selectivity of MS is achieved by identification of species coeluted during chromatography by their *m/z* [115]. Mass spectrometry is also high throughput approach [81] while typical dynamic range of standard MS instrument is 10^3-10^4 and more modern instruments using selective ion scanning methods have reached 10^5 [115]. Collision energy is required for fragmentation of the individual lipid molecules and it needs to be experimentally established [92]. The dwell time is time taken collecting data at each step during scanning in first quadrupole in triple quadrupole analyser. Usually sufficient dwell time is 10-50 ms but longer dwell time gives better sensitivity (i.e. signal to noise) at a cost of either lower resolution on the mass spectrum or fewer data points per unit time which makes quantification from liquid chromatography less reliable [115].

Utilizing the mass spectrometry is key in lipidomics [137–143]. Unfortunately, one single platform to fully characterize the lipids do not exist [86] and the best option is to combine several different techniques (e.g. MS imaging, LC-MS etc.) to yield the most complete lipidomic data set [144]. Due to lipid´s structural characteristics their identification from ion mass fragment spectra is generally easier to obtain than with other molecular compounds [81]. Limit of detection in MS lipidomics can be amol/mg protein of tissue or cell or amol/ml of body fluid [11]. In practice, most phospholipids are zwitterionic and their longer chain usually needs higher collision energy [115]. Wide range of lipids (e.g. phosphatidylcholines and phosphatidylethanolamines [115]) are analysed in a positive MS mode in which they form positive aducts [73,145], i.e. $[M]^+$ [115], $[M+H]^+$, $[M+Na]^+$ or $[M+NH_4]^+$ [145]. Especially sodium aducts highly occur because sodium is presented very often in natural sources and has high affinity to lipids (e.g. TG) [73]. Also, negative ionization provides superior results for certain lipid classes (e.g. phosphatidylinositol, phosphatidylserine, and phosphatidic acid [145]) as their phosphate group is deprotonized $[M-H]^-$ [115]. Although fatty acyls are measured more often in negative mode because they are ionized more efficiently under these conditions [146] they can form protonated molecules $[M+H]^+$ as well [87]. Of note, decay of molecules in fragmentation cell helps to get information about the distribution of fatty acyl chains and oxidation sites [115].

1.2.3.2. Instrumentation

Ion source

Molecules of analytes have to be ionized by ion source before their detection in mass spectrometer. The most common ion sources in lipidomics are electrospray (ESI), atmospheric pressure chemical ionization (APCI) and matrix assisted laser desorption/ionization (MALDI). All three belong to soft techniques which means that very little fragmentation occurs during the ionization process and monocharged molecular ions are provided [86]. These ion sources are "direct ionization sources," in which analytes are directly ionized from a surface (i.e. MALDI) or from a solution (i.e. ESI) [133].

First APCI, it works under atmospheric pressure and both solvent and analytes are in the gas phase [86]. Unfortunately, the technique is not soft enough [73] and it is often less susceptible to matrix effects (including ion suppression) as compared to ESI [133]. APCI is often used in clinical assays due to its compatibility with liquid chromatography [133]. Furthermore, MALDI utilize laser to ionize the analytes and it is appropriate for detection analytes directly from nonextracted samples, e.g. tissue surface/slices (so called mass spectrometry imaging), or spotted lipid extracts on MALDI plate [86]. Also, it can be used in LC-MS or shotgun lipidomics [11].

Electrospray (ESI)

Electrospray is sensitive ion source where ions are formed in solution or liquid phase and that works under atmospheric pressure [133]. Importantly, it is one of the softest platforms for ion ionization and the most popular quantitative technique for lipidomics [73] and clinical purposes [133]. The principle of ESI is as follows (see **Figure 8**). The sample is nebulized through a highly charged stainless steel capillary using heated nebulizing gas (typically nitrogen), producing fine aerosol [86]. It results in evaporation of the solvent and ionization of the molecules after which the ions [86] formed by desolvation [11] enter the mass spectrometer [86]. Therefore ESI source behaves as an electrophoretic device that selectively ionize a certain type of ions that is conducting with a continuously equilibrating mobile phase [73]. The technique is ideal for easily ionizated molecules [115] but ionization of less ionizable lipid can be enhanced by derivatization [147,148]. Of note, molecular ions can be formed in the source of the mass spectrometer without fragmentation [115].

Electrospray can be used for quantitative and qualitative analysis of all lipid species [86], for analysis of polar compounds [136] or complex dimers [73] and it allows simultaneous but specific analysis of multiple species with good sensitivity as well [115]. It is used in shotgun or LC-MS arrangement [11] while ESI mass spectrometry detection increases with decreasing liquid chromatography flow rate [58].

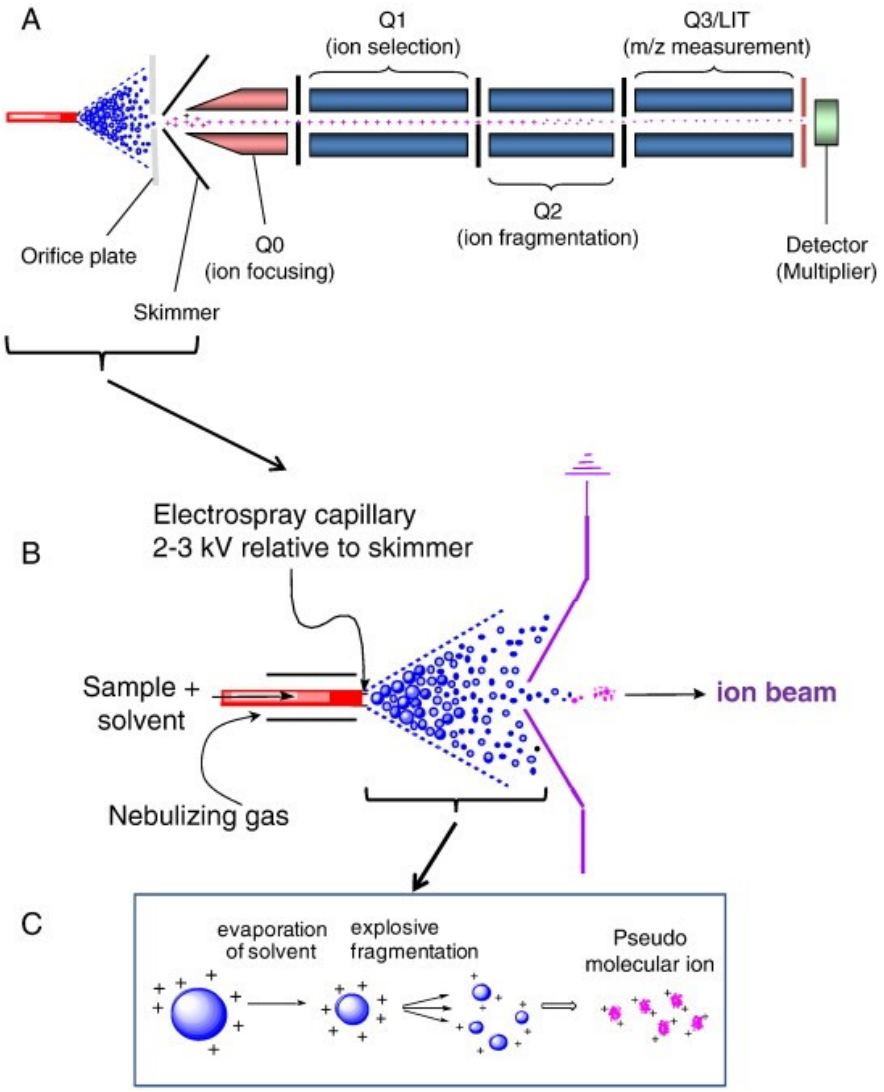

Figure 8. *Schematic diagram of an electrospray source showing formation of pseudo-molecular ions. (A) The geometry of a tandem or quadrupole–quadrupole–linear ion trap instrument. (B) The sample (in aqueous-organic solvent) is sprayed through a charged capillary and the solvent is evaporated by the sheath of nebulizing gas. (C) Pseudo-molecular ions form by explosive fragmentation as the droplet dries. Adapted from [115].*

Electrospray ionization has several advantages [137]. First, ESI can act as a separation device to selectively ionize a certain category of lipid molecular species based on the charge property of lipid class [73]. Therefore, it separates different lipid species with high efficiency without prior chromatographic separation [73] however ESI can be easily coupled to liquid

chromatography for further separation of analytes as well [93,115]. Second, ESI has a high ionisation efficiency, the limit of detection can be even fmol/µl [73], and wide dynamic range [149]. Third positive is that quantification of individual molecular species is possible through direct comparison of ion peak intensities of analyte and internal standard or through the peak-area measurement in the case of LC-MS [73]. Furthermore, there is a nearly linear relationship between an ion peak intensity of analyte and the concentration of that compound [149]. On the other hand, the main limitation of ESI is the occurrence of ion-suppression (matrix) effects that is caused by additives in the mobile phase (acids, bases) and coeluting impurities from biological samples. Unfortunately matrix effect influences the sensitivity of instrument but it can be minimized through sample clean-up by solid phase extraction or small sample volume (i.e. 2-10 µl). Practically, blank injection during measurement helps to monitor the background contamination [93].

Analyzers

Mass spectrometry analysers used in lipidomics are mainly Orbitrap [73], triple quadrupole and time-of-flight. These analysers combine high resolution with mass accuracy and provide high specificity of detection [86]. Time-of-flight (TOF) mass analyser separates ions based on their different flight times over a defined distance or flight path where travel time is calibrated to the *m/z* value [133]. TOF analyser measures all ion masses for each ion pulse [133] and detects unlimited *m/z* [121]. Moreover, it offers high sensitivity and capability of accurate and precise quantitative measurements [133]. Triple quadrupole and Orbitrap analysers are described below.

Hybrid MS is a spectrometer with combination of different mass filters (quadrupole, time-of-flight, ion trap etc.) and it can provide data-depending scanning. This approach can select one or more ions of interest for subsequent fragmentation (i.e. the product ion scan is performed for these selected ions) and thus it gives more structural information [86]. Hybrid instruments are for example QTRAP (for details see below) or Q-Orbitrap. The second mentioned combines a quadrupole with Orbitrap mass analyser while quadrupole performs precursor ion selection and Orbitrap product ion analysis. Q-Orbitrap can be used for protein sequencing and proteomic or metabolomic screening [133].

Triple quadrupole (QQQ)

Single quadrupole mass analyser consists of a set of four conducting rods arranged in parallel, with a space in the middle; the opposing pairs of rods are electrically connected to each other. This type of mass analyser separates ions based on the stability of their flight trajectories through an oscillating electric field in the quadrupole. The field is generated when a radio frequency (RF) voltage is applied between one pair of opposing rods within the quadrupole and direct current (DC) offset voltage is applied to the other pair of opposing rods. Then only ions of a certain *m/z* will have a stable flight path through the quadrupole in the resulting electric field; all other ions will have unstable trajectories and will not reach the detector. The RF and DC voltages can be fixed in a way that the quadrupole acts as a mass filter or analyte-specific detector for ions of a particular *m/z*. Alternatively, the analyst can scan for a range of *m/z* values by continuously varying the applied voltages. Single quadrupole mass spectrometer contains a single mass analyser and it can only measure ions formed in the instrument source [133].

A tandem quadrupole mass spectrometer, often called a triple quadrupole, consists of two quadrupole mass analysers separated by a collision cell (see **Figure 9**) [133]. The principle of triple quadrupole and multiple reaction monitoring mode (MRM) is following. Ion of interest is isolated in the first mass analyser (first quadrupole) and fragmented in a collision cell (second quadrupole) using gas, e.g. nitrogen or argon. Then product ions are scanned and selected by a second analyser (third quandrupole) and related back to their precursor ion [60,87,93] (see **Figure 9**). The pairs of precursor and product ions are called mass transitions and when the electric fields and collision energy are held constant, only analyte ions having a specified mass transition are able to reach the detector [133].

Triple quadrupole is sensitive, fast-scanning and reproducible with high dynamic range [111] and specificity [133]. Moreover, the signals are scanned many times per second and therefore the chromatographic peaks in the case of LC-MS are very reproduced and intensive [87]. The drawback of QQQ is limited resolution and lower sensitivity at higher acquisition rates and when scanning a wide mass range. Therefore it cannot be sufficient for metabolite identification based on the measured mass [86]. On the other hand, triple quadrupole is best for sensitive targeted quantitative analysis using MRM as it isolates and targets analytes of interest and excludes signal from the background matrix [111]. Of note, multidimensional mass spectrometry is combination of different scan types (neutral loss scan,

product and precursor ion scan-for details see below) applied on the same sample in triple quadrupole [86].

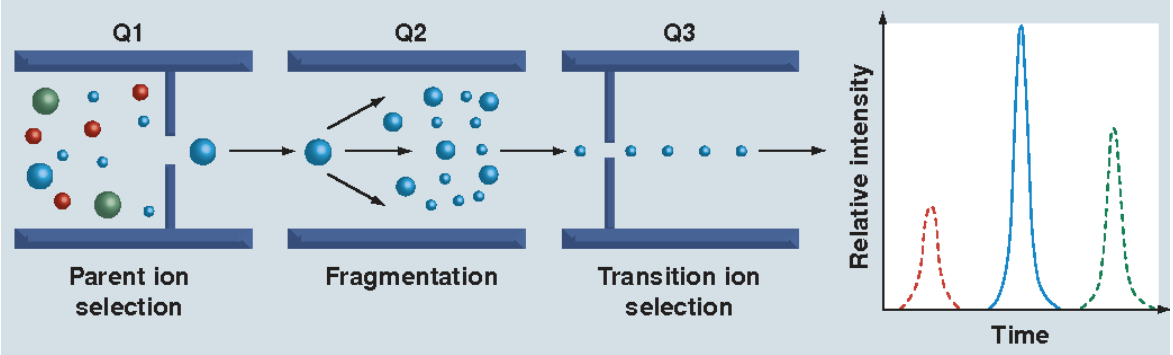

Figure 9. *Multiple reaction monitoring mass spectrometry A schematic of a triple quadrupole mass spectrometer commonly used in multiple reaction monitoring mass spectrometry (MRM-MS) analysis; Q represents a quadrupole in a triple quadrupole mass spectrometer. Relative intensities of measured transitions from three targeted peptides eluting at different retention times are monitored by MRM-MS (coloured in red, blue and green). MS/MS in Q2 illustrates the fragments in the second quadrupole Q2 (collision cell) for one of the three peptides (blue). An MRM-MS assay offers multiplexing capability of many target analytes in a single high-pressure liquid chromatography run. Adapted from [150].*

Ion traps

Ion trap mass analysers use an electromagnetic field to capture or "trap" ions inside the mass analyser. There are multiple configurations of ion traps including a 3D ion traps (Paul ion trap), a linear ion trap (2D trap), an electrostatic trap (Orbitrap), or a magnetic field-based trap (ion cyclotron resonance) [133]. Ion traps have relatively slow acquisition rate and thus they are not ideal for fast chromatography [86]. Also, some ion traps have tandem mass spectrometry (MS^n) capability (MS^n is discussed below).

First, a 3D ion trap basically works on the same principle as a quadrupole mass analyzer as it uses static DC current and RF oscillating electric fields but with hardware configured differently. The parallel rods are replaced with two hyperbolic metal electrodes (end caps) facing each other, and a ring electrode placed halfway between the end cap electrodes while ions are trapped in a circular flight path based on the applied electric field. Second, a linear ion trap uses a set of quadrupole rods coupled with electrodes on each end to facilitate the ion trapping. This configuration gives the linear ion trap a dual functionality, i.e. it can be used as a quadrupole mass filter or an ion trap. An ion cyclotron resonance trap uses a strong magnetic field to induce a radial orbit of ions, where the frequency of orbit in

the magnetic field is a function *m/z* for the ion. Finally, an Orbitrap mass spectrometer is a high-resolution instrument that consists of an inner spindle-like electrode and an outer barrel-like electrode. It stores all ions in stable flight path and detects them on the basis of their detected frequencies which is related to *m/z* [133]. Moreover, Orbitrap detects unlimited *m/z* [121], determinates the exact mass of the compounds and also resolves isobaric species and isotope fine structures [86].

Mass spectrometers that include an ion trap analyser are the most commonly used for qualitative work (e.g., metabolite or protein identification, and screening applications) [133] or for structural characterization of molecules [86]. Although examples of ion trap mass analysers for quantitative analysis do exist, their use in quantitative clinical MS to date is limited [133]. Ion traps are not also appropriate for precursor ion scanning, neutral loss scanning or multiple reaction monitoring modes (these modes are more discussed below) because they do not have two separate analysers [115].

We utilized hybrid instrument QTRAP mass spectrometer that combines a quadrupole mass analyser with a linear ion trap in our research. QTRAP is popular in toxicology screening for unknown agents or in quantitative analyses when the linear trap is operated as a quadrupole [133]. Specifically, our instrument QTRAP 5500 from Sciex is very flexible and sensitive [115] and it is capable of carrying out several mass spectrometry modes, i.e. Q1 MS, Q3 MS, product ion, precursor ion, neutral loss or gain, multiple reaction monitoring, enhanced MS, enhanced product ion, enhanced resolution, MS^3, TripleTrap™ scanning modes [151]. Furthermore, the instrument has the ability to switch polarity in less than 50 ms i.e. without delay in the cycle, and it has dwell time as low as 2 ms without losses in sensitivity [111]. On the other hand its limitation lies in the upper limits of mass scan range which is *m/z* 1000 for the trap and *m/z* 1250 for collision cell. For example, its limit of detection for a single phospholipid species is approximately 0.125 pmol (100 pg) using neutral loss scanning mode while precursor ion scanning mode gives 10-fold higher sensitivity in a case of 10 µl as an injection volume [115].

1.2.3.3. Mass spectrometry modes

Selected ion monitoring (SIM) detects ion intensities in a survey mode in which only a single *m/z* or limited *m/z* ratio is transmitted for quantification. Advantage of this platform is simple instrumentation because it is not a tandem technique. On the other hand monitored *m/z*

could represent combination of analyte and their isobaric counterparts and that leads to less specific identification and inaccurate quantification [121].

Tandem mass spectrometry (MS^n) involves multiple (-n) rounds of mass spectrometry in which precursor ions are either analysed or fragmented again n-times [86] (see **Figure 10**) while it results in product ions studied through a second mass analyser [93]. Tandem mass spectra are complicated because they contain fragments from all co-isolated precursors and from chemical background [74]. The plus is that MS^n can significantly reduce baseline noise by double filtering [121] but on the other hand it cannot separate isomers and isobaric compounds [152]. Also, in-source decay that generates fragments of the same mass-to-charge ratio occurs in MS^n and therefore suitable chromatographic technique is needed before MS detection in some cases [152]. In practice, MS^2 identifies the analytes by their specific fragmentation [57,74] whereas MS^3 is useful for enhanced structural identification of individual ions [115].

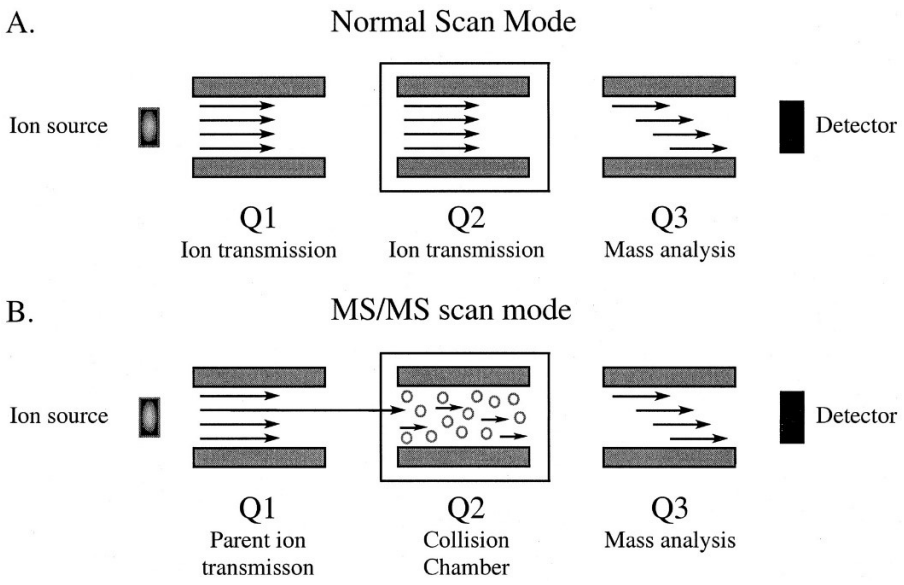

Figure 10. *MS/MS. Conventional and MS/MS modes of analysis in a triple-quadrupole mass spectrometer are shown. (A) In the normal scanning mode, all ions of a certain m/z range are transmitted through the first two quadrupoles for mass analysis in the third quadrupole. From this MS spectrum, a parent ion is selected for fragmentation in the collision cell. (B) In MS/MS mode, the parent ion is selectively transmitted into the collision chamber and fragmented, and the resulting daughter ions are resolved in the third quadrupole. Adapted from [153].*

Selected (SMR) or multiple reaction monitoring (MRM) modes use two mass analysers as static mass filters to monitor a particular fragment ion (i.e. product ion) of a selected precursor ion on triple quadrupole-like instruments (for details see above Triple quadrupole). The specific pair of *m/z* values associated with the precursor and product ions is

referred to as a ´transition´[11]. SRM monitors one transition while MRM monitors multiple transitions [133]. Both modes have high specificity and sensitivity of detection and enable us to analyse hundreds of compounds [59]. MRM is appropriate for quantifying certain predetermined species [115], i.e. target analyses [11], rather than investigating broader profile of analytes [115]. Specifically, multiple reaction monitoring mode is used for analysis of specific fatty acids in negative-ion mode or for headgroup analysis in positive ion mode [115].

Product ion scan (EPI) involves selecting a molecular ion of interest (i.e. precursor ion) in the first mass analyser, fragmenting it in the collision cell by collision with gas and detecting all the resultant fragment ions (i.e. product ions) in the second mass analyser (see **Figure 11**). The drawback of EPI is that it is time consuming as analyses have to be done individually for all components of a complex mixture. Further, this tandem mass technique is utilized for structural identification because it enables us to obtain *m/z* and information about the composition of the parent molecular ion (e.g. the position of acyl chain in the glycerol moiety) and information of functional group or their location within the carbon acyl chain [115]. In practice, product ion spectra can be acquired from different lipid class because lipids have diverse head groups and we got a various fragment ions from them [73].

Precursor ion scan (PIS) consists of the identification of molecular species that give rise to a particular product ion after fragmentation (see **Figure 11**). Specifically, the first analyser scans all the precursor ions through mass range and second analyser detects only *m/z* that belongs to specific fragment of analyte of interest [115]. The selected fragment ion corresponds with a common fragment ion of the precursors and thus all the precursors that produce specific fragments are monitored [11]. PIS is tandem mass spectrometry approach [11] that is appropriate for determination of analytes that have fragments with same polarity as analyte itself and for targeted detection or comparative analyses between controlled samples [115]. Of note, precursor ion scan is less quantitatively accurate than MRM [115].

Neutral loss scan (NLS) is a tandem mass technique where first analyser scans all precursor ions and the second mass analyser scans fragment ions set at an offset from the first analyser (see **Figure 11**). The offset corresponds to a common neutral loss from the precursor ions and all that neutral losses are monitored [11]. NLS is a powerful tool for a targeted detection but it is not commonly used for quantitative analysis because it is less accurate than for example MRM [115].

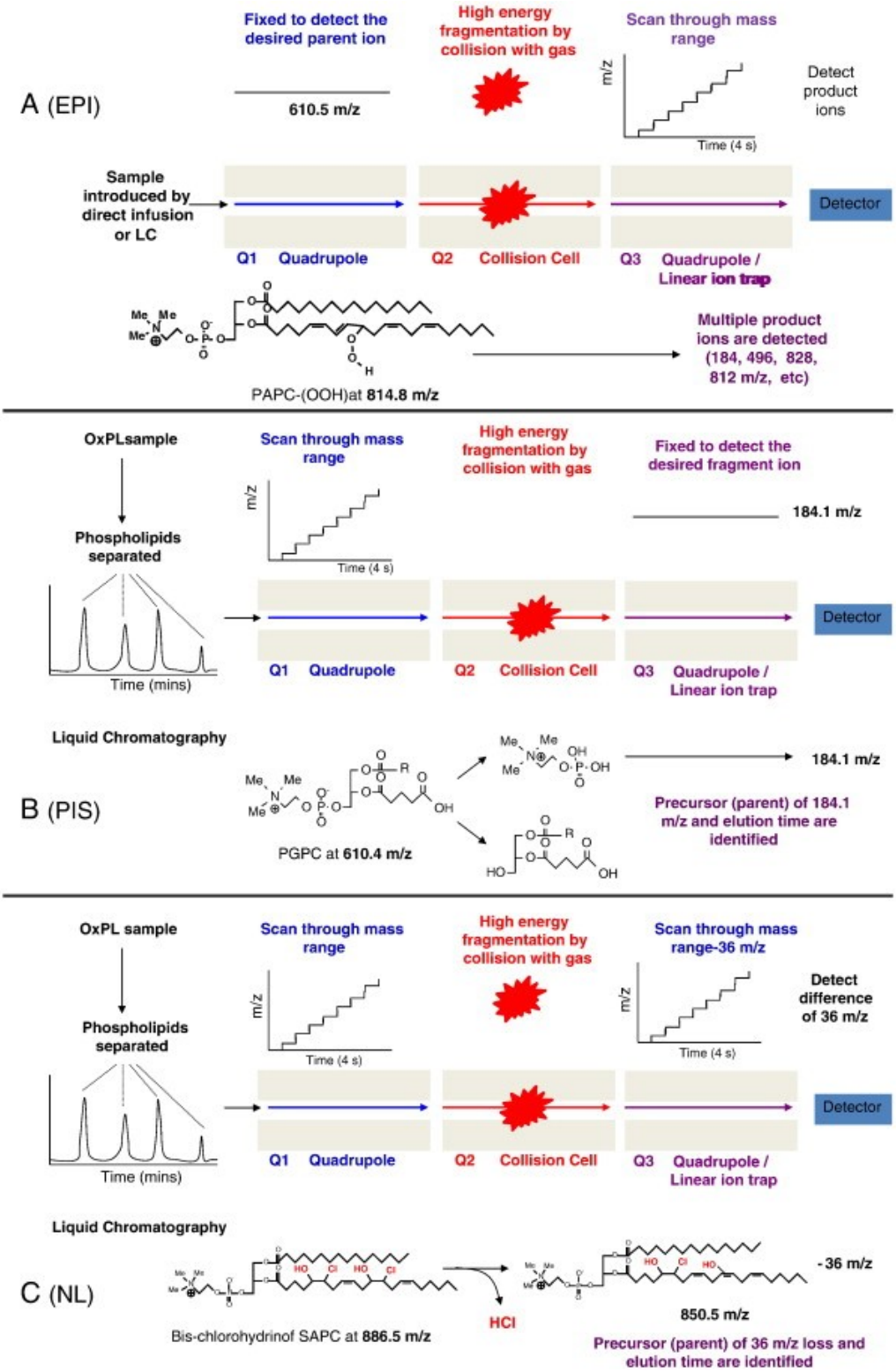

Figure 11. *Advanced MS routines for targeted detection of molecular species. (A) Product ion scanning (EPI) selects a specific molecular ion in Q1, fragments it in Q2, and scans to determine the m/z ratios of the product ions in Q3. (B) Precursor ion scanning mode scans through the mass range in Q1; at each step the molecular ions are fragmented in Q2, and Q3 is fixed to select the passage of a specific product ion, which can then be related to the precursor (parent) ion. (C) Neutral loss scanning mode scans both Q1 and Q3 simultaneously but with a fixed mass offset between them, so that precursor ions that fragment in Q2 by loss of a specific neutral fragment can be identified. Adapted from [115].*

1.2.3.4. Shotgun technique

The total lipid extracts of cells or tissues are directly infused in nanoliter-range into a mass spectrometer in shotgun mass spectrometry [74]. Then analyses are performed at constant concentration of extracted solution [11,121]. Moreover, shotgun approach has ´unlimited´ time and thus ions can be subjected to numerous MS scans and the measurement provides hundreds of spectra [11]. Also, every single peak in the full scan mass spectrum could represent one or more molecular species and identification of that species is achieved by knowledge of their product ion spectra or building block-related neutral loss scan/precursor ion scan spectra [73]. Of note, the complexity of sample can be reduced by sample preparation (e.g. extraction of different lipid classes) or selective ionization [11]. Shotgun MS is a high-throughput approach [11], its reproducibility is as high as 95% [137,154] and it also provides high accuracy of analysis [73]. Conversely, the limitations of that technique are ion-suppression effects [58,81,86], inability to distinguish certain isobaric or isomer species, unreliability to quantify low abundant lipids and difficulty in identifying unknown lipids [86]. Shotgun mass spectrometry can be used for global analyses of individual lipid species [73].

1.2.3.5. Quantitative analysis

The goal of quantification in analytical chemistry is to determine the relative or absolute abundance of analyte. Relative quantification measures the pattern changes of analytes of interest while absolute quantification determines the mass levels of individual analytes and derives total amount of them. The effective strategy to quantify the analytes of interest is to use external or internal standards. External standards are utilized for establishment of calibration curve while quantification is achieved by comparing the ion intensity of analyte with that curve. The advantage of the approach is that there is no concern of overlapping analyte and standard because they are analysed separately. On the other hand, it is necessary to have identical experimental conditions for both analyses [121].

Internal standard (IS) is analogue of the analyte and it is added to sample during sample preparation process (ideally as soon as possible). The sample with internal standard is analysed simultaneously in one analysis and therefore any possible variation during the entire process is compensated [121]. Nevertheless sometimes diverse retention times for internal

standard and analyte itself can be detected due to different ion suppression [86]. Using internal standard is very simple and accurate [121], it helps to reduce experimental errors [73] and it is also a useful approach when multiple peaks for one transition appear [63]. Internal standards are utilized for absolute quantification [115]. Concentration of analyte can be carried out using conventional equation according to where the analyte´s concentration is directly related to concentration of internal standard [155]. In practice, concentration of each individual molecular species can be calculated by comparing the ion-peak intensities (shotgun approach) or peak areas (in LC-MS technique) of analyte and internal standard [11,73].

Importantly, the internal standard should represent the physical properties of the entire chemical class, be chemically similar to the analyte of interest [114] and should not be in original sample or in very minimal level [121]. Using isotopically labelled or non-endogenous standards as internal standards is advantageous [121]. Isotopologue form of analyte is identical to the endogenous molecule except for mass [87] and therefore they are ionisable similarly [121]. Also, they can act as a carrier preventing the loss of trace amounts of analyte during extraction and analysis [156] or be utilized to confirm the presence of endogenous analyte in sample [87]. Unfortunately, stable isotope analogues do not exist for every biomarkers, sometimes only deuterated and structural analogues are available. Deuterated standards are separated slightly but significantly differently as compared to analyte of interest and using structural analogue is unsuitable because they have a different retention time and ionization properties than the analyte of interest [87]. In practice, dimyristoyl (C14:0/C14:0) or diheptadecanoyl (C17:0/C17:0) are very rare in mammalian tissues and thus they can be used as internal standard in lipid analyses [115].

2. METHODS

We adapted and optimized several methods based on liquid chromatography and mass spectrometry for our research [111,157–160]. First, metabolomic methods include a 10minutes long method, that is able to separate acylcarnitines (AC) and amino acids (AmA), and a more general method that is suitable for determination of other metabolites than AC and AmA. Subsequently, lipidomic methods comprise an analysis of eicosanoids and endocannabinoids (in 16 minutes) and a method for measurement of FAHFA compound. All

analyses were performed using an UPLC system (UltiMate 3000 Binary RSLC System, Thermo) coupled to QTRAP 5500 (Sciex, California, USA) mass spectrometer.

2.1. METABOLOMIC LC-MS METHODS

2.1.1. Acylcarnitine´s and amino acid´s 10minutes method

The method is based on HILIC Kinetex column, 50x2.1 mm, 1.7 µm (Phenomenex, USA) heated to 25 °C and it is able to separate 57 acylcarnitines and 21 amino acids in 10 minutes. Mobile phase A consists of 90/10 (v/v) acetonitrile and buffer, and phase B of 90/10 (v/v) water and buffer, while the buffer is 20 mM ammonium formate with pH 4. Gradient elution of mobile phase is in **Figure 12**. Briefly, analysis starts at 100 % of mobile phase A, then it decreases to 75 % of A and after that it rises to 99 % of A. Finally, gradient goes back to 100 % of A where it stayes till the end of analysis, i.e. time 9.5 min. Flow rate of mobile phase is 0.5 ml/min and injection volume of sample is 3 µl. AmA and AC are determined in positive multiple reaction monitoring (MRM) mode (list of MRM transitions is in **Table 1**) with electrospray as ion source. Importantly, we validated the method in sense of precision and accuracy according to [155]. Validation in practice, plasma samples from two mice strains, C57BL/6J and A/J, were divided into triplicates and analysed separately in three days to assess the inter-assay variability, and as a triplicate within one run to assess the intra-assay variability. The validation analyses were performed the same way as normal analyses.

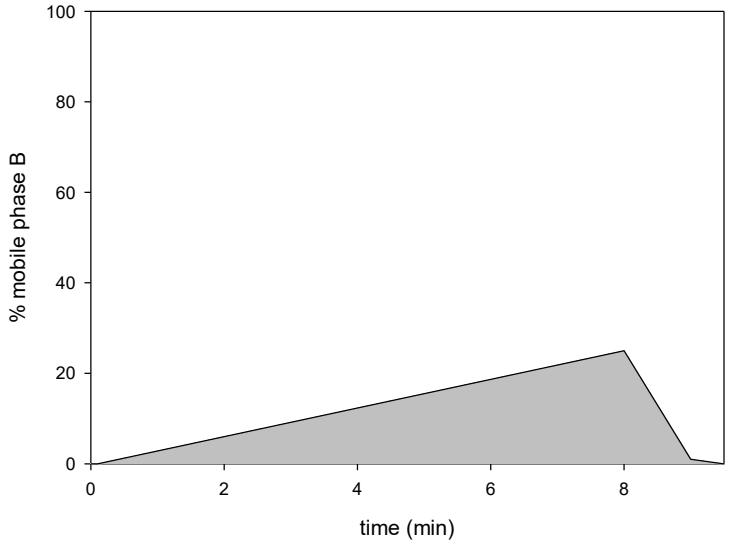

Figure 12. *Elution gradient of mobile phase in 10minutes method. Mobile phase A consists of 90/10 (v/v) acetonitrile and buffer, and phase B of 90/10 (v/v) water and buffer. The buffer is 20 mM ammonium formate (pH 4). Flow rate of mobile phase is 0.5 ml/min and injection volume of sample is 3 µl. HILIC Kinetex column heated to 25 °C. UPLC system (Thermo) and MS QTrap 5500 (Sciex).*

Table 1. *MRM transitions for acylcarnitines and amino acids in 10minutes method. CX is acylcarnitine with X carbons in acylchain, CXDC is dicarboxylcarnitine with X carbons in acylchain. CXOH is hydroxycarnitine with X carbons in acylchain. CX:Y is acylcarnitine with X carbons and Y double bonds in acylchain. CX:Y-OH is acylcarnitine with X carbons and Y double bonds in hydroxyacylchain. Analyte-D_x is deuterated analyte. Glycine-$^{12}C^{15}N$ is isotopic analogue of glycine .Mobile phase A consists of 90/10 (v/v) acetonitrile and buffer, and phase B of 90/10 (v/v) water and buffer. The buffer is 20 mM ammonium formate (pH 4). Flow rate of mobile phase is 0.5 ml/min and injection volume of sample is 3 µl. HILIC Kinetex column heated to 25 °C. UPLC system (Thermo) and MS QTrap 5500 (Sciex).*

ID	Q1	Q3	DP	CE	CXP
Glycine	76.0	30.1	60	19	16
Glycine-$^{12}C^{15}N$	79.1	32.1	60	19	16
Alanine	90.2	44.1	60	24	16
Alanine-D_4	94.1	48.2	60	24	16
Serine	106.0	60.0	60	15	16
Proline	116.1	70.1	70	21	16
Valine	118.1	72.0	70	25	16
Threonine	120.0	74.0	60	15	16
Proline-D_7	123.0	77.0	70	21	16
Valine-D_8	126.1	80.1	70	25	16
Hydroxyproline	132.0	68.2	60	30	16
Leucine/Isoleucine/Hydroxyproline	132.0	86.1	50	16	16
Ornithine	133.0	70.1	50	23	16
Asparagine	133.1	74.1	55	25	16
Aspartic acid	134.0	116.0	60	13	16
Leucine-D_3	135.1	89.1	50	16	16
Aspartic acid-D_3	137.0	119.0	60	13	16
Ornithine-D_6	139.0	76.1	50	23	16
Glutamine+Lysine	147.0	84.0	60	25	16
Lysine	147.0	67.0	50	30	16
Glutamic acid	148.1	130.0	60	13	16

Methionine	150.0	133.0	50	13	16
Methionine-D_3	153.0	136.1	51	13	16
Glutamic acid-D_5	153.0	135.0	60	13	16
Histidine	156.1	109.9	46	19	16
Carnitine	162.1	85.0	60	29	10
Phenylalanine	166.0	120.1	50	20	16
Carnitine-D_9	171.0	85.0	60	29	10
Phenylalanine-D_5	171.1	125.2	50	20	16
Arginine	175.1	70.0	55	35	16
Citrulline	176.1	113.0	31	23	16
Citrulline-D_2	178.1	115.0	31	23	16
Arginine-D_7	182.1	77.1	55	35	16
Tyrosine	182.1	136.0	55	21	16
Tyrosine-D_4	186.1	140.1	55	21	16
C2	204.2	84.9	51	27	16
Tryptophan	205.1	146.1	51	23	16
C2-D_3	207.0	85.0	51	27	16
C3	218.1	85.0	51	27	16
C3-D_3	221.1	85.1	51	27	16
C4:1	230.1	85.1	56	29	16
C4	232.1	85.1	56	29	16
C4-D_3	235.0	85.0	56	29	15
C5:1	244.2	85.0	50	29	16
C5	246.1	85.1	66	29	16
C3DC.C4OH	248.2	85.0	50	31	16
C5-D_9	255.2	85.0	66	29	16
C6:1	258.2	85.0	57	33	15
C6	260.1	85.1	51	31	16
C4DC.C5OH	262.2	85.0	60	31	16
C6-D_3	263.0	85.0	51	31	15
C5DC	276.1	85.1	70	35	16
C5DC-D_6	282.0	85.0	70	35	15
C8:1	286.2	85.0	60	31	16
C8	288.2	85.0	72	34	16
C6DC. C7OH	290.2	85.0	60	31	16
C8-D_3	291.0	85.0	72	34	15
C7DC	304.0	85.0	66	39	15
C10:2	312.2	85.0	70	35	16
C10:1	314.2	85.0	70	35	16
C10	316.2	84.9	79	38	16
C10-D_3	319.0	85.0	79	38	15
C12:1	342.3	85.0	70	35	16
C12	344.3	85.1	81	41	16
C12-D_3	347.0	850	81	41	15
C14:2	368.2	85.0	75	41	16
C14:1	370.2	85.0	80	45	16

C14	372.2	85.0	81	47	16
C12DC	374.3	85.0	86	45	15
C14-D_3	375.0	85.0	81	47	15
C14:2-OH	384.3	85.0	81	49	15
C14:1-OH	386.3	85.0	81	50	15
C14-OH	388.3	85.0	80	47	16
C16:2	396.3	85.0	83	51	15
C16:1	398.3	85.0	80	48	16
C16	400.3	85.0	90	47	16
C16-D_3	403.0	85.0	90	47	15
C16:2-OH	412.3	85.0	86	53	15
C16:1-OH	414.3	85.0	100	55	16
C16-OH	416.3	85.0	100	55	16
C18:3	422.3	85.0	98	57	15
C18:2	424.3	85.0	100	55	16
C18:1	426.3	85.0	100	55	16
C18	428.3	85.1	105	51	16
C18-D_3	431.0	85.0	105	51	15
C18:2-OH	440.3	85.0	100	55	16
C18:1-OH	442.3	85.0	100	55	16
C18-OH	444.3	85.0	100	55	16
C20:5	446.3	85.0	120	55	15
C20:4	448.3	85.0	120	55	16
C20:3	450.4	85.0	120	55	15
C20:2	452.4	85.0	102	60	15
C20:1	454.4	85.0	100	55	15
HpODE	456.3	85.0	100	55	15
C20	456.4	85.0	120	55	16
HETE	464.3	85.0	100	55	15
C22:6	472.3	85.0	120	55	16
C22:5	474.4	85.0	106	65	15
C22:4	476.4	85.0	110	55	15
HpETE	480.3	85.0	100	55	15
C16DC	524.0	85.0	100	55	16
C18DC	570.0	85.0	100	55	16

2.1.2. General metabolomic approach

More general metabolomic method detects as many as 254 metabolites (e.g. phosphorylated compounds) including AC and AmA in 40 minutes. The platform utilizes aminopropyl column, 150x2 mm, 3 µm (Phenomenex, USA) heated to 25 °C and the mobile phase acetonitrile (phase A) and alkaline buffer (phase B), i.e. ammonium acetate (20 mM,

pH = 9.45). The buffer was freshly prepared every 2 weeks to prevent pH change and was controlled before analysis. Elution gradient of mobile phase is in **Figure 13** while the flow rate is 0.3 ml/min. One µl of sample was determined in both positive and negative mode with scheduled multiple reaction monitoring mode (MRM transitions are in **Table 2**).

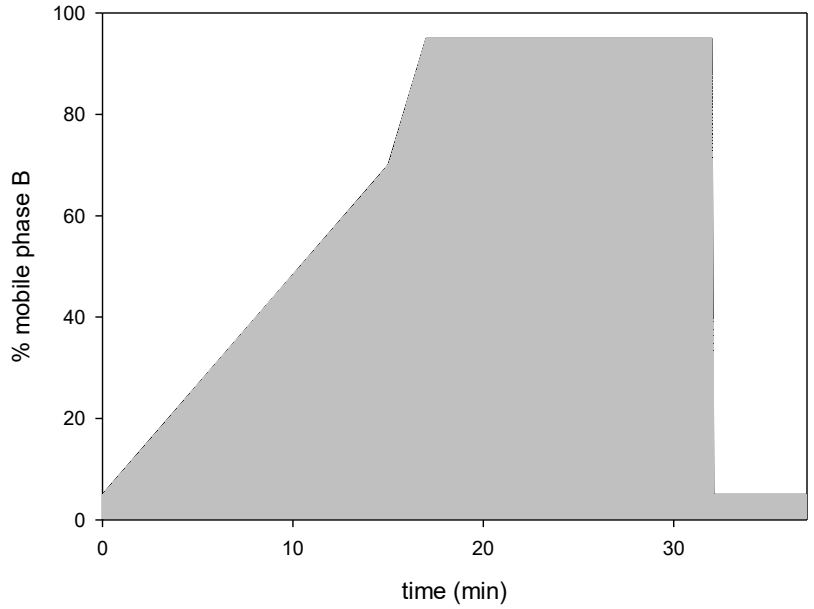

Figure 13. *Elution gradient of mobile phase in general 40 minutes metabolomic method. The mobile phase A is acetonitrile and phase B is ammonium acetate (20 mM, pH = 9.45). The flow rate of mobile phase is 0.3 ml/min and one µl of sample is analysed. Aminopropyl column heated to 25 °C. UPLC system (Thermo) and MS QTrap 5500 (Sciex).*

Table 2. *MRM transitions for metabolites in general 40 minutes metabolomic method in both positive and negative mode. CX is acylcarnitine with X carbons in acylchain, CXDC is dicarboxylcarnitine with X carbons in acylchain. CXOH is hydroxycarnitine with X carbons in acylchain. CX:Y is acylcarnitine with X carbons and Y double bonds in acylchain. The mobile phase A is acetonitrile and phase B is ammonium acetate (20 mM, pH = 9.45). The flow rate of mobile phase is 0.3 ml/min and one µl of sample is analysed. Aminopropyl column heated to 25 °C. UPLC system (Thermo) and MS QTrap 5500 (Sciex).*

ID	Q1	Q3	DP	CE	CXP
Cholesterol	387.1	105.0	146	21	10
N- acetylserotonin	218.9	159.9	101	21	14
Nicotinamide	122.9	79.9	10	27	8
Urea	61.1	44.2	60	25	10
C22:6	472.3	85.0	106	65	15
C20:5	446.3	85.0	102	60	15
C20:4	448.3	85.0	102	60	15
C18:2	424.3	85.1	89	54	15
C18:1	426.4	85.1	89	55	15
C16:1	398.3	85.1	84	51	15
C14:1	370.3	85.1	78	47	15
Creatinine	113.9	86.0	46	15	10
C16	400.3	85.1	84	51	15
C14	372.3	85.1	86	45	15

C18	428.4	85.1	96	63	15
C12	344.3	85.1	73	44	15
C12:1	342.3	85.1	73	44	15
C10	316.2	85.1	56	37	15
C8	288.2	85.1	66	33	15
C8:1	286.2	85.1	63	37	15
C6	260.2	85.1	56	27	15
C16DC	524.0	85.0	103	62	15
C5	246.2	85.1	46	29	15
C4OH	248.1	85.1	55	32	15
Homocystine	268.9	135.9	56	15	12
C6DC	290.2	85.1	63	37	15
C5:1	244.2	85.1	55	31	15
C4	232.2	85.1	46	29	15
C3	218.1	85.1	46	29	15
C5DC	276.2	85.1	61	35	15
C6OH	276.2	85.1	61	35	15
C5OH	262.2	85.1	58	33	15
Serotonin	160.0	115.0	90	25	15
C4DC	262.2	85.1	58	33	15
C2	204.1	85.1	41	27	15
C3DC	248.1	85.1	55	32	15
Leucine /Isoleucine/ Allo-isoleucine/Norleucine	132.0	85.9	46	15	10
Phenylalanine	165.9	119.9	36	19	12
Valine	117.9	72.1	56	17	8
Methionine	149.9	104.0	41	15	10
Taurocholate	516.0	337.1	120	33	15
Creatine/5-aminolevulinate	131.9	89.9	61	19	8
Tryptophan	204.9	145.8	41	25	14
Carnitine	161.9	102.9	56	23	10
Proline	115.9	69.9	31	21	8
Hydroxyproline	132.0	68.2	31	30	8
3-aminoisobutyrate	104.0	86.1	56	11	8
Alanine /Sarcosine	89.9	44.1	51	23	6
Dopamin	137.0	91.0	90	25	15
Tyrosine	181.9	136.0	46	19	12
Homocysteine	135.9	91.0	136	33	10
Threonine/homoserine	119.9	73.9	41	15	8
Glycine	75.9	29.9	41	27	8
Glutamine	146.9	83.9	66	25	10
Asparagine	132.9	74.1	36	21	8
Serine	105.8	60.0	16	15	8
Histidine	155.9	110.0	46	19	10
Choline	104.3	60.0	36	23	8
3-nitrotyrosine	227.1	181.1	60	20	10

Ornithine	132.9	115.6	51	13	12
Lysine	146.9	84.0	66	23	10
5-hydroxytryptophan	220.9	161.9	46	25	16
Glycerol	93.0	57.0	30	12	10
Adrenaline	183.9	100.8	61	23	10
NAD	664.0	136.0	71	69	15
Glutamate	147.8	83.9	41	23	8
Cystine	240.9	151.8	36	19	20
Cysteine	121.9	58.9	120	31	10
Glutathione reduced	307.9	178.9	41	17	16
Noradrenaline	170.0	107.0	61	23	10
Phosphocreatine	211.7	90.1	26	21	10
FAD	786.0	348.0	76	31	15
NADH	666.0	649.0	61	25	15
AMP	348.0	136.0	90	50	10
Glutathione oxidized	613.0	355.0	71	33	15
ADP	428.0	136.0	90	30	10
Acetyl-CoA	809.7	303.0	36	41	15
CoA	768.0	261.0	90	50	13
Propionyl-CoA	824.0	317.3	36	50	13
Butyryl-CoA	838.0	331.3	36	50	13
Malonyl-CoA	854.0	347.0	36	41	15
Succinyl-CoA	868.1	361.1	36	40	15
Acetoacetyl-CoA	852.0	345.0	36	50	13
3-hydroxy-3-methylglutaryl-CoA	910.0	408.0	36	43	15
ATP	508.0	136.0	90	40	10
Acetylcholine	146.1	87.1	40	20	8
Histamine	112.2	95.1	90	20	15
Anandamide	348.3	62.1	90	30	15
Glutamate	148.0	84.0	46	17	16
Asparate	134.0	73.9	45	15	30
cGMP-F1	346.1	152.1	70	27	10
cGMP-F2	346.1	135.1	70	65	8
Palmitoyl-CoA	1006.4	499.4	40	50	13

ID	Q1	Q3	DP	CE	CXP
Palmitic acid	255.1	45.1	-145	-54	-7
Palmitoleic acid	253.2	253.2	-145	-50	-7
Stearic acid	283.3	283.3	-145	-50	-7
Linolenic acid	277.3	277.3	-145	-50	-7
Linoleic acid	279.3	279.3	-145	-50	-7
Cyclic-AMP	328.1	134.0	-80	-36	-9
Cyclic-GMP	344.0	150.0	-80	-36	-9
FA 22:6 (DHA)	327.2	283.2	-140	-15	-15
Arachidonic acid	303.2	259.2	-140	-17	-15

Oleic acid	281.2	263.2	-140	-25	-15
FA 20:5 (EPA)	301.2	257.2	-140	-15	-15
Glucose/Fructose/Galactose/Mannose	178.9	88.9	-40	-12	-9
Glyoxylate	73.0	73.0	-30	-6	-15
Taurine	123.8	79.9	-45	-28	-7
Lactose/Maltose/Melibiose/Sucrose	340.9	161.0	-55	-12	-11
Lactose/Maltose/Melibiose/Sucrose	340.9	179.0	-40	-15	-15
Arginine	173.0	131.1	-55	-22	-17
Citrulline	174.0	131.2	-40	-16	-9
Oxalate	88.9	70.9	-45	-14	-9
Lactate	88.9	43.0	-30	-16	-7
Acetoacetate/2-oxobutanoate/Succinate semialdehyde	100.8	57.0	-30	-12	-7
2-oxoglutarate	144.9	101.0	-30	-10	-7
Isopentenyl diphosphate	245.0	79.0	-30	-34	-15
CDP-choline	487.0	428.0	-80	-18	-15
Glucuronic acid	193.0	113.0	-45	-18	-15
Aspartate	132.0	88.1	-35	-16	-7
4-aminobutyrate	102.0	102.0	-10	-6	-15
Pyruvate	86.9	43.1	-45	-12	-7
CDP-ethanolamine	445.0	79.0	-45	-82	-15
N-argininosuccinate	288.9	132.0	-70	-28	-9
Ethanolamine phosphate	139.8	78.9	-20	-16	-7
Phosphocreatine	209.8	78.8	-70	-16	-3
N-acetylglutamate	187.9	102.0	-45	-24	-9
2-hydroxyglutarate	146.9	128.9	-25	-16	-13
Suberate	172.9	111.0	-35	-20	-9
Glutaconate/Ketoleucine/Mevalonolactone/ 3-methyl-2-oxopentanoate	128.9	85.0	-36	-12	-7
Oxaloacetate/Glutarate/Ethylmalonate	130.8	86.8	-37	-16	-9
Methylsuccinate	131.0	87.0	-35	-15	-10
Succinate/Methylmalonate	116.8	73.0	-35	-14	-9
Sebacic acid	200.9	139.0	-65	-26	-13
Malate	132.9	115.0	-35	-15	-7
Glycerol-3-phosphate	170.9	78.9	-35	-34	-9
Malonate/3-hydroxybutanoate	102.9	59.0	-30	-14	-7
3-hydroxybutyrate	102.9	59.0	-30	-14	-7
Hydroxypyruvate	102.8	59.0	-35	-12	-5
Dihydroxyacetone phosphate	169.0	79.0	-40	-36	-15
Fumarate/Caproic acid	114.9	71.0	-38	-13	-7
Glyceraldehyde-3-phosphate	168.8	97.1	-40	-10	-5
Glucose-1-phosphate/Fructose-6-phosphate/ Galactose-1-phosphate/Glucose-6-phosphate	258.8	78.9	-40	-58	-9
Xylulose 5-phosphate	229.0	97.0	-35	-18	-15
CMP	322.0	79.0	-75	-62	-15
UMP	323.0	79.0	-60	-60	-15
GDP-Fucose	588.0	442.0	-75	-34	-15

Geranyl diphosphate	313.0	79.0	-25	-45	-15
GMP	362.0	79.0	-65	-62	-15
NADP	742.0	619.9	-90	-24	-15
Isocitrate	190.8	110.9	-40	-18	-11
Citrate	191.1	87.0	-40	-18	-11
3-phosphoglycerate/2-phosphoglycerate	184.8	78.9	-20	-50	-7
Aconitate	172.9	84.9	-35	-18	-7
UDP-glucuronic acid	579.0	403.0	-75	-32	-15
Phosphoenolpyruvate	166.8	78.9	-35	-24	-7
UDP	403.0	79.0	-60	-76	-15
Fructose-1,6-bisphosphate	339.1	96.9	-35	-30	-5
CDP	426.0	158.9	-90	-33	-15
GDP	442.0	79.0	-70	-82	-15
NADPH	744.0	407.9	-90	-39	-15
CTP	481.9	158.9	-70	-44	-15
UTP	483.0	79.0	-65	-90	-15
1,3-bisphosphoglycerate	265.0	79.0	-20	-37	-7
GTP	522.0	79.0	-60	-90	-15
Cholate	407.2	343.3	-145	-44	-5
Glycocholate	464.2	73.9	-140	-68	-11
Taurocholate	514.2	80.0	-165	-100	-11
Chenodeoxycholate	391.2	391.2	-140	-44	-8
Glycochenodeoxycholate	448.2	73.9	-105	-50	-10
Taurochenodeoxycholate	498.2	79.9	-195	-110	-5
Ribose	148.8	88.9	-30	-14	-17
3-methylglutaconic aciduria	143.0	55.0	-65	-20	-9
Prostaglandine E2	315.2	271.2	-70	-25	-15
Ribose-5-phosphate/Xylulose-5-phosphate	228.8	96.8	-45	-20	-13
Sedoheptulove-7-phosphate	288.9	97.1	-53	-23	-17
Fructose-6-phosphate	258.9	97.1	-50	-15	-17
Glyceraldehyde-3-phosphate	168.9	79.1	-42	-20	-15
Erythrose-4-phosphate	198.9	79.0	-43	-25	-17
Pantothenate	218.0	88.0	-51	-14	-16
UDP-glucose	564.8	323.1	-54	-26	-15
2-oxoglutarate	145.0	73.8	-45	-19	-7
6-phosphogluconate	275.0	97.0	-41	-20	-24
1,3-bisphosphoglycerate	265.0	167.2	-41	-18	-29

Acylcarnitines and amino acids elute at the beginning of elution gradient and therefore we could shorten the elution gradient to 12 min (**Figure 14**) to determine primarily them. In brief, 5 % of mobile phase B is at the beginning of analysis, then mobile phase B elevates to 70 % and after up to 95 %. Finally the gradient goes back to 5 % of B where it stayes till

12 min. The twelve minutes method enables separation of 31 AC, 24 AmA, and 27 metabolites (glucose, cholesterol etc.) in positive MRM mode.

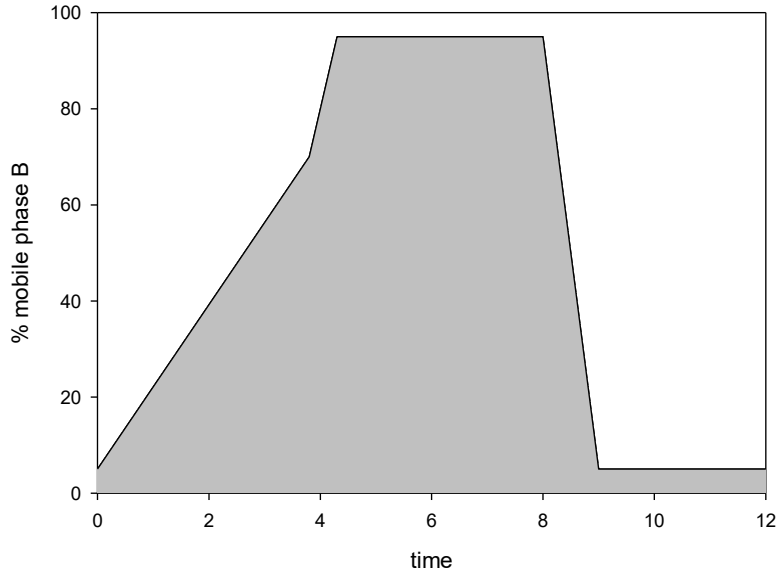

Figure 14. *Elution gradient of mobile phase in 12minutes metabolomics method. The mobile phase A is acetonitrile and phase B is ammonium acetate (20 mM, pH = 9.45). The flow rate of mobile phase is 0.3 ml/min and one µl of sample is analysed. Aminopropyl column heated to 25°C. UPLC system (Thermo) and MS QTrap 5500 (Sciex).*

2.2. LIPIDOMIC LC-MS METHODS

2.2.1. Eicosanoid´s and endocannabinoid´s method

We are able to separate 150 eicosanoids and endocannabinoids in 16 minutes. The method is based on octadecyl Kinetex column, 150x2.1 mm, 1.7 µm (Phenomenex, USA) heated to 50 °C and mobile phase consists of two parts. Mobile phase A is 30/70 (v/v) acetonitrile and 1.3 mM CH_3COONH_4 and part B is a mixture of acetonitrile and isopropanol 50/50 (v/v). Elution gradient of mobile phase is in **Figure 15** and the flow rate is 0.3 ml/min. Analytes were determined in 10 µl of sample in negative MRM mode (MRM transitions are in **Table 3**).

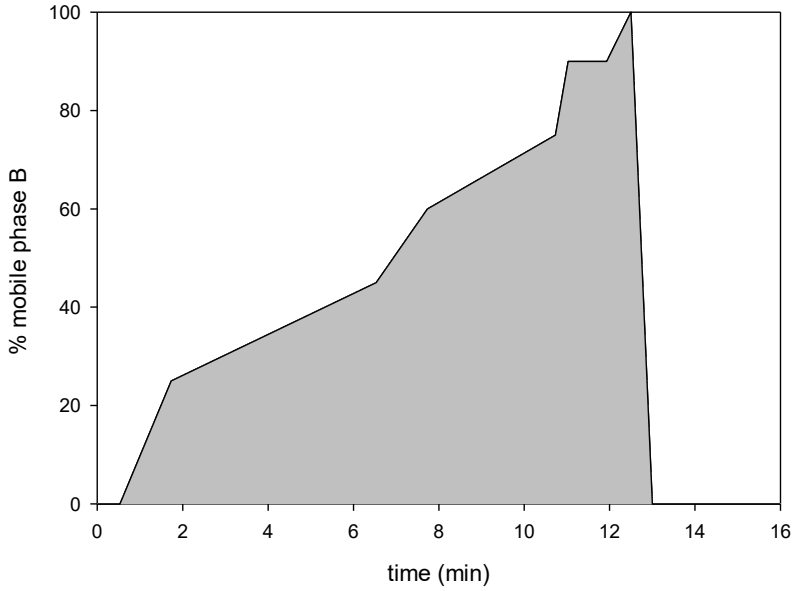

Figure 15. *Elution gradient of mobile phase in eicosanoids and endocannabinoids method. Mobile phase A is 30/70 (v/v) acetonitrile and 1.3 mM CH_3COONH_4 and part B is a mixture of acetonitrile and isopropanol 50/50 (v/v). The flow rate of mobile phase is 0.3 ml/min. Injection volume of sample is 10 µl. C18 Kinetex column heated to 50 °C. UPLC system (Thermo) and MS QTrap 5500 (Sciex).*

Table 3. *Multiple reaction monitoring transitions in eicosanoids and endocannabinoids method. FA is fatty acid. 12-HHT is 12-hydroxy-heptadecatrienoic acid. Y-oxo-ODE is Y-keto-octadecadienoic acid. X-HODE is X-hydroxy-octadecadienoic acid. 15d-PGX is 15-deoxyprostaglandin X (15-hydroxy-oxo-prostatetraenoic acid). PGX is prostaglandin X. X-HEPE is X-hydroxy-eicosapentaenoic acid. X-oxo-ETE is X-oxoicosa-tetraenoic acid. X-HETE is X-hydroxy-eicosatetraenoic acid. X,Y-EET is X,Y-epoxy-eicosatrienoic acid. X-HETrE is X-hydroxy-eicosatrienoic acid. LTX is leukotriene X (dihydroxy-eicosapentanenoic acid). 20-COOH-AA is 20-carboxyarachidonic acid. RvX is Resolvin X. HXY is hepoxilin Y (hydroxyl-epoxy-eicosatrienoic acid). X,Y DHET is X,Y-dihydroxyeicosatrienoic acid. X-HDoHE is X-hydroxy-docosahexaenoic acid. CUDA is 12-[(cyclohexylcarbamoyl)amino]dodecanoic acid. X,Y-EpDPE is X(Y)-epoxy-docosapentaenoic acid. dhk-PGE2 is 15-keto-13,14-dihydroprostaglandin E2. X-OH-LTB4 is X-hydroxy-leukotriene B4. X,Y,Z-TriHETrE isX,Y,Z-Trihydroxy-eicosatrienoic acid. X,Y-DiHDPA is X,Y-dihydroxy-docosapentaenoic acid. Mobile phase A is 30/70 (v/v) acetonitrile and 1.3 mM CH_3COONH_4 and part B is a mixture of acetonitrile and isopropanol 50/50 (v/v). The flow rate of mobile phase is 0.3 ml/min. Injection volume of sample is 10 µl. C18 Kinetex column heated to 50 °C. UPLC system (Thermo) and MS QTrap 5500 (Sciex).*

ID	Q1	Q3	DP	CE	CXP
FA 16:1 (Palmitoleoyl)	253.2	235.2	-140	-25	-15
FA 18:3 (γLinolenoyl)	277.2	233.2	-140	-20	-15
12-HHT	279.0	163.0	-60	-30	-15
FA 18:2 (Linoleoyl)	279.2	261.2	-140	-26	-15
FA 18:1 (Oleoyl)	281.3	263.3	-140	-25	-15
13-oxo-ODE	293.0	113.0	-100	-30	-15
9-oxo-ODE	293.0	185.0	-90	-25	-15
13-HODE	295.2	195.2	-90	-25	-15
9-HODE	295.2	171.1	-90	-25	-15
FA 20:5 (EPA)	301.2	257.2	-80	-15	-15
FA 20:4 (AA)	303.2	259.2	-140	-17	-15
EPA-D_5	306.0	262.0	-100	-15	-15
AA-D_8	311.3	267.0	-110	-20	-15
15d-PGJ3	313.0	269.0	-80	-15	-15
15d-PGJ2	315.2	271.3	-80	-15	-15
18-HEPE	317.0	259.0	-65	-18	-23
15-HEPE	317.0	219.0	-65	-19	-8

11-HEPE	317.0	121.0	-90	-24	-15
12-HEPE	317.0	179.0	-70	-21	-15
8-HEPE	317.0	127.0	-90	-25	-15
9-HEPE	317.0	149.0	-90	-20	-15
5-HEPE	317.0	115.0	-60	-22	-11
15-oxo-ETE	317.0	113.0	-70	-25	-15
12-oxo-ETE	317.0	153.0	-70	-25	-15
5-oxo-ETE	317.0	203.0	-70	-25	-15
9-HETE	319.0	151.0	-80	-20	-15
14,15-EET	319.0	219.0	-80	-15	-15
11,12-EET	319.0	167.0	-90	-20	-15
8,9-EET	319.0	155.0	-90	-20	-15
5,6-EET	319.0	191.0	-60	-20	-15
20-HETE	319.2	289.2	-95	-25	-15
18-HETE	319.2	261.0	-100	-25	-15
17-HETE	319.2	247.0	-100	-25	-15
16-HETE	319.2	189.0	-100	-25	-15
15-HETE	319.2	219.2	-70	-15	-18
11-HETE	319.2	167.2	-80	-20	-15
12-HETE	319.2	179.2	-80	-20	-15
8-HETE	319.2	155.1	-80	-20	-15
5-HETE	319.2	115.1	-80	-20	-22
15d-PGJ2-D_4	319.2	275.3	-110	-20	-15
15-HETrE	321.0	221.0	-90	-21	-15
FA 22:6 (DHA)	327.2	283.2	-140	-15	-15
5-HETE-D_8	327.3	116.1	-80	-20	-15
15-HETE-D_8	327.3	226.0	-80	-20	-15
12-HETE-D_8	327.3	183.0	-80	-20	-15
FA 22:5 (DPA)	329.3	285.3	-80	-15	-15
8, 9 EET-D_{11}	330.0	155.0	-90	-20	-15
PGJ3	331.2	269.0	-50	-20	-15
δ12-PGJ3	331.2	269.0	-100	-20	-15
DHA-D_5	332.0	234.0	-110	-20	-15
LTB5	333.0	195.0	-90	-25	-15
5,15-diHEPE	333.0	115.0	-110	-22	-17
20-COOH-AA	333.1	289.1	-125	-22	-15
PGB2	333.2	271.2	-60	-20	-15
δ12-PGJ2	333.2	271.0	-110	-15	-15
PGA2	333.2	235.3	-50	-20	-15
PGJ2	333.2	233.1	-50	-20	-15
15d-PGD2	333.2	271.2	-50	-20	-15
RvE3	333.3	201.1	-40	-22	-17
RvE2	333.3	253.2	-40	-22	-17
8,15-diHETE	335.0	127.0	-80	-25	-15
HXB3	335.0	183.0	-70	-20	-15
5,6-diHETE	335.0	163.0	-90	-25	-15

5,15-diHETE	335.2	115.2	-110	-22	-17
LTB4	335.2	195.1	-120	-22	-17
HXA3	335.2	171.1	-110	-20	-15
17,18-diHETE	335.3	247.2	-90	-25	-15
14,15-diHETE	335.3	207.2	-90	-25	-15
14,15-DHET	337.0	207.0	-90	-25	-15
11,12-DHET	337.0	167.0	-90	-25	-15
8,9-DHET	337.0	127.0	-90	-30	-15
5,6-DHET	337.0	145.0	-95	-25	-15
CUDA	339.2	214.1	-100	-20	-15
2,3-dinor-6-keto-PGF1α	341.0	135.0	-90	-30	-15
17-oxo-DHA	341.5	111.0	-90	-20	-15
20-HDoHE	343.0	241.0	-90	-20	-15
16-HDoHE	343.0	233.0	-105	-19	-15
17-HDoHE	343.0	245.0	-80	-20	-18
13-HDoHE	343.0	221.0	-90	-17	-15
14-HDoHE	343.0	205.0	-70	-21	-15
10-HDoHE	343.0	181.0	-80	-17	-15
11-HDoHE	343.0	149.0	-90	-19	-15
8-HDoHE	343.0	109.0	-100	-20	-15
7-HDoHE	343.0	141.0	-40	-18	-13
4-HDoHE	343.0	101.0	-40	-18	-13
19,20-EpDPE	343.5	281.2	-80	-20	-15
16,17-EpDPE	343.5	273.5	-80	-15	-15
8,9-DHET-D_{11}	348.0	127.0	-120	-30	-15
PGE3 +D3	349.2	269.0	-75	-25	-15
PGD3	349.2	189.0	-75	-25	-15
RvE1	349.2	195.1	-80	-24	-16
LXA5	349.0	115.0	-90	-25	-15
PGF3α	351.0	193.0	-105	-30	-15
dhk-PGE2	351.0	235.0	-70	-25	-15
dhk-PGD2	351.0	207.0	-70	-25	-15
LXB4	351.2	221.1	-90	-30	-21
LXA4	351.2	235.1	-95	-22	-11
PGE2+D2	351.2	271.2	-70	-25	-15
PGD2	351.2	189.0	-70	-25	-15
20-OH-LTB4	351.3	195.2	-90	-25	-15
dhk-PGF2α	353.0	291.0	-90	-25	-15
PGF2α	353.2	193.2	-80	-30	-15
8-iso-PGF2α	353.2	309.3	-80	-30	-15
PGE1	353.3	317.2	-80	-25	-15
PGD1	353.3	273.0	-80	-25	-15
11,12,15-TriHETrE	353.3	167.1	-100	-30	-15
PGF1α	355.0	293.0	-95	-30	-15
PGD2-D_4	355.2	275.2	-70	-25	-15
8-iso-PGF2α-D_4	357.0	197.0	-80	-30	-15

10,17-DiHDPA	359.0	153.0	-70	-20	-15
Maresin1	359.2	250.1	-40	-22	-17
19,20-DiHDPA	361.0	229.0	-90	-25	-15
PGF2α-D_9	362.0	193.0	-80	-30	-15
20-COOH-LTB4	365.3	347.2	-90	-25	-15
11-dh-TXB2	367.1	305.1	-70	-25	-15
TXB3	367.2	169.1	-70	-25	-15
11-dh-TXB3	367.2	169.1	-70	-25	-15
TXB2	369.2	169.1	-75	-25	-15
6-keto-PGF1α	369.3	163.2	-85	-35	-15
TxB1	371.0	171.0	-70	-25	-15
6k-PGF1α-D_4	373.3	167.1	-85	-35	-15
RvD2	375.2	141.2	-90	-24	-13
RvD1	375.2	215.2	-90	-22	-13
RvD2-D_5	380.0	175.0	-80	-40	-15
LTE4	438.2	333.2	-120	-30	-15
LTD4	495.0	177.0	-90	-25	-15
LTC4	624.3	272.1	-120	-30	-15

2.2.2. FAHFA analysis

Branched fatty acid hydroxy fatty acids (FAHFA) are determined on octadecyl stationary phase, 150x2.1 mm, 1.7 μm (Phenomenex, USA) warmed up to 50 °C. The mobile phase is 30/70 (v/v) acetonitrile and water with 0.01% acetic acid, pH 4 (part A) and 50/50 (v/v) acetonitrile and isopropanol (part B). Serum samples were analysed by gradient elution in 25 minutes (**Figure 16**) and structural analysis was done by isocratic elution with 20 % of mobile phase A in 60 minutes. Flow rate of mobile phase is 0.2 ml/min and injection volume of sample is 10 μl. DHAHLA compound was measured in negative multiple reaction mode, specifically 605.4>327.2, and the optimal collision energy was chosen as -35 V while declustering potential was -130 V. MRM transitions for FAHFA compouds are in **Table 4**.

Table 4. *MRM transitions for FAHFA compounds. Q1, precursor ion; Q3, product ion; FA, quantifier ion; HFA and HFA-H2O, qualifier ions. PAHSA is palmitic acid hydroxystearic acid, DHAHLA is docosahexaenoic acid hydroxylinoleic acid and DHAHDHA is docosahexaenoic acid hydroxydocosahexaenoic acid. Adapted from [99].*

ID	Q1 $[M-H]^-$	Q3 FA	Q3 HFA	Q3 HFA-H_2O
PAHSA	537.5	255.2	299.3	281.3
DHAHLA	605.4	327.2	295.2	277.2
DHAHDHA	653.4	327.2	343.2	325.2

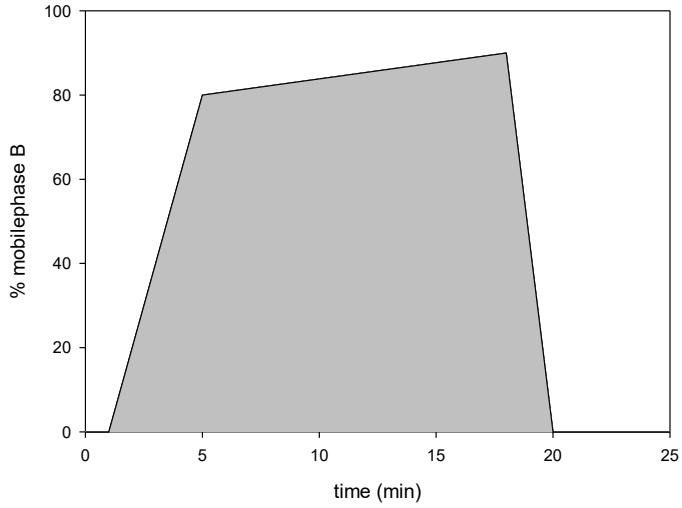

Figure 16. *Elution gradient of mobile phase in FAHFA analysis. Mobile phase A is 30/70 (v/v) acetonitrile and water with 0.01% acetic acid (pH 4) and mobile phase B is 50/50 (v/v) acetonitrile and isopropanol. Flow rate of mobile phase is 0.2 ml/min. Column C18 heated to 50 °C. Injection volume of sample is 10 µl. UPLC system (Thermo) and MS QTrap 5500 (Sciex).*

2.3. OTHER METHODS

2.3.1. Measurement of glycerol and non-esterified FAs

Media after co-incubation of adipocytes and macrophages were stored in -20 °C until time of analysis. Then free glycerol and non-esterified FAs were measured in media by spectrophotometric method using kits, specifically NEFA-HR(2), ACS-ACOD Method (Wako Chemicals USA Inc., USA) and Glycerol GLY (Randox, UK).

2.3.2. DNA measurement

DNA was measured in all parts of white adipose tissue (WAT) and WAT itself using Hoechst fluorescence stain. Hoechst increases in fluorescence in the presence of DNA, binding specifically and quantitatively [161]. The process in brief, TRIS, EDTA (both pH 7.4), water, 10% SDS and proteinase K solution were added to samples and heated to 56 °C for a night. Then we added buffer NaCl-Na_2HPO_4-EDTA (pH 7.4) and Hoechst (H33258) to samples and swayed them for 4 hours. Finally, we measured the fluorescence of sample by fluorescence spectrophotometer (Perkin-Elmer LS50B) with excitation at 356 nm

and emission at 458 nm. Of note, concentration of DNA was calculated using calibration curve prepared with DNA standard (Sigma-Aldrich, Czech Republic).

2.3.3. ELISA and quantitative polymerase chain reaction (qPCR)

The concentration of IL-6 was determined using IL-6 ELISA kit (Cayman Chemicals). The mRNA levels of cytokines IL-6, TNF-α, IL-1β and PTGS2 were determined by qPCR-based gene expression analyses that were performed according to standard protocols while the levels of transcripts were evaluated in total RNA isolated from cells.

2.4. PREPARATION OF SAMPLE

2.4.1. Samples for metabolomic methods

2.4.1.1. Acylcarnitine´s and amino acid´s 10minutes method

One µl of plasma sample was combined with extraction solution (i.e. methanol and 0.1% formic acid) and mixture of internal standards (MassChrome Amino Acids and Acylcarnitines kit, Chromsystems, Gräfelfing, Germany). Mass chrome kit includes labelled AC and AmA and represents an expanded screening panel of inborn metabolic disorders based on tandem mass spectrometry [68]. Afterwards, the sample was homogenized in an ultrasonic bath (Ultrasonic-cleaner US-10, Lab. Companion, USA) for 60 s burst, centrifuged (5 min, 15 000 g, 4 °C) and the supernatant was used for LC-MS measurement.

2.4.1.2. General metabolomic method

White adipose tissue was homogenized using a bead mill MM400 (Retsch, Germany) and extracted with 75% acetonitrile in which the internal standards (MassChrome Amino Acids and Acylcarnitines kit, Chromsystems, Gräfelfing, Germany) were dissolved. Serum and plasma samples were extracted in the same way apart from homogenization. The medium from co-culture experiment was replaced by 30% acetonitrile after the attempt. Macrophages that covered the well plates were frozen in liquid nitrogen and stored in -80 °C until analyses

when frozen cells with extraction solution were scraped off the wells and transferred to 1.5 ml tubes. After that, extracts of WAT, serum, plasma or cell samples were homogenized in ultrasonic bath (Ultrasonic-cleaner US-10, Lab. Companion, USA) for 60 s burst and centrifuged for 5 min (15 000 g, 4 °C). Finally, the supernatant was used for liquid chromatography-mass spectrometry analyses.

2.4.2. Samples for lipidomic methods

2.4.2.1. Liquid/liquid extraction

Bligh&Dyer and Folch methods are two well established liquid/liquid extraction approaches. Both utilize solution of chloroform, methanol and water and they were performed according to standard protocols [117,118] in our research.

2.4.2.2. Eicosanoid´s and endocannabinoid´s method

Solid phase extraction procedure was utilized to extract eicosanoids and endocannabinoids from WAT or cell samples. First in macrophages, the medium was replaced by 50% methanol after the co-culture experiment and macrophages grown on wells were frozen in liquid nitrogen and stored in -80 °C until analyses. Then frozen cells with extraction solution were scraped off the wells and transferred to 1.5 ml tubes. Subsequently, internal standards (their list is in **Table 5**), cold water and methanol were added to samples while final concentration is 15% methanol. Also, we added 46 µl hydrochloric acid to acidify 2.5 ml sample. SPE was carried out with Strata-X columns (60 mg, 3 ml, Phenomenex) that were washed by ethylacetate and conditioned with methanol and water. The samples were intercepted on columns and washed by water and hexane and elution of sample was achieved by adding methylformate and methanol. Finally, samples were evaporated in Speedvac and residues were dissolved in 30% acetonitrile and analysed by LC-MS. Second, WAT with methanol were homogenized in bead mill MM400 (Retsch, Germany) and centrifuged for 5 min (15 000 g, 4 °C). Then internal standards were added to samples and extraction procedure continued as described before. Adipocytes and SVF isolated from WAT were extracted same apart from homogenization as well as CD11b positive and CD11b negative

cells that were separated from SVF. Of note, it is crucial to keep all samples at ice to avoid the degradation of samples during extraction procedure.

Table 5. *List of internal standards (IS). Analyte-Dx is deuterated analyte with x-times deuterium. EPA is eicosapentaenoic acid. AA is arachidonic acid. DHA is docosahexaenoic acid. PGX is prostaglandin X . 15d-PGX is 15-deoxyprostaglandin X (15-hydroxy-oxo-prostatetraenoic acid). 8-iso-PGX is 8-iso-prostaglandin X. 6k-PGX is 6-ketoprostaglandin X. X-HETE is X-hydroxy-eicosatetraenoic acid. X,Y-EET is X,Y-epoxy-eicosatrienoic acid. X,Y DHET is X,Y-dihydroxyeicosatrienoic acid. RvX is Resolvin X.*

IS
EPA-D_5
AA-D_8
15d-PGJ2-D_4
5-HETE-D_8
15-HETE-D_8
12-HETE-D_8
8,9-EET-D_{11}
DHA-D_5
8,9-DHET-D_{11}
PGD2-D_4
8-iso-PGF2α-D_4
PGF2α-D_9
6k-PGF1α-D_4
RvD2-D_5

2.4.2.3. FAHFA analysis

DHAHLA´s extraction was based on Yore et al. [111]. Serum samples were extracted by liquid/liquid and solid phase extraction. First LLE, dichlormethane and methanol as organic phase and chilled citric acid buffer with pH 3.6 as water phase were added to sample (the final ratio is 2:1:1). The acidic pH in buffer suppresses the ionization of carboxylic group in DHAHLA and also lipids go willingly to organic phase. After, the organic phase was dried in Speed-vac (Savant SPD121P; ThermoFisher Scientific) and dissolved in dichloromethane. This sample underwent SPE that was performed on column Strata SI-I Silica columns (55 µm, 70 A, Sigma). The columns were conditioned by hexane, sample was applied on them and elution of DHAHLA was achieved by ethyl acetate. Finally, samples were evaporated, dissolved in methanol and analysed by liquid chromatography and mass spectrometry. Cells

were homogenized using a bead mill MM400 (Retsch, Germany) at first and then extraction procedure continued as described above. Importantly, LC-MS analyses have to be done immediately to avoid the decay of the DHAHLA compound because ester bond between DHA and HLA is very sensitive to hydrolysis.

Extraction of milk samples is slightly different than extraction of serum samples. First, milk samples (300 µl) were warmed to 25 °C in water bath and homogenized for 10 s in ultrasonic bath to disrupt fat globule membranes and ensure the consistent quality of sample. Later on, LLE with dichlormethane, methanol and citric acid buffer was performed as described before. The organic phase was collected, water phase was re-extracted and then organic phase was pooled, dried in a Speed-vac and dissolved in dichloromethane. Unfortunately, pulsed sonication as well as citric acid buffer in LLE lead to the formation of foamy cakes full of casein micelles that are very abundant in colostrum/transient milk samples and it complicated the collection of organic phase during extraction. After that solid phase extraction was performed on Hypersep column (500 mg/10 mL, 40–60 µm, 70 Å, Thermo) that provides cleaner samples even though it is related to lower DHAHLA yield. The analyte of interest was eluted from SPE columns with ethyl acetate as previously and it was concentrated using Speed-vac, dissolved in methanol and immediately analysed by LC-MS.

2.5. SAMPLES

2.5.1. Animals

Both mice strains, i.e. mice of the AJ and the C57BL/6J genetic background, fed standard maintenance diet (STD; Ssniff R/M-H diet, Ssniff Spezialdieten GmbH, Soest, Germany), containing 13.0 kJ/g as proteins (33%), carbohydrates (58%), and lipids (9%) or corn oil-based high-fat diet (HFD; lipids ~35% wt/wt) or diet with omega-3 PUFA concentrate (46% wt/wt DHA, 14% wt/wt EPA; product EPAX 1050 TG; EPAX, Alesund, Norway) replacing 15% wt/wt of dietary lipids (HFF diet).

Rats fed standard chow diet (control) (3300 kcal kg^{-1} ; Panlab, Barcelona, Spain) or cafeteria (high caloric) diet. The cafeteria diet includes: biscuits with a Majorcan sausage ('sobrasada') and with liver pate, salted peanuts, chocolate, candies, carrots, fresh bacon, cheese, sugared milk (20% w/v) and a Majorcan pastry ('ensaimada').

2.5.2. Cells

RAW 264.7 and bone marrow-derived macrophages were grown according to standard protocols as well as 3T3L1 murine cell model of adipocytes and human adipocytes (hMADs). Adipocytes and SVF were liberated from white adipose tissue of mice by collagenase solution according to published method [104] using Krebs Ringer bicarbonate medium with 5mM glucose and 4% BSA (fraction V, FA free, Sigma Aldrich). Specifically, collagenase-digested samples were passed through a sterile 250 μm nylon mesh and the suspension was centrifuged at 4 g for 5 min. The pellet was collected as SVF and the top buoyant layer was washed twice and collected as floating adipocytes.

Moreover, we utilized immunoprecipitation method using CD11b antibody bonded to a magnet to separate adipose tissue macrophages (ATM) from SVF. CD11b (Mac-1, αMβ2) is expressed on bone marrow-derived immune cells and is responsible for facilitating cell adhesion and transmigration across the endothelium or epithelium. Also, it traffics to the inflammation sites to mediate the inflammatory response [162]. Separation of ATM in practice, anti-CD11b antibody was coupled to magnetic beads, added to SVF and then CD11b positive cells were bonded to magnetic beads. Using a magnet, we were able to separate both CD11b positive (i.e. macrophages, monocytes) and negative (i.e. lymphocytes, endothelial and vascular cells) cells and analyse them separately.

2.6. CHEMICALS

All chemicals were purchased from Sigma-Aldrich (Prague, Czech Republic). Standard 5-PAHSA was purchased from Cayman Pharma (Neratovice, Czech Republic). The standard of 13-DHAHLA was synthetized in the Institute of Organic Chemistry and Biochemistry of the Czech Academy of Sciences and the organic synthesis was performed according to Steglich esterification [163]. Importantly, we store DHAHLA standard in brown glass tube with argon atmosphere to avoid chemical oxidation of the compound.

3. RESULTS

3.1. ANALYSES OF ACYLCARNITINES AND AMINO ACIDS

3.1.1. Introduction

We utilized mainly very sensitive approach UPLC-MS/MS to describe white adipose tissue (WAT) metabolism. At first, we wanted to find and optimize methods for analysis of acylcarnitines (AC) and amino acids (AmA). Acylcarnitines are intermediates of fatty acid and amino acid oxidation and they are important diagnostic markers [63]. Specifically, odd-numbered AC are newly discovered as potential markers of the metabolic syndrome and they influence development of insulin resistance [62] and impaired glucose tolerance in diabetes [63]. Therefore, our second goal was to reveal possible early biomarker of obesity-associated insulin resistance due to altered levels of AC and AmA in mice or rat´s plasma.

3.1.2. Analytical highlights

Acylcarnitine´s and amino acid´s 10minutes method. We have developed method based on hydrophilic interaction chromatography and high efficiency Kinetex chromatographic column. Mobile phase consists of water, acetonitrile and ammonium formate with acidic pH. AmA and AC are determined in positive MRM mode in less than 10 minutes while the method is able to separate 57 AC and 21 AmA.

Validation of acylcarnitine´s and amino acid´s 10minutes method. We used mice strains C57BL/6J and A/J for validation of 10minutes method while it included precision and accuracy. In practice, samples of mice plasma were divided into triplicates and analysed separately in three days to assess the inter-assay validation, and as a triplicate within one run to assess the intra-assay validation. The validation analyses were performed same as normal analysis.

Preparation of sample for acylcarnitine´s and amino acid´s 10minutes method. One µl of plasma sample was combined with methanol and 0.1% formic acid and mixture of

internal standards. Afterwards the sample was homogenized in an ultrasonic bath, centrifuged and the supernatant was used for LC-MS measurement.

General metabolomic LC-MS method. The platform is based on aminopropyl column and mobile phase that consists of acetonitrile and alkaline ammonium acetate. The method analyses 254 metabolites including phosphorylated compounds as well as acylcarnitines and amino acids in 40 minutes. Shortened method for determination primarily AmA and AC takes only 12 min and enables to separate 31 AC, 24 AmA, and 27 metabolites (glucose, cholesterol etc.). All metabolites are measured in positive MRM mode.

Preparation of sample for general metabolomic LC-MS method. Plasma samples were extracted with 75% acetonitrile with internal standards while then they were homogenized in an ultrasonic bath and centrifuged for 5 min. Finally, the supernatant was used for liquid chromatography-mass spectrometry analysis.

Internal standards. We added mixture of deuterated labelled AC and AmA as internal standards (IS) to samples during extraction process to provide quantitative analysis. For analytes without corresponding IS, analyte-IS pairs were selected due to the most similar chemical structure and according to the closest retention times.

3.1.3. Results

3.1.3.1. Metabolomic methods

In general

The quantification of acylcarnitines is challenging because they have various species, e.g. positional isomers or isobaric compounds, and they also occur in low concentration [63]. Positional isomers have the same functional groups at different substituent positions [164] and therefore they have similar mass transition [63], for example hydroxybutyrylcarnitine C4OH can have hydroxyl group bonded on different carbons. On the other hand isobaric substances

are compounds of the same nominal mass but of different elemental composition [165]. Isobaric species are for example C4OH and C3DC or C5OH and C4DC. Structure of C4OH and C3DC is in **Figure 17**. Separation of these isobaric species is important because they describe different setting of metabolism as they come from various metabolic pathways. Acylcarnitines are usually analysed by direct infusion ESI-MS/MS which is very fast and cheap but it cannot separate isobaric species. Also, all acylcarnitines have a similar product ion (*m/z* 85) and thus it is difficult to separate them only by their mass using direct infusion mass spectrometry. For that reason, chromatographic separation before MS measurement can improve the analysis. Furthermore, several enhancements can be done, for example scheduled MRM mode provides shorter analysis time and more scan cycles per peak and ammonium acetate in mobile phase increases the ionization efficiency of the analysis of AC [63] etc.

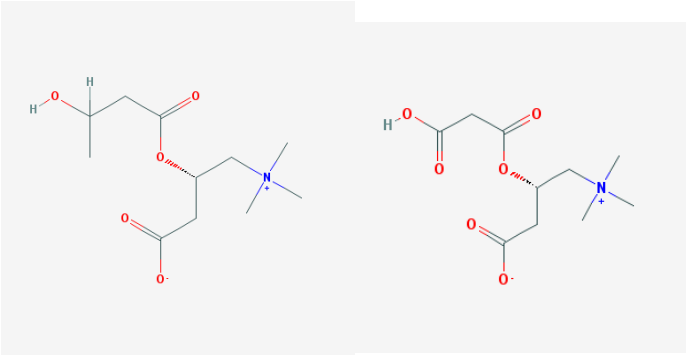

Figure 17. *Hydroxybutyrylcarnitine C4OH and malonylcarnitine C3DC. Adapted from [166,167]*

We added mixture of deuterated labelled AC and AmA to samples as internal standards (IS) to provide quantitative analysis. Analyte-internal standard pairs are in **Table 6**. For analytes without corresponding IS, analyte-IS pairs were selected due to the most similar chemical structure and according to the closest retention time. Coelution of IS and corresponding analyte confirmed the analytes in sample. Importantly, we obtained the analyte´s concentration by comparing the analyte´s and IS´s peak area according to [63].

Table 6. *Analyte-internal standard pairs utilized for quantitative analysis. CX is acylcarnitine with X carbons in acylchain, CXDC is dicarboxylcarnitine with X carbons in acylchain. CXOH is hydroxycarnitine with X carbons in acylchain. CX:Y is acylcarnitine with X carbons and Y double bonds in acylchain. CX:Y-OH is acylcarnitine with X carbons and Y double bonds in hydroxyacylchain. Analyte-Dx is deuterated analyte with x-times deuterium. Glycine-$^{12}C^{15}N$ is isotopic analogue of glycine.*

Analyte	**IS**	**Analyte**	**IS**
Carnitine	Carnitine-D_9	Glycine	Glycine-$^{12}C^{15}N$
C2	C2-D_3	Alanine	Alanine-D_4
C3	C3-D_3	Serine	Alanine-D_4
C4:1	C4-D_3	Proline	Proline-D_7
C4	C4-D_3	Valine	Valine-D_8
C5:1	C5-D_9	Threonine	Alanine-D_4
C5	C5-D_9	Hydroxyproline	Proline-D_7
C3DC,C4OH	C4-D_3	Leucine+Isoleucine+ +hydroxyProline	Leucine-D_3
C6	C6-D_3	Ornithine	Ornithine-D_6
C4DC,C5OH	C5-D_9	Asparagine	Arginine-D_7
C5DC	C5DC-D_6	Aspartic acid	Aspartic acid-D_3
C8:1	C8-D_3	Glutamine+Lysine	Arginine-D_7
C8	C8-D_3	Lysine	Arginine-D_7
C6DC, C7OH	C8-D_3	Glutamic acid	Glutamic acid-D_5
C10:2	C10-D_3	Methionine	Methionine-D_3
C12:1	C12-D_3	Histidine	Arginine-D_7
C12	C12-D_3	Phenylalanine	Phenylalanine-D_5
C14:2	C14-D_3	Arginine	Arginine-D_7
C14:1	C14-D_3	Citrulline	Citrulline-D_2
C14OH	C14-D_3	Tyrosine	Tyrosine-D_4
C14	C14-D_3	Tryptophane	Tyrosine-D_4
C16	C16-D_3		
C16-1OH	C16-D_3		
C16OH	C16-D_3		
C18:2	C18-D_3		
C18:1	C18-D_3		
C18	C18-D_3		
C18:2-OH	C18-D_3		
C18:1-OH	C18-D_3		
C18OH	C18-D_3		
C14DC	C18-D_3		
C16DC	C18-D_3		
C18DC	C18-D_3		
C20	C18-D_3		
C20:4	C18-D_3		
C22	C18-D_3		
C24	C18-D_3		
C26	C18-D_3		
C22:6	C18-D_3		

Acylcarnitine´s and amino acid´s 10minutes method

First method for analysis of acylcarnitines and amino acids was based on HILIC column and was able to separate 57 AC and 21 AmA in less than 10 minutes (for details see Analytical highlights or Methods). Validation study of that method comprised two mice strains because we processed both strains in our animal experiments. Validation was performed as follows according to [155]. In practice, samples of mice plasma were divided into triplicates and analysed separately in three days to assess the inter-assay validation, and as a triplicate within one run to assess the intra-assay validation. The validation analysis and sample preparation were performed same as common measurement. Of note, we excluded several analytes from validation study because evaluation of their peak areas was complicated due to asymmetrical and/or broad peaks. Specifically, we eliminated acylcarnitines C5DC, C12:1, C4:1, C5:1, C10:2, C8:1, C14:2-OH, C14:1-OH, C16:2-OH, C18:2-OH, C22:4 and amino acid glycine. As a result, overall average inter-assay precision obtained from measurement in different days was 9.43 % for acylcarnitines and 10.79 % for amino acids for both mice strains. Simultaneously, intra assay precision acquired from analyses of replicates was 8.65 % for AC and 5.55 % for AmA. All validation data are summarized in **Table 7**. Validation of standards can reveal potential changes in sample preparation. Nevertheless, analyses of sample replicates showed small alteration in AC´s and AmA´s concentrations and therefore it was not deemed necessary to analyse standards which is also in line with procedure in [155]. To sum up the validation study, 10minutes method was validated with good precision and accuracy up to 11 %.

Table 7. *Validation data for 10minutes method. Mobile phase A consists of 90/10 (v/v) acetonitrile and buffer, and phase B of 90/10 (v/v) water and buffer. The buffer is 20 mM ammonium formate (pH 4). Flow rate of mobile phase is 0.5 ml/min and injection volume of sample is 3 µl. HILIC Kinetex column heated to 25°C. UPLC system (Thermo) and MS QTrap 5500 (Sciex).*

	RSD of acylcarnitines (%)			**RSD of aminoacids (%)**		
	Bl/6 strain	AJ strain	Overall	Bl/6 strain	AJ strain	Overall
inter assay validation (different days)	10.69	8.16	9.43	11.42	10.15	10.79
intra assay validation (in triplicates)	9.64	7.66	8.65	5.71	5.39	5.55

Several rules were applied for qualitative analysis. For example it is known that retention time is shorter for AC with longer chain [71] and we saw this phenomenon in our

experiment as well (**Figure 18**). Moreover, we focused on separation of isobaric species that is challenging (for details see above). Chromatogram of isobaric species C4OH and C3DC is in **Figure 19**. It was complicated that both isobaric species weren´t visible in every sample and thus we had to find exact retention time for all that species to interpret the results correctly. In practice, chromatogram with both isobaric species gave us the retention times of that analytes and then we could easily find correct isobaric species in other chromatograms.

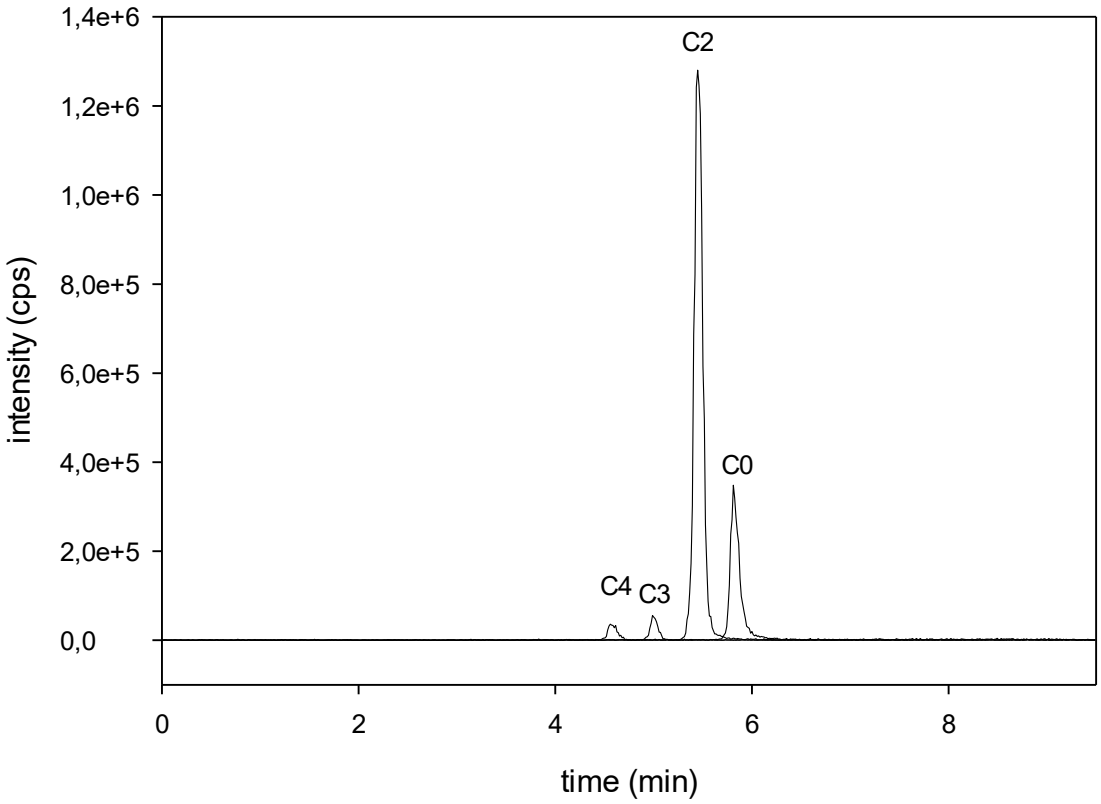

***Figure 18**.Chromatogram of carnitine (C0) and acylcarnitines (C1-C4) measured by 10minutes method. Mobile phase A consists of 90/10 (v/v) acetonitrile and buffer, and phase B of 90/10 (v/v) water and buffer. The buffer is 20 mM ammonium formate (pH 4). Flow rate of mobile phase is 0.5 ml/min and injection volume of sample is 3 µl. HILIC Kinetex column heated to 25°C. UPLC system (Thermo) and MS QTrap 5500 (Sciex).*

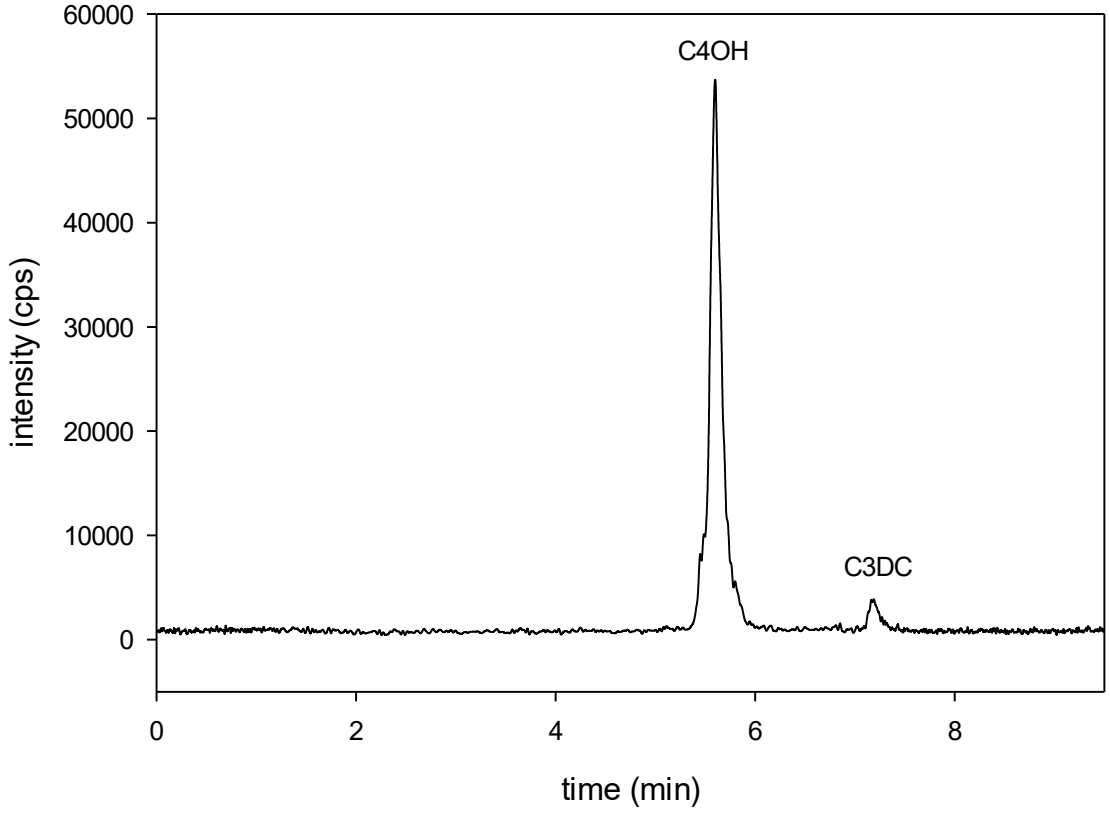

Figure 19. *Chromatogram of isobaric C4OH and C3DC measured by 10minutes method Mobile phase A consists of 90/10 (v/v) acetonitrile and buffer, and phase B of 90/10 (v/v) water and buffer. The buffer is 20 mM ammonium formate (pH 4). Flow rate of mobile phase is 0.5 ml/min and injection volume of sample is 3 µl. HILIC Kinetex column heated to 25°C. UPLC system (Thermo) and MS QTrap 5500 (Sciex).*

General metabolomic method

Afterwards, we improved the analyses due to our new UPLC-MS/MS metabolomic method. It is more general method separating AC, AmA and many other metabolites (up to 254 compounds). The 10minutes method, previously used for measurement of AC and AmA, was fast and sensitive. Our new more general metabolomic approach with aminopropyl column (for details see Analytical highlights or Methods) was fast as well and it achieved better resolution than the previously used method for some AC and AmA. Also, certain peaks of acylcarnitines and amino acids were more symmetrical using this platform and it simplified peak integration process and saved peak review time.

3.1.3.2. Biological application

In general

We wanted to find potential candidates of AC and AmA which might be indicative of higher propensity for a dysmetabolic state or predict the predisposition to obesity in two rodent experiments. It may help early diagnosis and implementation of prevention strategies. For details of experiment´s methodologies see [68,168].

Prediction an obesity in different mice genders

First experiment strives to reveal which levels of AC and AmA predict the mice obesity, also with respect to different mice genders. The attempt was carried out on both genders of C57BL/6J mice that were fed high fat (HFD) or control diet. Plasma samples collected before and after weight gain were analysed by our validated AC´s and AmA´s 10minutes method (for details see [68]).

Gender-specific differences in response to high fat diet were observed in several levels of acylcarnitines and amino acids. For example plasma acylcarnitines´s levels of female mice were higher in case of C5, C14:2, C16:1-OH and lower in case of C18:1, C18:1-OH, C20:4 in comparison to male´s samples. Regarding amino acids, ornithine was increased in female mice while lysine was increased in HFD males. Importantly, long chain acylcarnitines and carnitine were the most discriminating factor in the pre-obese state of male mice. They represent complex early biomarker of obesity in male C57BL/6J mice together with even short AC species (C4, C6), branch-chained amino acid derived C4DC and amino acids tyrosine, alanine, ornithine and threonine. The situation was more complicated in the case of female mice. It seems that AC and amino acids do not represent the main process underlying the development of obesity and insulin resistance in female mice. Thus we could not determinate the biomarker of obesity in this gender.

Prediction an obesity in different rat´s models and feeding conditions

The second experiment was based on two rat´s models with different metabolic programming outcomes and different feeding conditions. Specifically, attempt was carried out on offspring of dams fed a cafeteria diet during lactation (O-CAF, with a thin-outside-fat inside phenotype, model 1) and the offspring of diet-induced obese dams submitted to a dietary normalization before gestation (O-PCaf, non-altered phenotype, model 2). Plasma samples collected in fasting or *ad libitum* feeding state in all animal groups were measured by our general metabolomic methodology (for details see [168]).

Regarding model 1, PLS-DA score plot showed clear separated groups according to both, feeding/fasting conditions and to maternal diet during lactation (control or cafeteria diet). The variables with the highest contribution were the long-chain AC species C18, C18:1, C18:2, C16:1 and C16DC, and the amino acids glycine, alanine, isoleucine, serine and proline. These analytes predict the later dysmetabolic phenotype observed in the offspring and indicate a poor nutrition during lactation due to maternal unbalanced diet intake.

O-PCaf and control animals presented a similar profile of circulating AC as well as AmA in model 2. On the other hand short-chain AC levels decreased and medium- and long-chain AC levels increased upon fasting. Thus, PLS-DA score showed significantly separated groups according to fed and fasting conditions but did not separate O-PCaf and control groups.

3.1.4. Conclusion

We established two UPLC-MS/MS methodologies for analyses of acylcarnitines and amino acids. Also, we aimed to find possible AC´s or AmA´s biomarkers of propensity to obesity in animal´s experiments using these platforms.

First method is based on HILIC column and is able to separate about 80 analytes in less than 10 minutes. The method was validated with good precision and accuracy. We utilized this approach for mice experiment where we revealed several acylcarnitines, i.e. long chain ACs, carnitine, acylcarnitines C4 and C6, C4DC, as well as amino acids, i.e. tyrosine,

alanine, ornithine and threonine, that could serve as complex, gender-specific biomarker of propensity to obesity and partially also as biomarker of obesity-associated insulin resistance.

Second, general metabolomic method is based on aminopropyl column and is able to separate up to 254 metabolites, including AC and AmA. This approach is relatively fast, sensitive and provides good peak shapes. Importantly, it simplified peak integration process in comparison to AC´s and AA´s 10minutes method. We utilized this platform for rat´s experiment where we uncovered that maternal intake of a cafeteria diet during lactation in rats entails an alteration in the plasma profile of AC and AmA. Specifically, changes were apparent in case of acetylcarnitine and medium- and long-chain AC, as well as in case of glycine, alanine, isoleucine, serine and proline, in the offspring, which is more evident under feeding conditions.

3.2. INTERACTION OF ADIPOCYTES AND MACROPHAGES

3.2.1. Introduction

Subsequently, we wanted to describe WAT metabolism regarding mutual interaction between adipocytes and adipose tissue macrophages in WAT. Adipocytes are the main cellular components of adipose tissue and they are principal storage depots of the energy in form of TG droplets [169]. Almost all types of immune cells are present in WAT [170] but particularly adipose tissue macrophages (ATM) are associated with changes in metabolic state of the tissue [41–43]. It is known that the interaction between adipocytes and macrophages are key to the integrated control of adipose tissue inflammation and lipid metabolism in obesity but it is still unknown how the macrophages interact with neighbouring adipocytes [49]. Also, we specially focused on the effect of omega-3 PUFA on that interaction because it seems to be crucial for amelioration of low-grade inflammation [7]. We hypothesized that beneficial effect of omega-3 PUFA is caused by stimulation of M2 macrophages lipid processing.

We performed several *in vitro* experiments where we co-incubated different types of macrophages and adipocytes or WAT explants, as source of fatty acids, to broaden our knowledge about WAT metabolism and we utilized mainly general metabolomic UPLC-MS/MS platform established before (see part 3.1.) for that. First, we described basic process in WAT, i.e. WAT lipolysis, by determination of free fatty acids and glycerol in

medium after the experiment using spectrophotometric method. Afterwards, we analysed both macrophages and adipocytes (or explants) after the experiments and therefore we gave insight the mutual interaction between these cells presented in WAT.

3.2.2. Analytical highlights

LC-MS method for analysis of eicosanoids and endocannabinoids. Eicosanoids and endocannabinoids are separated on octadecyl Kinetex column heated to 50 °C. Mobile phase consists of two parts, part A is 30/70 (v/v) acetonitrile and 1.3 mM CH_3COONH_4 and part B is mixture of acetonitrile and isopropanol 50/50 (v/v). The analytes are analysed in negative MRM mode in 16 minutes.

Extraction of eicosanoids. Medium after the co-culture experiment was replaced by 50% methanol and cells grown on wells were frozen in liquid nitrogen and stored in -80 °C until analyses. Lately, frozen macrophages with extraction solution were scraped off the wells and transferred into 1.5 ml tubes while internal standards, cold water, methanol and hydrochloric acid were added to samples. Afterwards solid phase extraction was done with Strata-X column washed by ethylacetate. The columns were conditioned with methanol and water and samples were applied on them. Then both column and sample were washed with water and hexane. Importantly, elution of sample was achieved by adding methylformate and methanol. Acquired samples were evaporated in Speedvac and residues were dissolved in 30% acetonitrile and analysed by LC-MS.

General metabolomic LC-MS method. See part 3.1.

Sample preparation for general metabolomic LC-MS method. White adipose tissue was homogenized using a bead mill and extracted with 75% acetonitrile in which the internal standards were dissolved. Medium after co-culture experiment was replaced by 30% acetonitrile and macrophages grown on well plate were frozen in liquid nitrogen. Then macrophages were scraped off from the wells and transferred into 1.5 ml tubes. Extracts of WAT or cell samples were homogenized in an ultrasonic bath and centrifuged for 5 min. Finally, the supernatant was used for liquid chromatography-mass spectrometry analysis.

Measurement of free fatty acids and glycerol. Medium after co-incubation was stored in -20 °C till analyses. Subsequently, free glycerol and non-esterified FAs in media were measured according to kit by spectrophotometric method.

3.2.3. Results

We co-incubated RAW macrophages (polarized to M1 or M2 state) and primary adipocytes from HF or HFF fed mice for 2h in first type of experiment. Then we prepared primary BDMD macrophages polarized into M1 and M2 form, or kept naïve (M0), respectively. These macrophages were exposed to explants from HF or HFF mice for 24h (for details see [99]). Both types of attempts simulated real situation in white adipose tissue.

3.2.3.1. Lipolysis in WAT

First, we focused on basic process of WAT, i.e. lipolysis. We measured non-esterified fatty acids and glycerol released during lipolysis in medium after the experiments by spectrophotometric methods. Our approach revealed that adipocytes alone or with M1 macrophages released glycerol and fatty acid to the medium in ratio 1:1 (**Figure 20 panel A, B, C**). It corresponds to the situation when 2 fatty acids from 3 are re-esterified back to TG. Same situation was for adipocytes from HF and HFF fed animals. Interestingly, HF adipocytes released more glycerol and fatty acids to the medium when exposed to M2 macrophages. Specifically, the ratio for glycerol was 1.4 and for FA was 2.2 (**Figure 20 panel A, B, C**). It suggests that less FA are re-esterified back to glycerol and the process of lipolysis and FA re-esterification is in favour of lipolysis and thus lipid storage is smaller than with M1 macrophages. It corresponds to the fact that M2 macrophages are predominant in lean WAT [1]. Co-incubation of M2 and HFF adipocytes denoted altered levels of glycerol and FA as well (**Figure 20 panel A, B, C**). Specifically, their significantly decreased levels, in compares to co-incubation of M2 and HF adipocytes, indicate higher FA re-esterification. Also, increased levels of M2 and HFF adipocytes, contrary to co-incubation of adipocytes with M1, suggest that less FA are re-esterified back to glycerol. Taken together, our results show that macrophages modulate the lipolysis and FA re-esterification in adipocytes.

Specifically, their modulation depends on polarization state of macrophages and it responses to dietary omega-3 PUFA supplementation.

Of note, our previous mice experiment (see section 3.1.) revealed that non-esterified FA were higher in plasma of mice fed standard diet (STD) than mice fed high fat diet (HFD). It is in agreement with results from our *in vitro* experiment when we co-incubated macrophages and adipocytes from mice fed STD or HFD and where we elucidated higher levels of non-esterified FA in medium with adipocytes from mice fed STD as well (data not shown).

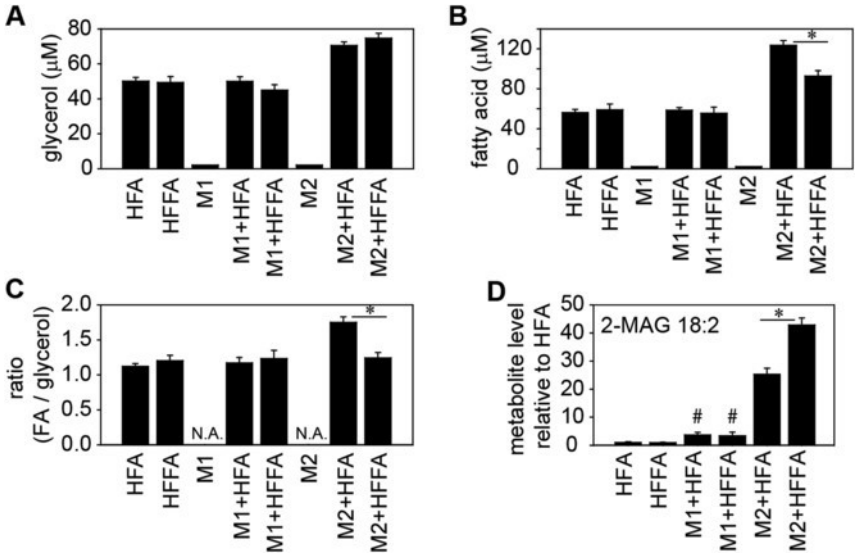

Figure 20. *Lipolysis in adipocytes co-incubated with macrophages. Freshly isolated adipocytes from HF-fed mice (HFA) or HFF-fed mice (HFFA) were incubated for 2 h either alone or in the presence of M1 or M2 polarized macrophages. Panel A: free glycerol, B: non-esterified FA were measured in the incubation media and re-esterification ratio (FA/glycerol) was calculated (panel C). Values are means ± SE, n = 16, representative of 3 independent experiments. Panel D: relative levels of 2-linoleoylglycerol in adipocytes co-incubated with macrophages. Values are means±SE, n = 6, representative of 2 independent experiments. Adapted from [49].*

3.2.3.2. Metabolic profile of macrophages and source of FA after their co-incubation

We analysed both adipocytes and macrophages after their co-incubation by our general metabolomic approach to look for changes reflecting the interaction between them. The metabolic profile of adipocytes was not significantly altered by the co-incubation with macrophages when compared with macrophages. In contrast, macrophages responded dynamically to the presence of adipocytes (**Figure 21**) and therefore we discuss data obtained from them in further paragraphs.

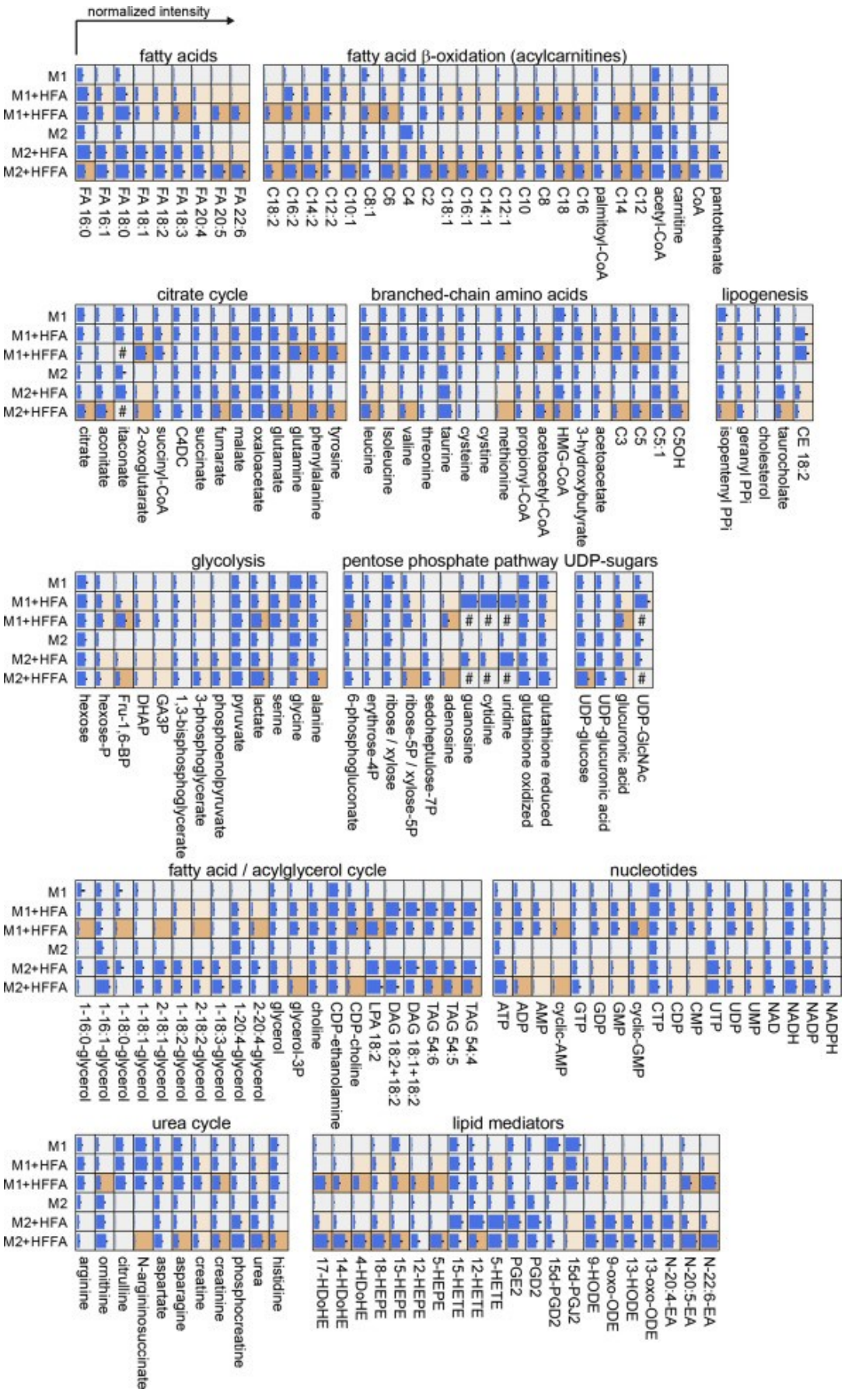
normalized intensity
fatty acids
fatty acid β-oxidation (acylcarnitines)
M1
M1+HFA
M1+HFFA
M2
M2+HFA
M2+HFFA
FA 16:0
FA 16:1
FA 18:0
FA 18:1
FA 18:2
FA 18:3
FA 20:4
FA 20:5
FA 22:6
C18:2
C16:2
C14:2
C12:2
C10:1
C8:1
C6
C4
C2
C18:1
C16:1
C14:1
C12:1
C10
C8
C18
C16
palmitoyl-CoA
C14
C12
acetyl-CoA
carnitine
CoA
pantothenate
citrate cycle
branched-chain amino acids
lipogenesis
citrate
aconitate
itaconate
2-oxoglutarate
succinyl-CoA
C4DC
succinate
fumarate
malate
oxaloacetate
glutamate
glutamine
phenylalanine
tyrosine
C5OH
C5:1
C5
C3
acetoacetate
3-hydroxybutyrate
HMG-CoA
acetoacetyl-CoA
propionyl-CoA
methionine
cystine
cysteine
taurine
threonine
valine
isoleucine
leucine
isopentenyl PPi
geranyl PPi
cholesterol
taurocholate
CE 18:2
glycolysis
pentose phosphate pathway
UDP-sugars
hexose
hexose-P
Fru-1,6-BP
DHAP
GA3P
1,3-bisphosphoglycerate
3-phosphoglycerate
phosphoenolpyruvate
pyruvate
lactate
serine
glycine
glycerone
alanine
6-phosphogluconate
erythrose-4P
ribose / xylose
ribose-5P / xylose-5P
sedoheptulose-7P
adenosine
guanosine
cytidine
uridine
glutathione oxidized
glutathione reduced
UDP-glucose
UDP-glucuronic acid
glucuronic acid
UDP-GlcNAc
fatty acid / acylglycerol cycle
nucleotides
1-16:0-glycerol
1-16:1-glycerol
1-18:0-glycerol
2-18:1-glycerol
1-18:1-glycerol
2-18:2-glycerol
1-18:2-glycerol
2-18:2-glycerol
1-18:3-glycerol
1-20:4-glycerol
2-20:4-glycerol
glycerol
glycerol-3P
choline
CDP-ethanolamine
CDP-choline
LPA 18:2
DAG 18:2+18:2
DAG 18:1+18:2
TAG 54:6
TAG 54:5
TAG 54:4
ATP
ADP
AMP
cyclic-AMP
GTP
GDP
GMP
cyclic-GMP
CTP
CDP
CMP
UTP
UDP
UMP
NAD
NADH
NADP
NADPH
urea cycle
lipid mediators
arginine
ornithine
citrulline
N-argininosuccinate
aspartate
asparagine
creatine
creatinine
phosphocreatine
urea
histidine
17-HDoHE
14-HDoHE
4-HDoHE
18-HEPE
15-HEPE
12-HEPE
5-HEPE
15-HETE
12-HETE
5-HETE
PGE2
PGD2
15d-PGD2
15d-PGJ2
9-HODE
9-oxo-ODE
13-HODE
13-oxo-ODE
N-20:4-EA
N-20:5-EA
N-22:6-EA

Figure 21. *Metabolic profile of macrophages after their co-incubation with adipocytes. X-HETE is X-hydroxy-eicosatetraenoic acid. X-HEPE is X-hydroxy-eicosapentaenoic acid. X-HDoHE is X-hydroxy-docosahexaenoic acid. 15d-PGX is 15-deoxyprostaglandin X (15-hydroxy-oxo-prostatetraenoic acid). PGX is prostaglandin X. Y-oxo-ODE is Y-keto-octadecadienoic acid. CX is acylcarnitines with X carbons in acylchain. TAG is triacylglycerol. DAG is diacylglycerol. CE is cholesterol ester. FA is fatty acid. EA is ethanolamine. X-HODE is X-hydroxyoctadecadienoic acid. LPA is lysophosphatidic acid. DHAP is dihydroxyacetone phosphate. GA3P is glyceraldehyde 3-phosphate.Fru-1,6-BP is fructosa-1,6-bisphosphate. HMG-CoA is 3-hydroxy-3-methylglutaryl-CoA. GlcNAc is N-acetylglukosamin. The mobile phase A is acetonitrile and phase B is ammonium acetate (20 mM, pH = 9.45). The flow rate of mobile phase is 0.3 ml/min and one µl of sample is analysed. Aminopropyl column heated to 25 °C. UPLC system (Thermo) and MS QTrap 5500 (Sciex). Adapted from [49].*

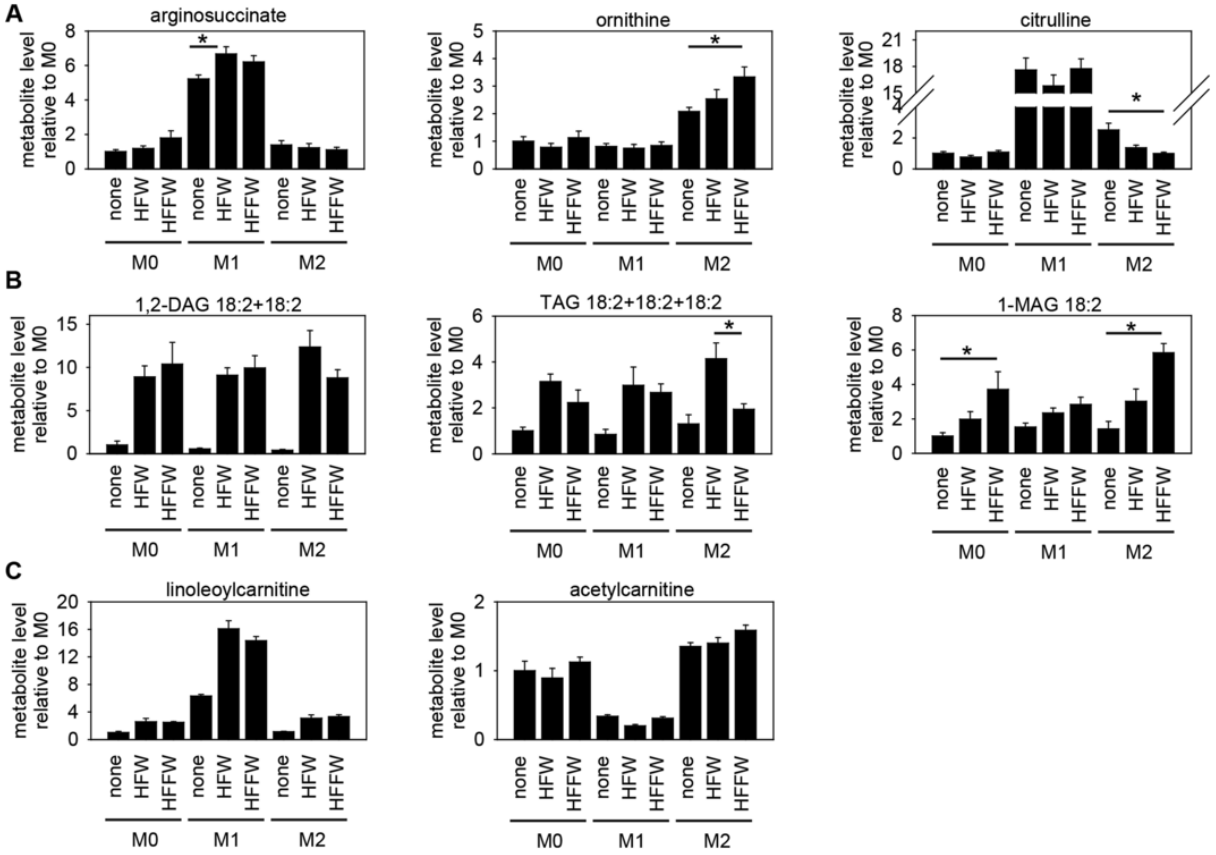

Figure 22. *Polarization and FA re-esterification in ATMs. Bone marrow-derived macrophages were kept naive M0, polarized into M1 or M2 state using cytokines and co-incubated with WAT explants from HF (HFW) or HFF (HFFW) mice or without explants (none) for 24 h. Metabolomics analysis was performed as before. A: markers of polarization; B: acylglycerols containing linoleic acid, 1,2-DAG denotes both 1,2- and 2,3-isomers; C: levels of acylcarnitines. Values are expressed as mean±SE, relative to "M0 none", n = 7–10, representative of 3 independent experiments. Adapted from [49].*

First, we verified that macrophages were polarized well in our experiment. M2 macrophages are characterized by expression of the enzyme arginase that hydrolyzes arginine to ornithine and urea. On the other hand M1 macrophages can synthesize arginine in a cyclic fashion while during nitric acid synthesis, arginine is converted to nitric acid and citrulline [171]. Therefore high level of ornithine confirmed that macrophages were polarized well to M2 form whereas increased level of citrulline bore out the correct M1 polarization

(Figure 22 panel A). Also, augmented level of ornithine in case of co-incubation M2 and HFF explants showed the shift this polarization marker more toward M2-like metabotype. The analogous phenomenon was visible for citrulline in same co-culture, this time represented by decreased level of citrulline because it is polarization marker of M1 **(Figure 22 panel A).**

Lipolysis of TG results in DG and lately in MG due to several enzymes (for details see [172]). Also, glycerol-3-phosphate is starting point of Kennedy's pathway, i.e. precursor of DG and TG. Our first experiment with RAW macrophages and adipocytes revealed that M1 in co-culture with adipocytes had higher levels of glycerol-3-phosphate than M2 with adipocytes regardless of adipocytes were from mice fed HF or HFF diet (**Figure 23 panel B**). Same trend was visible for macrophages alone but it was more noticeable when macrophages were in co-culture with adipocytes. Further, we denoted higher levels of MG in M2 that were co-incubated with adipocytes in compares to M1 with adipocytes (**Figure 23 panel D**). Both results suggest that lipolysis in anti-inflammatory M2 macrophages is under way from TG to DG and MG whereas M1 macrophages support lipolysis from TG to DG and vice versa.

Second experiment with primary macrophages and explants uncovered higher amount of MG in M2 with explants. It signifies that M2 provide lipolysis from TG up to MG **(Figure 22 panel B)** and corresponds to the results of previous attempt (**Figure 23 panel D**). This phenomenon was more noticeable when M2 were co-incubated with explants from HFF fed animals. We could observe this effect unlike in previous experiment probably due to longer time of macrophages in the co-culture. Also, it confirms our hypothesis that beneficial effect of omega-3 PUFA is caused by stimulation of M2 macrophages lipid processing. On the other hand lower level of MG in M1 signifies that M1 carry out lipolysis from TG to DG while there is no changes for M1 with HFF explants. M0 levels were comparable with M1 levels but we could observe the augmented levels in M0 with HFF explants equally as in M2 with HFF explants. Results of these two types of experiments indicate that the processes of lipolysis and FA re-esterification in M1 are faster and thus it supports higher lipid storage of TG in WAT. It is in line with fact that M1 is prevailing in obese individuals [1].

Also, our outcomes displayed that M2 in co-culture with both types of adipocytes contained more acylcarnitines than M1 macrophages with adipocytes. This result indicates that M2 use excess of FA to β-oxidation because acylcarnitines are the intermediates of β-oxidation [63]. Indeed, level of acylcarnitines was higher when the co-culture was with omega-3 PUFA supplemented adipocytes (**Figure 23 panel D**). It suggests complex

stimulation of β-oxidation by omega-3 PUFA. Therefore, the highest β-oxidation is expected for co-culture of M2 and adipocytes from HFF fed animals and we confirmed that as well (**Figure 23 panel D**). It corresponds to the fact that M2 as well as omega-3 supplementation have beneficial effects on WAT because they utilize FA to β-oxidation rather than storage them to TG.

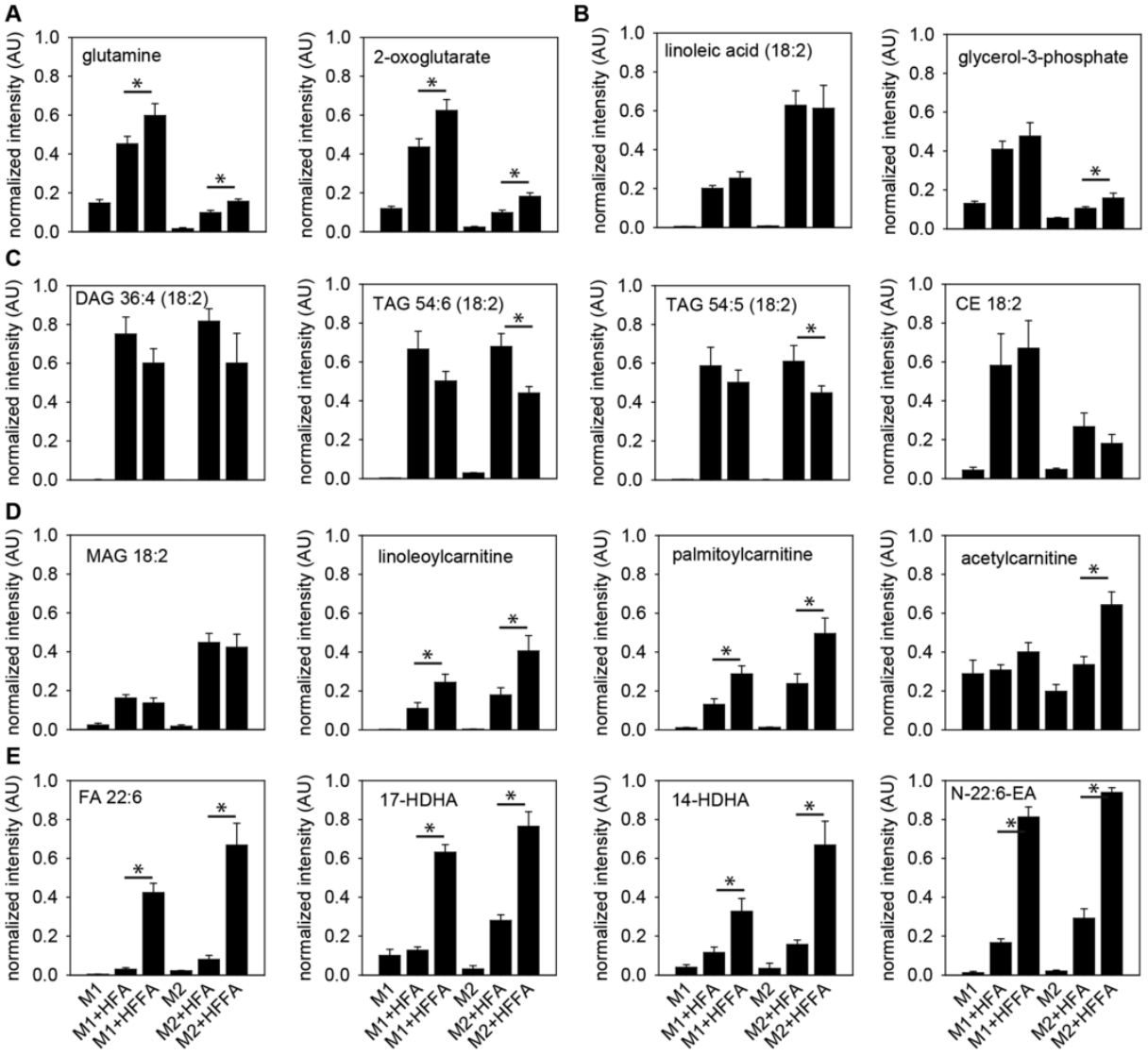

Figure 23. *Metabolic pathways in M1 and M2 macrophages upregulated by co-incubation with adipocytes from HF and HFF mice. A: glutamine to 2-oxoglutarate pathway; B: free FA and glycerol-3 phosphate, starting point of the Kennedy pathway; C: levels of neutral lipids; D: lipid degradation and oxidation pathway; E: synthesis of pro-resolving lipid mediators. Values are expressed as mean±SE, n = 8–16, representative of 5 independent experiments. For the scheme of relevant metabolic pathways and other metabolites, see Figs. S1 and S2, respectively. CE, cholesteryl ester; DAG, diacylglycerol; EA, ethanolamine; HDHA, hydroxy-DHA; MAG, monoacylglycerol; TAG, triacylglycerol. Adapted from [49].*

3.2.4. Conclusion

We utilized our general metabolomic UPLC-MS/MS approach to describe WAT metabolism regarding mutual interaction between different cells in WAT. The principal finding of this study is that M2 macrophages specifically modulate lipolysis and FA re-esterification in WAT of dietary obese mice. Also, our metabolic profiling of macrophages revealed that M2 macrophages are under way from triacylglycerol to diaclyglycerol and monoacylglycerol whereas M1 macrophages support lipolysis from TG to DG and vice versa. Therefore M1 support higher lipid storage of TG in WAT. Of note, we confirmed that M2 as well as omega-3 PUFA supplementation have beneficial effects on WAT.

3.3. LIPID MEDIATORS IN DIFFERENT PARTS OF WAT

3.3.1. Introduction

We focused on metabolism of WAT and we utilized several UPLC-MS/MS methods to describe main processes there, i.e. lipolysis, FA re-esterification and β-oxidation, as well as we determined acylcarnitines as possible biomarkers of obesity, in previous parts of the thesis. Here, we wanted to explore another important players in WAT metabolism, i.e. lipid mediators. Primary aim of this section was to find how different cell types in WAT modulate levels of lipid mediators there. We analysed separately adipocytes, both subfractions of stromal vascular fraction (i.e. adipose tissue macrophages and rest of SVF), SVF itself and whole WAT by UPLC-MS/MS to achieve this. WAT samples were obtained from mice fed HF, HFF or ST diet. Also, we were concentrated on omega-3 PUFA supplementation in diet and how it influences pro and anti-inflammatory lipid mediators in WAT. Another goal was to explore the effect of omega-3 PUFA on adipose tissue macrophages while they are present in WAT due to obesity.

3.3.2. Analytical highlights

General metabolomic LC-MS method. See part 3.1.

Sample preparation for general metabolomic LC-MS method. See part 3.2.

LC-MS method for analysis of eicosanoids and endocannabinoids. See part 3.2.

Extraction of eicosanoids. First, white adipose tissue with methanol were homogenized in bead mill and centrifuged for 5 min. Then standards, cold water, methanol and hydrochloric acid were added to samples. Solid phase extraction was done with Strata-X column washed by ethylacetate and columns were conditioned with methanol and water. Afterwards samples were applied on columns while after both column and sample were washed with water and hexane. Importantly, elution of sample was achieved by adding methylformate and methanol. Finally, acquired sample was evaporated in Speedvac and residues were dissolved in 30% acetonitrile and analysed by LC-MS. Second, adipocytes and SVF isolated from WAT were extracted same apart from homogenization as well as CD11b positive and CD11b negative cells that were separated from SVF. Eicosanoids in macrophages after co-incubation were extracted as described in part 3.2.

DNA measurement. DNA was measured in all parts of white adipose tissue and WAT itself. DNA was determined using Hoechst fluorescence stain and its concentration was calculated using calibration curve prepared with DNA standard.

3.3.3. Results

3.3.3.1. Lipid mediators in WAT

Initially, we analysed WAT, adipocytes and SVF from mice fed HF, HFF or ST diet. We specially focused on protectin D1 (PD1), which is anti-inflammatory lipid mediator that improves insulin sensitivity in obese mice, and its precursor 17-HDHA. Cellular origin of PD1 and its role in metabolism are not very well explored [104]. Also, PD1 is very sensitive to degradation and thus it has to be analysed immediately after collection. As a result, we confirmed that levels of lipid mediators PD1 and 17-HDHA were elevated after the omega-3 PUFA administration (**Figure 24**) which is in line with previously published data [104]. Measurement of DNA content in WAT ensured that 72% of cells were adipocytes and 13% were SVF (data not shown). Measuring DNA is a good measure of total cell number due to the invariability of cellular DNA content during even extreme physiological conditions

and the excellent correlation with the cell number [173]. Similar levels of 17-HDHA were detected both in adipocytes and SVF (**Figure 24**). Comparing these levels with DNA content indicate that SVF is responsible for production of 17-HDHA and PD1 as well. Of note, protectin D1 was not detected in isolated adipocytes and although their absolute levels could be influenced by collagenase digestion, the distribution pattern responded to levels measured in intact WAT. Interestingly, levels of 17-HDHA and PD1 were significantly elevated in CD11b negative cells when compared to CD11b positive subfraction, i.e. macrophages, (**Figure 25 panel A**) which is novel finding.

Our research of lipid mediators further focused on endocannabinoids, specifically two best known, anandamide (AEA) and 2-arachidonoylglycerol (2-AG). Both are pro-inflammatory endocannabinoids that are associated with obesity [8]. Our research confirmed that amount of 2-AG and AEA were increased after high fat diet feeding in contrast to standard diet feeding. On the other hand, omega-3 supplementation counteracted the effect of HF feeding in that endocannabinoids (**Figure 24**) which is in line with findings in obese mice [7]. Levels of 2-AG were two orders higher than AEA which is in accord with our previous results [174]. Interestingly, levels of 2-AG were similar in adipocytes and SVF. Both AEA and endocannabinoid DHEA were detected in WAT and adipocytes but not in SVF (**Figure 24**). It indicates that these compounds have a higher rate of degradation in SVF.

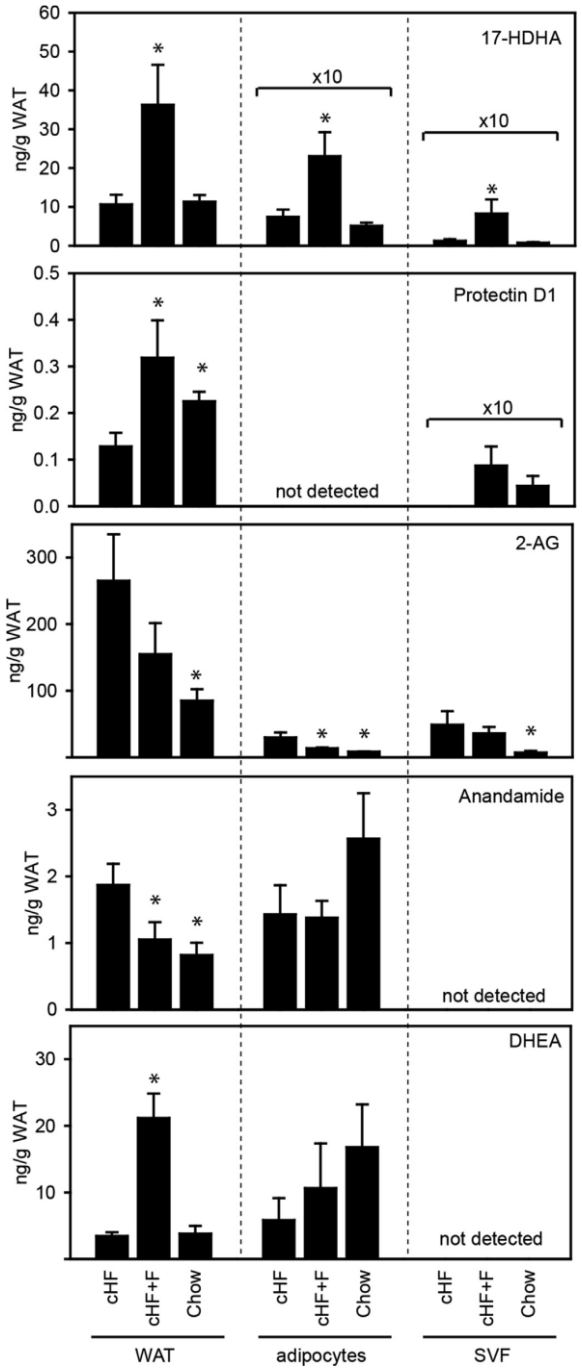

Figure 24. *Source of lipid mediators in adipose tissue. Epididymal WAT, isolated adipocytes and SVF cells were collected from mice fed different diets and lipid mediators were analyzed using LC-MS/MS. 17-HDHA, (±)17-hydroxy-docosahexaenoic acid; protectin D1, 10R,17S-dihydroxy-docosahexaenoic acid; 2-AG, 2-arachidonoylglycerol; anandamide, N-arachidonoylethanolamine; DHEA, N docosahexaenoylethanolamine. x10 e values were multiplied by 10 to fit the range. Values are expressed as mean ± SE, n ¼ 5e7 mice, ng per g of source WAT, representative of 2 experiments. *Significantly different from cHF diet. Adapted from [8].*

3.3.3.2. Influence of omega-3 PUFA on ATM

Subsequently, we wanted to explore the beneficial effect of omega-3 PUFA on adipose tissue macrophages. Therefore we separated CD11b positive cells (i.e. macrophages)

and CD11b negative cells from SVF of mice fed HF or HFF diet. As a result, we denoted that CD11b positive cells (i.e. macrophages) had significantly lower levels of arginosuccinate in groups supplemented by omega-3 PUFA (**Figure 25 panel E**). Activation of macrophages into M1 metabotype was represented by high levels of arginosuccinate [171] and thus lower levels of arginosuccinate in macrophages isolated from HFF adipose tissue indicated that they reduced WAT inflammation. It is in agreement with omega-3 PUFA modulation of ATM metabolism towards M2 polarization and thus less inflammatory state of tissue (see part 3.2.). Also, we revealed that omega-3 PUFA lowered levels of TG while it corresponds to beneficial properties of omega-3 PUFA (**Figure 25 panel D**).

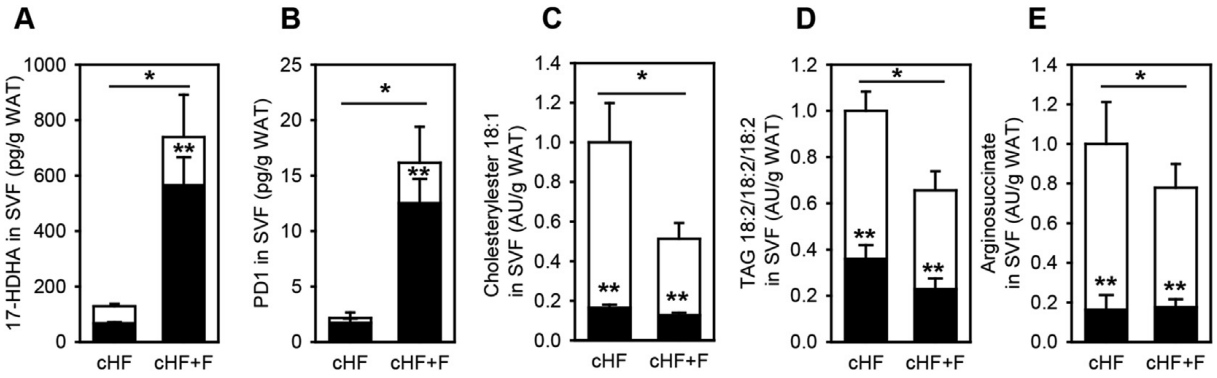

Figure 25. *CD11b-positive ATMs in SVF. Concentration of 17-HDHA (A) and protectin D1 (B) in CD11b-positive (empty bars) and CD11b-negative (black bar) cells isolated from SVF after stimulation with calcium ionophore A23187 (see Fig. 1). *Significantly different levels with respect to diets, **significantly different separation according to CD11b marker, p < 0.05, n ¼ 5, means ± SE. Relative levels of oleoyl (18:1) ester of cholesterol (C), tri-linoleoyl glycerol (D) and arginosuccinate (E) in CD11b positive (empty bars) and CD11b-negative (black bar) cells isolated from SVF. Values as means ± SE relative to cHF, n ¼ 7, representative of 2 independent experiments. Adapted from [8].*

3.3.4. Conclusion

Our results showed the interplay between several cell types in WAT. Cell type specific production of different lipid mediators was involved in the control of WAT inflammation and metabolism. Specifically, we were able to track protectin D1 to SVF cells and confirmed that PD1 levels were upregulated by omega-3 PUFA. Surprisingly, the PD1 production was associated with CD11b negative cells and not with adipose tissue macrophages. Omega-3 PUFA had a beneficial effect on WAT metabolism while we documented here their ability to lower the inflammation in WAT.

3.4. ANALYSIS OF NOVEL MEMBER OF FAHFA LIPID CLASS

3.4.1. Introduction

Another part of the thesis focused on branched fatty acid hydroxy fatty acids (FAHFA) lipid molecules that have probably anti-inflammatory properties and potentially influence WAT metabolism as well. We concentrated on novel member of this family, i.e. docosahexaenoic acid hydroxylinoleic acid (DHAHLA) that is derived from omega-3 PUFA. We utilized UPLC-MS/MS methodology for FAHFA analysis to identify DHAHLA compound by its fragmentation scheme and detected several isomers in murine serum as well. Another aim was to investigate whether different cell types from WAT could synthesize DHAHLA compound. Finally, last goal was to prove the anti-inflammatory properties of the analyte of interest.

3.4.2. Analytical highlights

LC-MS method for FAHFA analysis. Branched fatty acid hydroxy fatty acids are determined on octadecyl column warmed up to 50 °C. The mobile phase is 30/70 (v/v) acetonitrile and water with 0.01% acetic acid, pH 4 (part A) and 50/50 (v/v) acetonitrile and isopropanol (part B). Serum samples were analysed by gradient elution in 25 minutes whereas structural analysis was done by isocratic elution in 60 minutes. DHAHLA compound is measured in negative multiple reaction mode.

Extraction of FAHFA. First in serum samples, samples were extracted by liquid/liquid and solid phase extraction. First LLE, dichlormethane and methanol as organic phase and chilled citric acid buffer as water phase were added to sample. After, the organic phase was dried in a Speed-vac and dissolved in dichloromethane. SPE was performed on Strata SI-I Silica columns conditioned by hexane, sample was applied on columns and elution of FAHFA was achieved by ethylacetate. Finally, samples were evaporated, dissolved in methanol and analysed by liquid chromatography and mass spectrometry. Cells were homogenized using a bead mill at first and then extraction procedure continued as described above.

Standard of 13-DHAHLA. Standard was synthetized in the Institute of Organic Chemistry and Biochemistry of the Czech Academy of Sciences.

General metabolomic LC-MS method. See part 3.1. The methodology was utilized to prove the anti-inflammatory properties of DHAHLA compound.

3.4.3. Results

3.4.3.1. Methodology for DHAHLA analysis

The method for FAHFA analysis was optimized by Marie Brezinova and it is discussed in her diploma thesis (see [175]). She analysed palmitic acid hydroxystearic acid (PAHSA) but the same approach was used for DHAHLA analysis in my project. The methodology based on liquid chromatography coupled to hybrid tandem mass with linear ion trap spectrometry is described in Methods and Analytical highlights.

3.4.3.2. Fragmentation of DHAHLA compound

Mass spectrometer is able to switch from sensitive triple quadrupole scan modes to highly sensitive full-scan ion trap mode within one analysis. Therefore, using MS/MS and MS/MS/MS technique we were able to reliably identify the structure of docosahexaenoic acid hydroxylinoleic acid by its fragmentation scheme (**Figure 26 panel A**). Specifically, DHAHLA was ionized in negative mode to $[M-H]^-$ ion *m/z* 605.457 which is molecular ion. Fragmentation by collision-induced dissociation (i.e. MS/MS) resulted in daughter ion $[13\text{-HLA-H}]^-$ *m/z* 295.228 (**Figure 26 panel B**). Further fragmentation of that ion in the linear ion trap (i.e. MS/MS/MS) gave rise to the ions *m/z* 179.144 and 195.139, that are specific to the position of the hydroxyl group on the hydroxyoctadecadienoic acid (HLA) backbone, i.e. 13-DHAHLA (**Figure 26 panel C**) [111]. Alternatively, specific fragment for 9-DHAHLA is *m/z* 171.10.

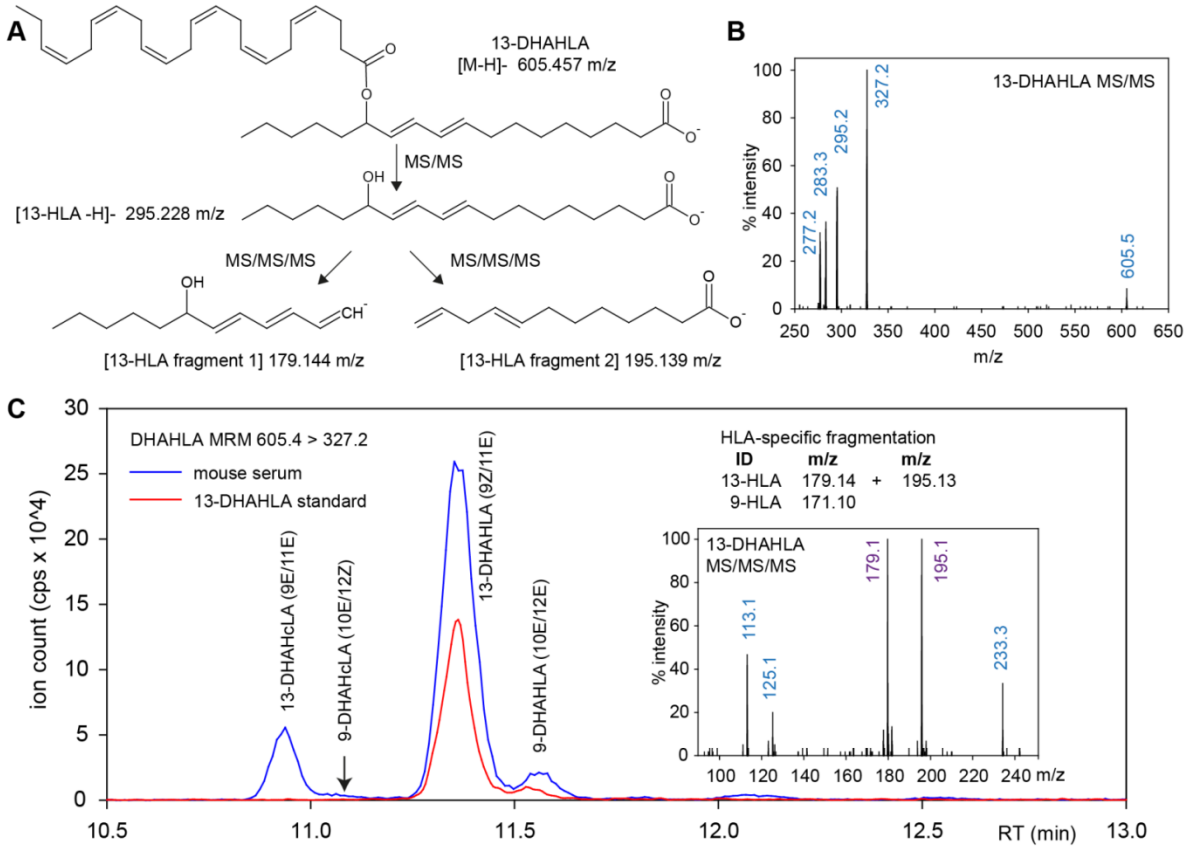

Figure 26. *Analysis of DHAHLA isomers. A: A fragmentation scheme of 13-DHAHLA with 13-HLA-specific fragments. B: MS/MS spectrum of 13-DHAHLA. C: Chromatographic profile of DHAHLA isomers (MRM 605.4 > 327.2) detected in murine serum sample (blue line) overlaid with synthetic standard of 13-DHAHLA (red line). Inserted table summarizing MS/MS/MS fragments specific to individual positional isomers of the hydroxyl group on HLA and MS/MS/MS spectra of 13-DHAHLA. Specific fragments highlighted in magenta. HcLA, hydroxy-conjugated-LA. Adapted from [99].*

3.4.3.3. DHAHLA analysis in murine serum

DHAHLA has several isomers [99]. We detected four separated DHAHLA peaks in murine serum samples (**Figure 26 panel C**) by method described previously. Structural characterization in the linear ion trap (see above) revealed that 2 major peaks were 13-DHAHLA and 2 minor peaks were 9-DHAHLA cis-trans isomers of double bonds in HLA acyl chains. This is in agreement with the high concentrations of 9(S)- and 13(S)-HODE (HLA aka HODE), enzymatic products of 15-lipoxygenase in the organism. Identity of the backbone fragmentation was confirmed using synthetic standards for 9(S)-HODE and 13(S)-HODE.

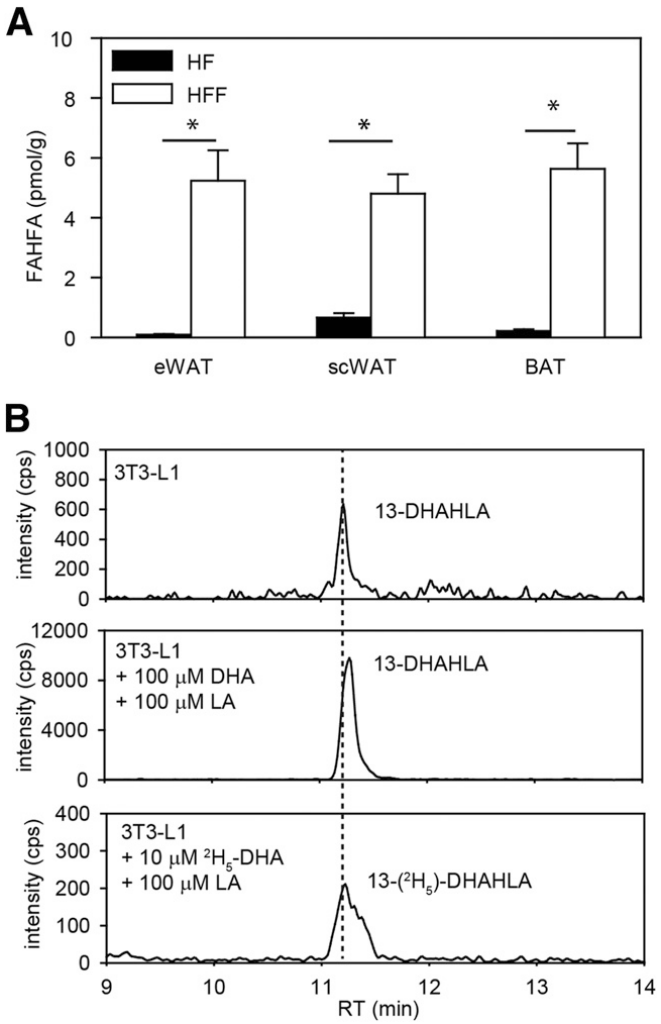

Figure 27. *13-DHAHLA in adipose tissue. A: Levels of 13-DHAHLA in murine epididymal WAT (eWAT), subcutaneous WAT (scWAT) and interscapular brown adipose tissue (BAT) with and without omega-3 PUFA supplementation. Black bars, mice on high-fat diet; empty bars, mice on high-fat diet supplemented with omega-3 PUFA. Values are expressed as mean ± SE, n=4-8. B: Chromatographic profile of 13-DHAHLA in naïve 3T3-L1 adipocytes, adipocytes supplemented with 100 μM DHA and LA for 24 hours, and adipocytes supplemented with deuterium-labelled DHA and cold LA for 24 hours, as indicated. Adapted from [99].*

3.4.3.4. Cells in white adipose tissue can synthetize DHAHLA

Generally, branched fatty acid hydroxy fatty acids are released by adipocytes [99,111]. We have detected DHAHLA compound in adipose tissue of human and mice (data not shown, for details see [99]). The goal of this section was to reveal whether adipocytes and macrophages, main parts of adipose tissue, could synthetize DHAHLA. We used *in vitro* models of adipocytes and macrophages treated with DHA and LA to achieve this. Specifically, we utilized murine cell model of adipocytes (i.e. 3T3-L1) and human adipocytes (i.e. multipotent adipose-derived stem cells, hMADS) and RAW macrophages. DHAHLA analyses were performed by method described previously.

As a result, we revealed that both types of adipocytes were capable to synthesize DHAHLA isomers (**Figure 27 panel B, Figure 28**). Cell model of macrophages did not behave similarly with same level of substrates. Nevertheless when macrophages were exposed to higher concentrations of DHA and LA, they were able to synthetize DHAHLA as well (**Figure 28**).

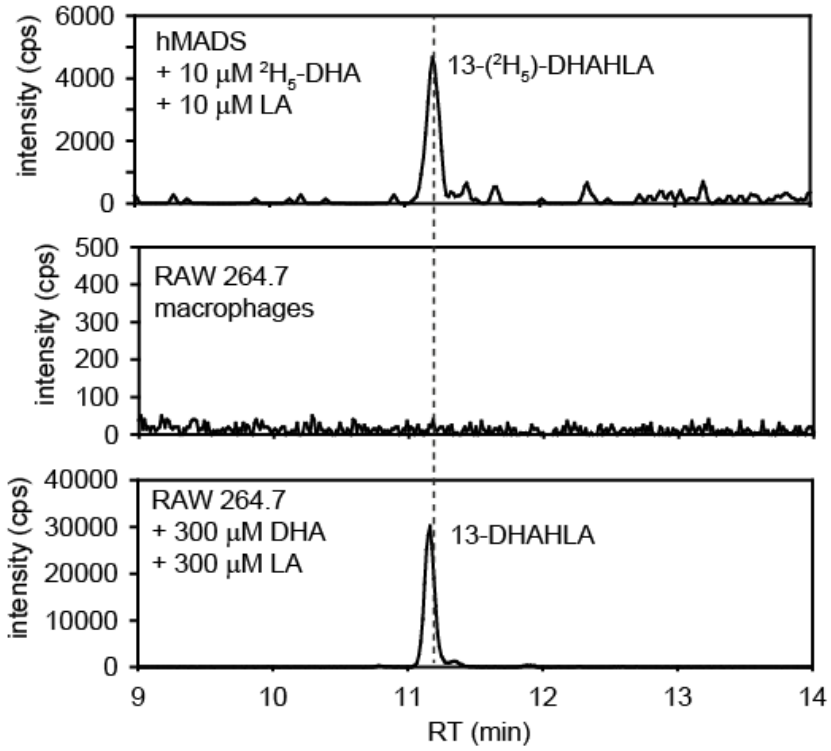

Figure 28. *Chromatographic profile of 13-DHAHLA in hMADS (adipocytes) supplemented with 10 µM $^2H_5$-DHA and LA for 24 hours, naïve RAW 264.7 macrophages and RAW 264.7 macrophages supplemented with 300 µM DHA and LA for 24 hours, as indicated. Adapted from [99].*

3.4.3.5. Anti-inflammatory and pro-resolving effects of DHAHLA

PAHSA, a known member of FAHFA family, have anti-inflammatory properties [111]. Also, DHA and its metabolites have a beneficial effect on adipose tissue inflammation. Thus we hypothesized that DHAHLA could have immunomodulatory properties as well. We performed several cell line experiments to prove the anti-inflammatory behaviour of DHAHLA compound and we utilized mainly general metabolomics UPLC-MS/MS methodology established in part 3.1 for that.

First, RAW macrophages were stimulated with 100 ng/ml lipopolysaccharide (LPS) to activate the macrophages and 10 µM 13-DHAHLA complexed to BSA (in ratio 3:1) was

added or not to medium. Then the effect of 13-DHAHLA on cells was analysed by qPCR and ELISA measurement. The rate of inflammation is represented by bars of IL-6. Importantly, it was shown that DHAHLA prevented the increase pro-inflammatory IL-6 concentrations in media (**Figure 29 panel A**). DHAHLA decreased mRNA levels of inflammatory cytokines IL-6, TNF-α, IL-1β and PTGS2 in cells as well (**Figure 29 panel A**). Therefore it suggests that 13-DHAHLA prevented macrophage activation. Further, we wanted to explore the lowest effective concentration of 13-DHAHLA that reduces macrophages activation. We used RAW macrophages that were stimulated by 10 ng/ml LPS and incubated with different 13-DHAHLA concentration for 18 h experiment. As a result, we discovered that 10 nM of 13-DHAHLA was sufficient concentration that had an effect on cell activation (**Figure 29 panel E**).

Then we utilized murine BMDM that are more relevant to real macrophages in mice WAT for another hypothesis. First, an effect of 13-DHAHLA on the stimulation by pro-inflammatory cytokine IFN-γ (50 ng/ml) was tested. BMDM were incubated in the absence (unstimulated) or presence of IFN-γ (50 ng/ml) with 10 μM 13-DHAHLA. Macrophages activation corresponded to the high level of intracellular citrulline and we utilized the metabolomic profiling to determinate that metabolite. The level of citrulline was decreased after 13-DHAHLA supplementation (**Figure 29 panel G**) and thus we were able to confirm that 13-DHAHLA prevented macrophage activation. Next, FAHFA might serve as a pool of FA, and the anti-inflammatory properties of 13-DHAHLA could be partially mediated by DHA released via DHAHLA hydrolysis. To test this, BMDM were stimulated with 100ng/ml LPS for 18 h and the effects of 10 μM 13-DHAHLA and 10 μM DHA on macrophage activation were analysed using metabolipidomics [8,176]. We used the ratio of the intracellular concentrations of (citrulline+ornithine)/(arginine+aspartate) to evaluate this experiment. The ratio summarizes the intermediates of the related metabolic pathways of nitrogen oxide and reactive oxygen species production and it is assumed as the most sensitive early marker of macrophage activation [176]. The attempt showed that the pro-inflammatory effect of LPS was significantly reduced by both 13-DHAHLA and DHA (**Figure 29 panel C**). It indicates that the effect of DHAHLA can be partially mediated by DHA.

Afterwards, we carried out experiment with human peripheral blood mononuclear cell (PBMCs), another type of immune cells, to test the immunomodulatory potential of 13-DHAHLA. In practice, freshly isolated PBMCs from buffy coats were preincubated with 1 mmol/L 13-DHAHLA for 30 min and then exposed to lectin phytohemagglutinin for 24 hours. Lectin activates T-helper type 1 lymphocytes and also the indoleamine

2,3-dioxygenase (IDO) pathway in macrophages. IDO is the rate-limiting enzyme of the essential amino acid tryptophan catabolism toward kynurenine while its activation causes tryptophan depletion, reduces the growth of microbes [177], and serves as an immune checkpoint [99]. Activation of that enzyme was indicated by a strong increase in the kynurenine/tryptophan ratio that was measured in the media. Increased level of kynurenine/tryptophan ratio after 13-DHAHLA preincubation confirmed that 13-DHAHLA was able to partially prevent IDO activation in PBMCs stimulated with lectin, and to limit immunosuppression caused by tryptophan depletion (**Figure 29 panel B**) [177]. The results from experiments with RAW and BMDM macrophages as well as human immune cells document that 13-DHAHLA exerts anti-inflammatory and pro-resolving properties.

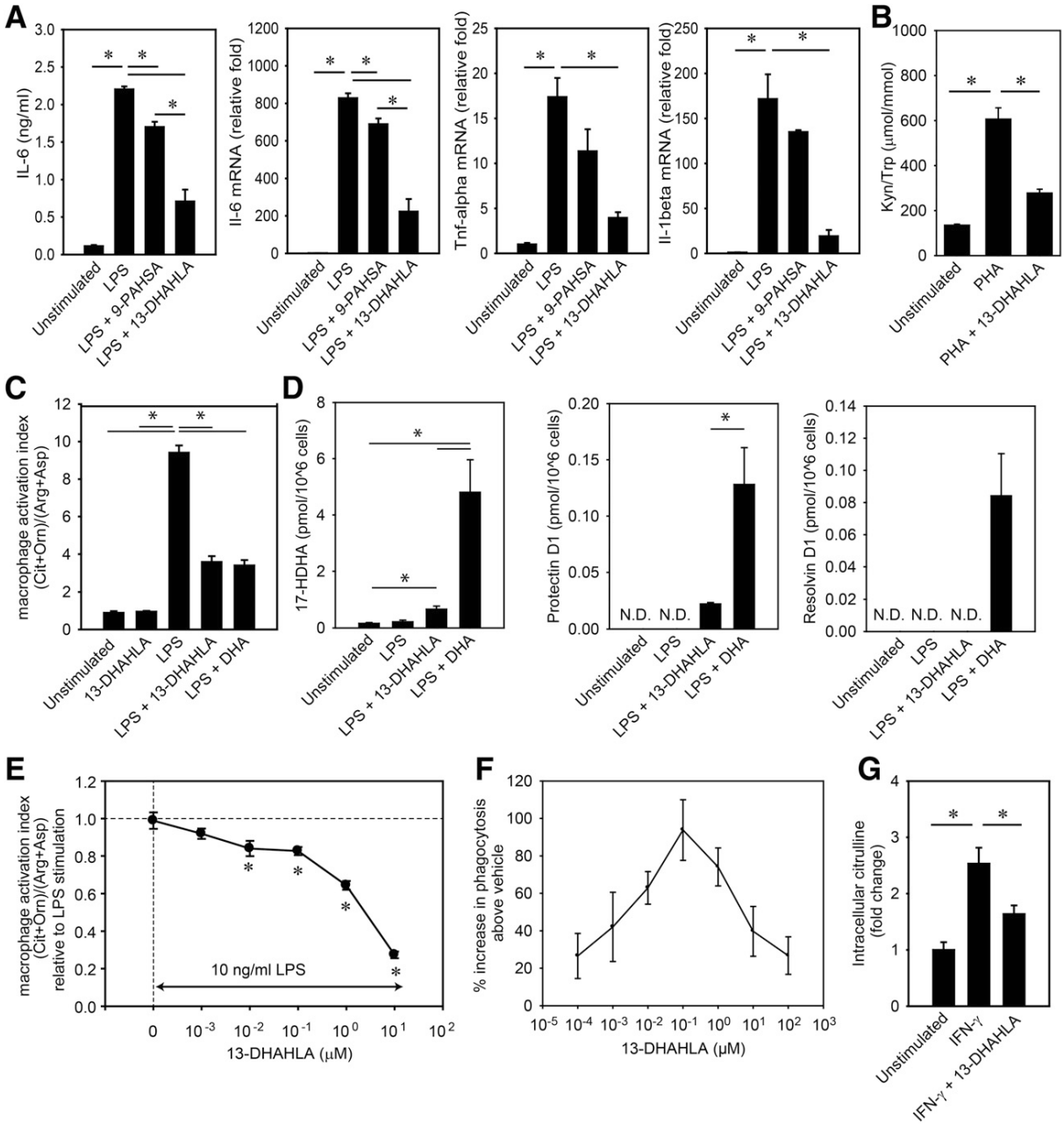

Figure 29. *Anti-inflammatory effects of 13-DHAHLA. A: RAW 264.7 macrophages were incubated in the absence (Unstimulated) or presence of LPS (100 ng/mL) for 18 h, and the effect of 9-PAHSA (10 mmol/L) and 13-DHAHLA (10 mmol/L) on macrophage activation was tested. IL-6 protein levels in the medium, and IL-6, TNF-a, IL-1b, and Ptgs2 mRNA in cells. Values are expressed as the mean ± SE. n = 6, representative of three experiments. B: Human PBMCs were freshly isolated from a buffy coat, preincubated with 1 mmol/L 13-DHAHLA, and stimulated with phytohemagglutinin (PHA; 10 mg/mL) for 24 h. Levels of tryptophan and kynurenine were measured in the medium. Values are expressed as the mean ± SE. n = 8, representative of 3 PBMC isolations. C: BMDMs were incubated in the absence (Unstimulated) or presence of LPS (100 ng/mL) for 18 h, and the effect of 13-DHAHLA (10 mmol/L) and DHA (10 mmol/L) on macrophage activation was tested. Cells were either extracted for metabolomics (Cit+Orn)/(Arg+Asp) macrophage activation index (relative fold)—or processed for the metabolipidomics of lipid mediators. D: Levels of DHA-derived lipid mediators 17-HDHA, protectin D1, and resolvin D1. Values are expressed as the mean ± SE. n = 6, representative of three experiments. N.D., not detected. E: RAW 264.7 macrophages were stimulated with LPS (10 ng/mL) and incubated in the presence of various concentrations of 13-DHAHLA for 18 h to explore dosedependent inhibition of macrophage activation. The LPS-stimulated state is set as a reference point. Values are expressed as the mean ± SE. n = 6, representative of two experiments. F: BMDMs were pretreated for 15 min with 13-DHAHLA, as indicated, and were incubated with fluorescein labelled zymosan for 30 min. Extracellular fluorescence was quenched with trypan blue and fluorescence measured using a plate reader. Values are expressed as the mean ± SE. n = 8, representative of three experiments. G: BMDMs were incubated in the absence (Unstimulated) or presence of IFN-g (50 ng/mL) for 18 h, and the effect of 13-DHAHLA (10 mmol/L) on macrophage activation (intracellular citrulline levels) was tested. Values are expressed as the mean ± SE. n = 6. *P < 0.05. Adapted from* [99].

3.4.4. Conclusion

To summarize it, our metabolipidomic methodology using UPLC-MS/MS enabled us to identify novel compound of FAHFA lipid class derived from DHA and LA, i.e. docosahexaenoic acid hydroxylinoleic acid. Also, we detected several isomers of that compound in murine serum. Our cell line experiments elucidated that DHAHLA were synthetized by adipocytes and macrophages in WAT. Also, this substance was involved in the beneficial anti-inflammatory effects attributed to omega-3 PUFA and therefore DHAHLA may improve the metabolism of adipocyte in obesity [99].

3.5. ANALYSIS OF DHAHLA COMPOUND IN MILK SAMPLES

3.5.1. Introduction

Synthesis of FAHFA is linked with de novo lipogenesis [111] which is tightly regulated in the lactating human mammary gland [178]. Previously, we have quantified the amount of docosahexaenoic acid hydroxylinoleic acid (DHAHLA), novel compound of FAHFA family with anti-inflammatory and anti-diabetic properties, in human and mice WAT and plasma samples (data not shown, for details see [99]). Here, we continued with analysis of DHAHLA compound presented in previous section but this time in human breast milk where we hypothesized should be found for the first time. Then we focused whether FAHFA in breast milk could appear in the circulation of infants. This type of experiment is problematic due to ethical reasons and thus we performed mice experiment to explore that.

3.5.2. Analytical highlights

LC-MS method for FAHFA analysis. See part 3.4.

Extraction of FAHFA in milk samples. Extraction in milk samples is slightly different than extraction in serum samples. First, milk samples were warmed to 25 °C in water bath and homogenized for 10s in ultrasonic bath. Later on, LLE with dichlormethane, methanol and citric acid buffer was performed as described before. The organic phase was collected, water phase was re-extracted and then organic phase was pooled, dried in a Speed-vac and dissolved

in dichloromethane. After that solid phase extraction was performed on Hypersep columns. FAHFA were eluted from SPE columns with ethyl acetate as previously and they were concentrated using Speed-vac, dissolved in methanol and analysed by LC-MS.

3.5.3. Results

3.5.3.1. Analyses of milk sample

LC-MS/MS analyses of milk samples were done as FAHFA analyses before (for details see part 3.4.). We discovered FAHFA composition of human milk (data not shown, for details see [179]). The compound 13-DHAHLA was also found in human breast milk but only in samples from mothers who were supplemented with omega-3 PUFA during pregnancy (**Figure 30**). It is in line with finding that synthesis of DHA-derived FAHFA depends on omega-3 PUFA intake.

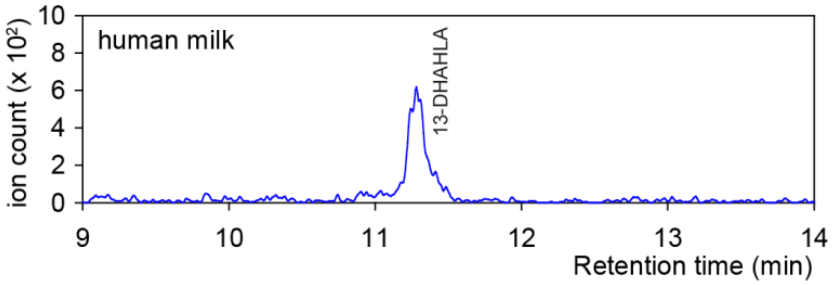

Figure 30. *Profile of 13-DHAHLA in human milk. MRM profile of 13-DHAHLA in breast milk from a single mother who reported omega-3 PUFA supplementation during pregnancy. Adapted from [179].*

3.5.3.2. Bioavailability of orally administrated FAHFA

Mice were gavaged by 5-PAHSA or not for three days to reveal the bioavailability of orally administrated PAHSA. Then levels of that compound were determined in mice plasma. As a result, we uncovered that administration of 5-PAHSA elevated its level in mice plasma (**Figure 31**) while it suggests that PAHSA from breast milk might reach newborn´s circulation.

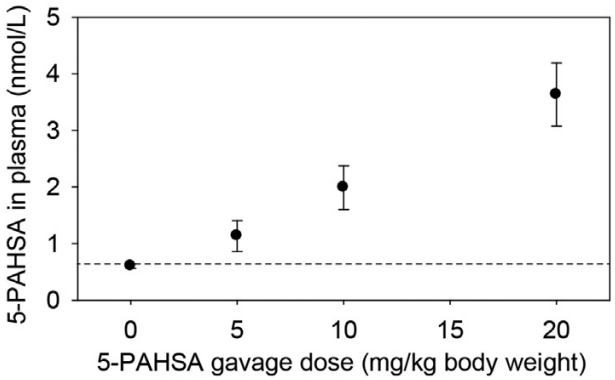

Figure 31. *Bioavailability of digested 5-PAHSA. Male mice were gavaged with 5, 10, and 20 mg 5-PAHSA/kg body weight or an equivalent volume of vehicle (50% PEG400, 0.5% Tween-80, 49.5% H_2O [180] once daily for 3 days, followed by the analysis of 5-PAHSA levels in plasma. Data are expressed as mean ± S.E., n = 3. Adapted from [179].*

3.5.4. Conclusion

To sum up this part, we detected DHAHLA compound in human breast milk for the first time while it has been only reported in human serum and adipose tissue previously. Also, our animal´s experiment suggests that administration of FAHFA analytes may reach infants´s circulation and thus potentially positively influence their metabolism.

4. SUMMARY

This dissertation thesis is focused on adipose tissue metabolism. Firstly, we wanted to find and optimize UPLC-MS/MS methods for the analysis of acylcarnitines (AC) and amino acids (AmA), because these metabolites are associated with obesity and they are important diagnostic markers. We also aimed to find new AC or AmA biomarkers with propensity to obesity in animal experiments using these platforms. The first method used for analysis of acylcarnitines and amino acids was based on the HILIC column and was able to separate 57 AC and 21 AmA in less than 10 minutes. Moreover, the method was validated with good precision and accuracy up to 11 %. Importantly, these analyses enabled us to separate isobaric species C4OH and C3DC which is not usually possible. We utilized this approach in mice experiment where we identified several acylcarnitines, i.e. long chain ACs, carnitine, acylcarnitines C4 and C6, C4DC, as well as amino acids, i.e. tyrosine, alanine, ornithine and threonine, that could serve as complex, gender-specific biomarkers of propensity to obesity and partially also as a biomarker of obesity-associated insulin resistance. Afterwards, we adapted the UPLC-MS/MS general metabolomic method with an aminopropyl column that allowed us to separate as many as 254 metabolites including AC and AmA in 40 minutes. This simplified the peak integration process in comparison to the AC´s and AmA´s 10minutes method. We utilized this platform in an experiment using rats where we discovered that maternal intake of a cafeteria diet during lactation entails an alteration in the plasma profile of AC and AmA. Specifically, changes were apparent in their offspring in the case of C2 and medium- and long-chain AC, as well as in the case of glycine, alanine, isoleucine, serine and proline.

Next, we utilized mainly the general metabolomic UPLC-MS/MS method established before to explore adipose tissue metabolism regarding mutual interactions between main cell types of adipose tissue, i.e. adipocytes and adipose tissue macrophages. We were especially interested in the effect of omega-3 PUFA on that interaction. The co-culture experiment with adipocytes and macrophages showed that macrophages modulate lipolysis and FA re-esterification in adipocytes while this effect depends on the polarization state of macrophages and their response to dietary omega-3 PUFA supplementation. Moreover, the metabolic profile of adipocytes is not significantly altered by co-incubation with macrophages but macrophages react dynamically to the presence of adipocytes. Our analyses showed that inflammatory M1 and anti-inflammatory M2 macrophages act differently. For example,

lipolysis in M2 macrophages happens from TG to DG and MG whereas lipolysis in M1 macrophages occurs only from TG to DG and vice versa. Thus, M1 macrophages store fatty acids in neutral lipids whereas M2 use them for β-oxidation. Of note, omega-3 PUFA further support β-oxidation. The results confirmed our hypothesis that the beneficial effect of omega-3 PUFA is caused by stimulation of M2 macrophages lipid processing and that M2 macrophages specifically modulate lipolysis and FA re-esterification in adipose tissue of dietary obese mice.

Subsequently, we concentrated on lipid mediators that are produced in white adipose tissue (WAT) and their effect on adipose tissue metabolism. Specifically, we studied how different cell types in WAT modulate levels of lipid mediators and how omega-3 PUFA affect them. Our results showed the interplay between several cell types in WAT and cell type specific production of different lipid mediators that is involved in the control of WAT inflammation and metabolism. In addition, we were able to find the origin of anti-inflammatory lipid mediator protectin D1 and determined several endocannabinoids in different cell types of adipose tissue. Importantly, we confirmed that adipose tissue macrophages isolated from WAT supplemented by omega-3 PUFA are able to reduce WAT inflammation. Beneficial properties of omega-3 PUFA were documented by lowered levels of TG in adipose tissue.

Another part of this thesis focused on FAHFA lipid molecules that have strong anti-inflammatory properties and potentially influence WAT metabolism. We identified a novel compound of this family, docosahexaenoic acid hydroxylinoleic acid (DHAHLA) which is derived from omega-3 PUFA. We utilized MS/MS and MS/MS/MS techniques to identify its structure by fragmentation scheme and UPLC-MS/MS methodology to detect several isomers of DHAHLA in murine serum. We have detected 13-DHAHLA in adipose tissue and therefore were interested in whether adipocytes or macrophages, the main parts of adipose tissue, could synthetize DHAHLA. As a result, the cell lines of adipocytes are able to synthesize 13-DHAHLA as well as macrophages but with a higher concentration of substrates in this case. We mainly utilized the general metabolomic UPLC-MS/MS approach established before to explore the potential anti-inflammatory properties of the 13-DHAHLA compound. The outcome from cultured cell experiments showed that 13-DHAHLA exerts anti-inflammatory and pro-resolving properties. We found that 10 nM 13-DHAHLA is the lowest effective concentration that reduces activation of macrophages. Our attempt also indicated that the anti-inflammatory effect of 13-DHAHLA could be partially mediated by

DHA released from DHAHLA via hydrolysis. Later on, we hypothesized that 13-DHAHLA could be found in human milk. The compound was truly discovered but only in samples from mothers who were supplemented with omega-3 PUFA during pregnancy. Of note, we performed experiment on mice suggesting that FAHFA from breast milk reach a newborn's circulation.

To sum up, we concentrated on adipose tissue metabolism and we utilized several UPLC-MS/MS methods to describe the main processes in adipose tissue - lipolysis, FA re-esterification and β-oxidation. Moreover, we analysed different compounds that influence adipose tissue metabolism, specifically, acylcarnitines, amino acids as well as lipid mediators and FAHFA compounds. We performed mainly experiments on mice and cell line to achieve our goals. All the experiments included omega-3 PUFA supplementation because it has a beneficial metabolic effect on adipose tissue and we tried to clarify its effect on this over a long term period.

5. CITATION

1 Rose, D., Gracheck, P. and Vona-Davis, L. (2015) The Interactions of Obesity, Inflammation and Insulin Resistance in Breast Cancer. Cancers **7**, 2147–2168.

2 Bourgeais, V., Agafitei, L. and Hrkal, J. (2016) Almost 1 adult in 6 in the EU is considered obese, Eurostat.

3 Bernlohr, D. A., Jenkins, A. E. and Bennaars, A. A. (2002) Adipose tissue and lipid metabolism. Biochem. Lipids Lipoproteins Membr. 4th Edn **36**, 263–289.

4 Luo, L. and Liu, M. (2016) Adipose tissue in control of metabolism. J. Endocrinol. **231**, R77–R99.

5 Nuttall, F. Q. (2015) Body Mass Index: Obesity, BMI, and Health. Nutr. Today **50**, 117–128.

6 Serra, D., Mera, P., Malandrino, M. I., Mir, J. F. and Herrero, L. (2013) Mitochondrial Fatty Acid Oxidation in Obesity. Antioxid. Redox Signal. **19**, 269–284.

7 Kuda, O., Rossmeisl, M. and Kopecky, J. (2018) Omega-3 fatty acids and adipose tissue biology. Mol. Aspects Med.

8 Kuda, O., Rombaldova, M., Janovska, P., Flachs, P. and Kopecky, J. (2016) Cell type-specific modulation of lipid mediator's formation in murine adipose tissue by omega-3 fatty acids. Biochem. Biophys. Res. Commun. **469**, 731–736.

9 Haka, A. S., Barbosa-Lorenzi, V. C., Lee, H. J., Falcone, D. J., Hudis, C. A., Dannenberg, A. J. and Maxfield, F. R. (2016) Exocytosis of macrophage lysosomes leads to digestion of apoptotic adipocytes and foam cell formation. J. Lipid Res. **57**, 980–992.

10 Fitzgibbons, T. P. and Czech, M. P. (2016) Emerging evidence for beneficial macrophage functions in atherosclerosis and obesity-induced insulin resistance. J. Mol. Med. **94**, 267–275.

11 Yang, K. and Han, X. (2016) Lipidomics: Techniques, Applications, and Outcomes Related to Biomedical Sciences. Trends Biochem. Sci. **41**, 954–969.

12 Hertzel, A. V., Thompson, B. R., Wiczer, B. M. and Bernlohr, D. A. (2008) Lipid metabolism in adipose tissue. In Biochemistry of Lipids, Lipoproteins and Membranes (Fifth Edition), pp 277–304, Elsevier.

13 Oh, W., Abu-Elheiga, L., Kordari, P., Gu, Z., Shaikenov, T., Chirala, S. S. and Wakil, S. J. (2005) Glucose and fat metabolism in adipose tissue of acetyl-CoA carboxylase 2 knockout mice. Proc. Natl. Acad. Sci. U. S. A. **102**, 1384–1389.

14 Heeren, J. and Scheja, L. (2018) Brown adipose tissue and lipid metabolism: Curr. Opin. Lipidol. 1.

15 Chusyd, D. E., Wang, D., Huffman, D. M. and Nagy, T. R. (2016) Relationships between Rodent White Adipose Fat Pads and Human White Adipose Fat Depots. Front. Nutr. **3**.

16 Seale, P., Conroe, H. M., Estall, J., Kajimura, S., Frontini, A., Ishibashi, J., Cohen, P., Cinti, S. and Spiegelman, B. M. (2011) Prdm16 determines the thermogenic program of subcutaneous white adipose tissue in mice. J. Clin. Invest. **121**, 96–105.

17 Foster, M. T., Shi, H., Seeley, R. J. and Woods, S. C. (2011) Removal of intra-abdominal visceral adipose tissue improves glucose tolerance in rats: Role of hepatic triglyceride storage. Physiol. Behav. **104**, 845–854.

18 Choe, S. S., Huh, J. Y., Hwang, I. J., Kim, J. I. and Kim, J. B. (2016) Adipose Tissue Remodeling: Its Role in Energy Metabolism and Metabolic Disorders. Front. Endocrinol. **7**.

19 Bora, P. and Majumdar, A. S. (2017) Adipose tissue-derived stromal vascular fraction in regenerative medicine: a brief review on biology and translation. Stem Cell Res. Ther. **8**.
20 Lee, M.-J., Wu, Y. and Fried, S. K. (2013) Adipose tissue heterogeneity: Implication of depot differences in adipose tissue for obesity complications. Mol. Aspects Med. **34**, 1–11.
21 Jeanson, Y., Carrière, A. and Casteilla, L. (2015) A New Role for Browning as a Redox and Stress Adaptive Mechanism? Front. Endocrinol. **6**.
22 Cannon, B. and Nedergaard, J. (2004) Brown Adipose Tissue: Function and Physiological Significance. Physiol. Rev. **84**, 277–359.
23 Zechner, R. (2015) FAT FLUX: enzymes, regulators, and pathophysiology of intracellular lipolysis. EMBO Mol. Med. **7**, 359–362.
24 Lass, A., Zimmermann, R., Oberer, M. and Zechner, R. (2011) Lipolysis – A highly regulated multi-enzyme complex mediates the catabolism of cellular fat stores. Prog. Lipid Res. **50**, 14–27.
25 Boström, P., Wu, J., Jedrychowski, M. P., Korde, A., Ye, L., Lo, J. C., Rasbach, K. A., Boström, E. A., Choi, J. H., Long, J. Z., et al. (2012) A PGC1-α-dependent myokine that drives brown-fat-like development of white fat and thermogenesis. Nature **481**, 463–468.
26 Harms, M. and Seale, P. (2013) Brown and beige fat: development, function and therapeutic potential. Nat. Med. **19**, 1252–1263.
27 Cohen, P., Levy, J. D., Zhang, Y., Frontini, A., Kolodin, D. P., Svensson, K. J., Lo, J. C., Zeng, X., Ye, L., Khandekar, M. J., et al. (2014) Ablation of PRDM16 and Beige Adipose Causes Metabolic Dysfunction and a Subcutaneous to Visceral Fat Switch. Cell **156**, 304–316.
28 Bargut, T. C. L., Silva-e-Silva, A. C. A. G., Souza-Mello, V., Mandarim-de-Lacerda, C. A. and Aguila, M. B. (2016) Mice fed fish oil diet and upregulation of brown adipose tissue thermogenic markers. Eur. J. Nutr. **55**, 159–169.
29 Algire, C., Medrikova, D. and Herzig, S. (2013) White and brown adipose stem cells: From signaling to clinical implications. Biochim. Biophys. Acta BBA - Mol. Cell Biol. Lipids **1831**, 896–904.
30 Pahlavani, M., Razafimanjato, F., Ramalingam, L., Kalupahana, N. S., Moussa, H., Scoggin, S. and Moustaid-Moussa, N. (2017) Eicosapentaenoic acid regulates brown adipose tissue metabolism in high-fat-fed mice and in clonal brown adipocytes. J. Nutr. Biochem. **39**, 101–109.
31 Ameer, F., Scandiuzzi, L., Hasnain, S., Kalbacher, H. and Zaidi, N. (2014) De novo lipogenesis in health and disease. Metabolism **63**, 895–902.
32 Lodhi, I. J., Wei, X. and Semenkovich, C. F. (2011) Lipoexpediency: de novo lipogenesis as a metabolic signal transmitter. Trends Endocrinol. Metab. **22**, 1–8.
33 Jensen-Urstad, A. P. L. and Semenkovich, C. F. (2012) Fatty acid synthase and liver triglyceride metabolism: Housekeeper or messenger? Biochim. Biophys. Acta BBA - Mol. Cell Biol. Lipids **1821**, 747–753.
34 Ahmadian, M., E Duncan, R., Jaworski, K., Sarkadi-Nagy, E. and Sul, H. S. (2007) Triacylglycerol metabolism in adipose tissue. Future Lipidol. **2**, 229–237.
35 Harris, C. A., Haas, J. T., Streeper, R. S., Stone, S. J., Kumari, M., Yang, K., Han, X., Brownell, N., Gross, R. W., Zechner, R., et al. (2011) DGAT enzymes are required for triacylglycerol synthesis and lipid droplets in adipocytes. J. Lipid Res. **52**, 657–667.
36 Langin, D. (2006) Control of fatty acid and glycerol release in adipose tissue lipolysis. C. R. Biol. **329**, 598–607.
37 Strable, M. S. and Ntambi, J. M. (2010) Genetic control of *de novo* lipogenesis: role in diet-induced obesity. Crit. Rev. Biochem. Mol. Biol. **45**, 199–214.

38 Naukkarinen, J., Heinonen, S., Hakkarainen, A., Lundbom, J., Vuolteenaho, K., Saarinen, L., Hautaniemi, S., Rodriguez, A., Frühbeck, G., Pajunen, P., et al. (2014) Characterising metabolically healthy obesity in weight-discordant monozygotic twins. Diabetologia **57**, 167–176.
39 Chung, K.-J., Nati, M., Chavakis, T. and Chatzigeorgiou, A. (2018) Innate immune cells in the adipose tissue. Rev. Endocr. Metab. Disord.
40 Rodriguez-Prados, J.-C., Traves, P. G., Cuenca, J., Rico, D., Aragones, J., Martin-Sanz, P., Cascante, M. and Bosca, L. (2010) Substrate Fate in Activated Macrophages: A Comparison between Innate, Classic, and Alternative Activation. J. Immunol. **185**, 605–614.
41 Chawla, A., Nguyen, K. D. and Goh, Y. P. S. (2011) Macrophage-mediated inflammation in metabolic disease. Nat. Rev. Immunol. **11**, 738–749.
42 Kosteli, A., Sugaru, E., Haemmerle, G., Martin, J. F., Lei, J., Zechner, R. and Ferrante, A. W. J. (2010) Weight loss and lipolysis promote a dynamic immune response in murine adipose tissue.
43 Xu, X., Grijalva, A., Skowronski, A., van Eijk, M., Serlie, M. J. and Ferrante, A. W. (2013) Obesity Activates a Program of Lysosomal-Dependent Lipid Metabolism in Adipose Tissue Macrophages Independently of Classic Activation. Cell Metab. **18**, 816–830.
44 Hotamisligil, G. S., Shargill, N. S. and Spiegelman, B. M. (1993) Adipose Expression of Tumor Necrosis Factor-x:Direct Role in Obesity-Linked Insulin Resistance, Science.
45 Weisberg, S. P., McCann, D., Desai, M., Rosenbaum, M., Leibel, R. L. and Ferrante, A. W. (2003) Obesity is associated with macrophage accumulation in adipose tissue. J. Clin. Invest. **112**, 1796–1808.
46 Xu, H., Barnes, G. T., Yang, Q., Tan, G., Yang, D., Chou, C. J., Sole, J., Nichols, A., Ross, J. S., Tartaglia, L. A., et al. (2003) Chronic inflammation in fat plays a crucial role in the development of obesity-related insulin resistance. J. Clin. Invest. **112**, 1821–1830.
47 Giordano, A., Murano, I., Mondini, E., Perugini, J., Smorlesi, A., Severi, I., Barazzoni, R., Scherer, P. E. and Cinti, S. (2013) Obese adipocytes show ultrastructural features of stressed cells and die of pyroptosis. J. Lipid Res. **54**, 2423–2436.
48 Kloting, N., Fasshauer, M., Dietrich, A., Kovacs, P., Schon, M. R., Kern, M., Stumvoll, M. and Bluher, M. (2010) Insulin-sensitive obesity. AJP Endocrinol. Metab. **299**, E506–E515.
49 Rombaldova, M., Janovska, P., Kopecky, J. and Kuda, O. (2017) Omega-3 fatty acids promote fatty acid utilization and production of pro-resolving lipid mediators in alternatively activated adipose tissue macrophages. Biochem. Biophys. Res. Commun. **490**, 1080–1085.
50 Masoodi, M., Kuda, O., Rossmeisl, M., Flachs, P. and Kopecky, J. (2015) Lipid signaling in adipose tissue: Connecting inflammation & metabolism. Biochim. Biophys. Acta BBA - Mol. Cell Biol. Lipids **1851**, 503–518.
51 Kratz, M., Coats, B. R., Hisert, K. B., Hagman, D., Mutskov, V., Peris, E., Schoenfelt, K. Q., Kuzma, J. N., Larson, I., Billing, P. S., et al. (2014) Metabolic Dysfunction Drives a Mechanistically Distinct Proinflammatory Phenotype in Adipose Tissue Macrophages. Cell Metab. **20**, 614–625.
52 Oh, D. Y., Talukdar, S., Bae, E. J., Imamura, T., Morinaga, H., Fan, W., Li, P., Lu, W. J., Watkins, S. M. and Olefsky, J. M. (2010) GPR120 Is an Omega-3 Fatty Acid Receptor Mediating Potent Anti-inflammatory and Insulin-Sensitizing Effects. Cell **142**, 687–698.

53 Van den Bossche, J., Baardman, J. and de Winther, M. P. J. (2015) Metabolic Characterization of Polarized M1 and M2 Bone Marrow-derived Macrophages Using Real-time Extracellular Flux Analysis. J. Vis. Exp.
54 Wahli, W. and Michalik, L. (2012) PPARs at the crossroads of lipid signaling and inflammation. Trends Endocrinol. Metab. **23**, 351–363.
55 Lumeng, C. N., DelProposto, J. B., Westcott, D. J. and Saltiel, A. R. (2008) Phenotypic Switching of Adipose Tissue Macrophages With Obesity Is Generated by Spatiotemporal Differences in Macrophage Subtypes. Diabetes **57**, 3239–3246.
56 Sun, Y. V. and Hu, Y.-J. (2016) Integrative Analysis of Multi-omics Data for Discovery and Functional Studies of Complex Human Diseases. In Advances in Genetics, pp 147–190, Elsevier.
57 Buchholz, A., Hurlebaus, J., Wandrey, C. and Takors, R. (2002) Metabolomics: quantification of intracellular metabolite dynamics. Biomol. Eng. **19**, 5–15.
58 Ding, J., Sorensen, C. M., Zhang, Q., Jiang, H., Jaitly, N., Livesay, E. A., Shen, Y., Smith, R. D. and Metz, T. O. (2007) Capillary LC Coupled with High-Mass Measurement Accuracy Mass Spectrometry for Metabolic Profiling. Anal. Chem. **79**, 6081–6093.
59 Buescher, J. M., Moco, S., Sauer, U. and Zamboni, N. (2010) Ultrahigh Performance Liquid Chromatography−Tandem Mass Spectrometry Method for Fast and Robust Quantification of Anionic and Aromatic Metabolites. Anal. Chem. **82**, 4403–4412.
60 Wei, R., Li, G. and Seymour, A. B. (2010) High-Throughput and Multiplexed LC/MS/MRM Method for Targeted Metabolomics. Anal. Chem. **82**, 5527–5533.
61 Cai, Z., Song, F. and Yang, M. S. (2002) Capillary liquid chromatographic–high-resolution mass spectrometric analysis of ribonucleotides, Journal of chromatography A.
62 Pietiläinen, K. H., Naukkarinen, J., Rissanen, A., Saharinen, J., Ellonen, P., Keränen, H., Suomalainen, A., Götz, A., Suortti, T., Yki-Järvinen, H., et al. (2008) Global transcript profiles of fat in monozygotic twins discordant for BMI: pathways behind acquired obesity. PLoS Med **5**, e51.
63 Giesbertz, P., Ecker, J., Haag, A., Spanier, B. and Daniel, H. (2015) An LC-MS/MS method to quantify acylcarnitine species including isomeric and odd-numbered forms in plasma and tissues. J. Lipid Res. **56**, 2029–2039.
64 Rinaldo, P., Cowan, T. M. and Matern, D. (2008) Acylcarnitine profile analysis. Genet. Med. **10**, 151–156.
65 Newgard, C. B., An, J., Bain, J. R., Muehlbauer, M. J., Stevens, R. D., Lien, L. F., Haqq, A. M., Shah, S. H., Arlotto, M., Slentz, C. A., et al. (2009) A Branched-Chain Amino Acid-Related Metabolic Signature that Differentiates Obese and Lean Humans and Contributes to Insulin Resistance. Cell Metab. **9**, 311–326.
66 Mihalik, S. J., Goodpaster, B. H., Kelley, D. E., Chace, D. H., Vockley, J., Toledo, F. G. S. and DeLany, J. P. (2010) Increased Levels of Plasma Acylcarnitines in Obesity and Type 2 Diabetes and Identification of a Marker of Glucolipotoxicity. Obesity **18**, 1695–1700.
67 Adams, S. H., Hoppel, C. L., Lok, K. H., Zhao, L., Wong, S. W., Minkler, P. E., Hwang, D. H., Newman, J. W. and Garvey, W. T. (2009) Plasma Acylcarnitine Profiles Suggest Incomplete Long-Chain Fatty Acid -Oxidation and Altered Tricarboxylic Acid Cycle Activity in Type 2 Diabetic African-American Women. J. Nutr. **139**, 1073–1081.
68 Horakova, O., Hansikova, J., Bardova, K., Gardlo, A., Rombaldova, M., Kuda, O., Rossmeisl, M. and Kopecky, J. (2016) Plasma Acylcarnitines and Amino Acid Levels As an Early Complex Biomarker of Propensity to High-Fat Diet-Induced Obesity in Mice. PLOS ONE **11**, e0155776.

69 Xia, T., Fu, S., Wang, Q., Wen, Y., Chan, S., Zhu, S., Gao, S., Tao, X., Zhang, F. and Chen, W. (2018) Targeted metabolomic analysis of 33 amino acids and biogenic amines in human urine by ion-pairing HPLC-MS/MS: Biomarkers for tacrolimus nephrotoxicity after renal transplantation. Biomed. Chromatogr. **32**, e4198.
70 Wu, G. (2009) Amino acids: metabolism, functions, and nutrition. Amino Acids **37**, 1–17.
71 Soeters, M. R., Sauerwein, H. P., Duran, M., Wanders, R. J., Ackermans, M. T., Fliers, E., Houten, S. M. and Serlie, M. J. (2009) Muscle acylcarnitines during short-term fasting in lean healthy men. Clin. Sci. **116**, 585–592.
72 Sailer, M., Dahlhoff, C., Giesbertz, P., Eidens, M. K., de Wit, N., Rubio-Aliaga, I., Boekschoten, M. V., Müller, M. and Daniel, H. (2013) Increased Plasma Citrulline in Mice Marks Diet-Induced Obesity and May Predict the Development of the Metabolic Syndrome. PLoS ONE (Covasa, M., ed.) **8**, e63950.
73 Wang, C., Wang, M. and Han, X. (2015) Applications of mass spectrometry for cellular lipid analysis. Mol BioSyst **11**, 698–713.
74 Papan, C., Penkov, S., Herzog, R., Thiele, C., Kurzchalia, T. and Shevchenko, A. (2014) Systematic Screening for Novel Lipids by Shotgun Lipidomics. Anal. Chem. **86**, 2703–2710.
75 Fahy, E. (2005) A comprehensive classification system for lipids. J. Lipid Res. **46**, 839–862.
76 Koletzko, B. (2016) Human Milk Lipids. Ann. Nutr. Metab. **69**, 28–40.
77 Sala-Vila, A., Castellote, A. I., Rodriguez-Palmero, M., Campoy, C. and López-Sabater, M. C. (2005) Lipid composition in human breast milk from Granada (Spain): Changes during lactation. Nutrition **21**, 467–473.
78 Sokol, E., Ulven, T., Faergeman, N. J. and Ejsing, C. S. (2015) Comprehensive and quantitative profiling of lipid species in human milk, cow milk and a phospholipid-enriched milk formula by GC and MS/MS ^{ALL}: Comparative lipid analysis of milk and milk products. Eur. J. Lipid Sci. Technol. **117**, 751–759.
79 Han, X., Yang, J., Yang, K., Zhao, Z., Abendschein, D. R. and Gross, R. W. (2007) Alterations in Myocardial Cardiolipin Content and Composition Occur at the Very Earliest Stages of Diabetes: A Shotgun Lipidomics Study †. Biochemistry (Mosc.) **46**, 6417–6428.
80 Orešič, M., Hänninen, V. A. and Vidal-Puig, A. (2008) Lipidomics: a new window to biomedical frontiers. Trends Biotechnol. **26**, 647–652.
81 Rolim, A. E. H., Henrique-Araújo, R., Ferraz, E. G., de Araújo Alves Dultra, F. K. and Fernandez, L. G. (2015) Lipidomics in the study of lipid metabolism: Current perspectives in the omic sciences. Gene **554**, 131–139.
82 Wenk, M. R. (2010) Lipidomics: New Tools and Applications. Cell **143**, 888–895.
83 Shevchenko, A. and Simons, K. (2010) Lipidomics: coming to grips with lipid diversity. Nat. Rev. Mol. Cell Biol. **11**, 593–598.
84 Klose, C., Surma, M. A. and Simons, K. (2013) Organellar lipidomics—background and perspectives. Curr. Opin. Cell Biol. **25**, 406–413.
85 Lee, C.-H., Olson, P. and Evans, R. M. (2003) Minireview: Lipid Metabolism, Metabolic Diseases, and Peroxisome Proliferator-Activated Receptors. Endocrinology **144**, 2201–2207.
86 Vaz, F. M., Pras-Raves, M., Bootsma, A. H. and van Kampen, A. H. C. (2015) Principles and practice of lipidomics. J. Inherit. Metab. Dis. **38**, 41–52.
87 Ciccimaro, E. and Blair, I. A. (2010) Stable-isotope dilution LC–MS for quantitative biomarker analysis. Bioanalysis **2**, 311–341.

88 The ACCORD Study Group. (2010) Effects of Combination Lipid Therapy in Type 2 Diabetes Mellitus. N. Engl. J. Med. **362**, 1563–1574.
89 Adibhatla, R. M. and Hatcher, J. F. (2010) Lipid oxidation and peroxidation in CNS health and disease: from molecular mechanisms to therapeutic opportunities. Antioxid. Redox Signal. **12**, 125–169.
90 Perera, R., Riley, C., Isaac, G., Hopf-Jannasch, A. S., Moore, R. J., Weitz, K. W., Pasa-Tolic, L., Metz, T. O., Adamec, J. and Kuhn, R. J. (2012) Dengue Virus Infection Perturbs Lipid Homeostasis in Infected Mosquito Cells. PLoS Pathog. (Heise, M. T., ed.) **8**, e1002584.
91 Blaho, V. A., Buczynski, M. W., Brown, C. R. and Dennis, E. A. (2009) Lipidomic Analysis of Dynamic Eicosanoid Responses during the Induction and Resolution of Lyme Arthritis. J. Biol. Chem. **284**, 21599–21612.
92 Calder, P. C. (2013) Omega-3 polyunsaturated fatty acids and inflammatory processes: nutrition or pharmacology?: Omega-3 fatty acids and inflammation. Br. J. Clin. Pharmacol. **75**, 645–662.
93 Massey, K. A. and Nicolaou, A. (2013) Lipidomics of oxidized polyunsaturated fatty acids. Free Radic. Biol. Med. **59**, 45–55.
94 Plewes, M. R., Burns, P. D., Hyslop, R. M. and George Barisas, B. (2017) Influence of omega-3 fatty acids on bovine luteal cell plasma membrane dynamics. Biochim. Biophys. Acta BBA - Biomembr. **1859**, 2413–2419.
95 Burdge, G. C. and Calder, P. C. (2006) Dietary α-linolenic acid and health-related outcomes: a metabolic perspective. Nutr. Res. Rev. **19**, 26.
96 Calder, P. C. (2008) The relationship between the fatty acid composition of immune cells and their function. Prostaglandins Leukot. Essent. Fatty Acids **79**, 101–108.
97 Calder, P. C. (2010) The 2008 ESPEN Sir David Cuthbertson lecture: Fatty acids and inflammation – From the membrane to the nucleus and from the laboratory bench to the clinic. Clin. Nutr. **29**, 5–12.
98 Calder, P. C. (2011) Fatty acids and inflammation: The cutting edge between food and pharma. Eur. J. Pharmacol. **668**, S50–S58.
99 Kuda, O., Brezinova, M., Rombaldova, M., Slavikova, B., Posta, M., Beier, P., Janovska, P., Veleba, J., Kopecky, J., Kudova, E., et al. (2016) Docosahexaenoic Acid–Derived Fatty Acid Esters of Hydroxy Fatty Acids (FAHFAs) With Anti-inflammatory Properties. Diabetes **65**, 2580–2590.
100 Veleba, J., Kopecky, J., Janovska, P., Kuda, O., Horakova, O., Malinska, H., Kazdova, L., Oliyarnyk, O., Skop, V., Trnovska, J., et al. (2015) Combined intervention with pioglitazone and n-3 fatty acids in metformin-treated type 2 diabetic patients: improvement of lipid metabolism. Nutr. Metab. **12**.
101 WHO | 5. Population nutrient intake goals for preventing diet-related chronic diseases. WHO.
102 Awada, M., Meynier, A., Soulage, C. O., Hadji, L., Géloën, A., Viau, M., Ribourg, L., Benoit, B., Debard, C. and Guichardant, M. (2013) n-3 PUFA added to high-fat diets affect differently adiposity and inflammation when carried by phospholipids or triacylglycerols in mice. Nutr. Metab. **10**, 23.
103 Titos, E., Rius, B., González-Périz, A., López-Vicario, C., Morán-Salvador, E., Martínez-Clemente, M., Arroyo, V. and Clària, J. (2011) Resolvin D1 and Its Precursor Docosahexaenoic Acid Promote Resolution of Adipose Tissue Inflammation by Eliciting Macrophage Polarization toward an M2-Like Phenotype. J. Immunol. **187**, 5408–5418.
104 Flachs, P., Rühl, R., Hensler, M., Janovska, P., Zouhar, P., Kus, V., Macek Jilkova, Z., Papp, E., Kuda, O., Svobodova, M., et al. (2011) Synergistic induction of lipid

catabolism and anti-inflammatory lipids in white fat of dietary obese mice in response to calorie restriction and n-3 fatty acids. Diabetologia **54**, 2626–2638.
105 Neuhofer, A., Zeyda, M., Mascher, D., Itariu, B. K., Murano, I., Leitner, L., Hochbrugger, E. E., Fraisl, P., Cinti, S., Serhan, C. N., et al. (2013) Impaired Local Production of Proresolving Lipid Mediators in Obesity and 17-HDHA as a Potential Treatment for Obesity-Associated Inflammation. Diabetes **62**, 1945–1956.
106 Lewis, R., Austen, K. F. and Soberman, R. (1990) Leukotrienes and other products of the 5-lipoxygenase pathway. N. Engl. J. Med. **323**, 645–655.
107 Tilley, S. L., Coffman, T. M. and Koller, B. H. (2001) Mixed messages: modulation of inflammation and immune responses by prostaglandins and thromboxanes. J. Clin. Invest. **108**, 15–23.
108 Kroetz, D. L. and Zeldin, D. C. (2002) Cytochrome P450 pathways of arachidonic acid metabolism. Curr. Opin. Lipidol. **13**, 273–283.
109 Di Marzo, V. (2008) The endocannabinoid system in obesity and type 2 diabetes. Diabetologia **51**, 1356–1367.
110 Silvestri, C. and Di Marzo, V. (2013) The Endocannabinoid System in Energy Homeostasis and the Etiopathology of Metabolic Disorders. Cell Metab. **17**, 475–490.
111 Yore, M. M., Syed, I., Moraes-Vieira, P. M., Zhang, T., Herman, M. A., Homan, E. A., Patel, R. T., Lee, J., Chen, S., Peroni, O. D., et al. (2014) Discovery of a Class of Endogenous Mammalian Lipids with Anti-Diabetic and Anti-inflammatory Effects. Cell **159**, 318–332.
112 Zerkowski, J. A. (2008) Estolides: From structure and function to structured and functionalized. Lipid Technol. **20**, 253–256.
113 Smith, U. and Kahn, B. B. (2016) Adipose tissue regulates insulin sensitivity: role of adipogenesis, *de novo* lipogenesis and novel lipids. J. Intern. Med. **280**, 465–475.
114 Dunn, W. B., Broadhurst, D., Begley, P., Zelena, E., Francis-McIntyre, S., Anderson, N., Brown, M., Knowles, J. D., Halsall, A., Haselden, J. N., et al. (2011) Procedures for large-scale metabolic profiling of serum and plasma using gas chromatography and liquid chromatography coupled to mass spectrometry. Nat. Protoc. **6**, 1060–1083.
115 Spickett, C. M., Reis, A. and Pitt, A. R. (2011) Identification of oxidized phospholipids by electrospray ionization mass spectrometry and LC–MS using a QQLIT instrument. Free Radic. Biol. Med. **51**, 2133–2149.
116 Humbert, L., Hoizey, G. and Lhermitte, M. (2014) Drugs Involved in Drug-Facilitated Crimes (DFC). In Toxicological Aspects of Drug-Facilitated Crimes, pp 159–180, Elsevier.
117 Folch, J., Lees, M. and Stanley, S. (1957) A simple method for the isolation and purification of total lipides from animal tissues. J Biol Chem **226**, 497–509.
118 Bligh, E. G. and Dyer, W. J. A RAPID METHOD OF TOTAL LIPID EXTRACTION AND PURIFICATION 7.
119 Solid Phase Extraction/SPE Guide : Waters.
120 Peterson, B. L. and Cummings, B. S. (2006) A review of chromatographic methods for the assessment of phospholipids in biological samples. Biomed. Chromatogr. **20**, 227–243.
121 Wang, M., Wang, C. and Han, X. (2017) Selection of internal standards for accurate quantification of complex lipid species in biological extracts by electrospray ionization mass spectrometry-What, how and why?: INTERNAL STANDARDS FOR QUANTIFICATION OF LIPIDS IN LIPIDOMICS. Mass Spectrom. Rev. **36**, 693–714.
122 Coulier, L., Bas, R., Jespersen, S., Verheij, E., van der Werf, M. J. and Hankemeier, T. (2006) Simultaneous Quantitative Analysis of Metabolites Using Ion-Pair Liquid

Chromatography−Electrospray Ionization Mass Spectrometry. Anal. Chem. **78**, 6573–6582.
123 Wu, Y., Engen, J. R. and Hobbins, W. B. (2006) Ultra performance liquid chromatography (UPLC) further improves hydrogen/deuterium exchange mass spectrometry. J. Am. Soc. Mass Spectrom. **17**, 163–167.
124 Luo, B., Groenke, K., Takors, R., Wandrey, C. and Oldiges, M. (2007) Simultaneous determination of multiple intracellular metabolites in glycolysis, pentose phosphate pathway and tricarboxylic acid cycle by liquid chromatography–mass spectrometry. J. Chromatogr. A **1147**, 153–164.
125 Pabst, M., Grass, J., Fischl, R., Léonard, R., Jin, C., Hinterkörner, G., Borth, N. and Altmann, F. (2010) Nucleotide and Nucleotide Sugar Analysis by Liquid Chromatography-Electrospray Ionization-Mass Spectrometry on Surface-Conditioned Porous Graphitic Carbon. Anal. Chem. **82**, 9782–9788.
126 Bi, H., Krausz, K. W., Manna, S. K., Li, F., Johnson, C. H. and Gonzalez, F. J. (2013) Optimization of harvesting, extraction, and analytical protocols for UPLC-ESI-MS-based metabolomic analysis of adherent mammalian cancer cells. Anal. Bioanal. Chem. **405**, 5279–5289.
127 Díez, C., Guillarme, D., Staub Spörri, A., Cognard, E., Ortelli, D., Edder, P. and Rudaz, S. (2015) Aminoglycoside analysis in food of animal origin with a zwitterionic stationary phase and liquid chromatography–tandem mass spectrometry. Anal. Chim. Acta **882**, 127–139.
128 Jandera, P. and Janás, P. (2017) Recent advances in stationary phases and understanding of retention in hydrophilic interaction chromatography. A review. Anal. Chim. Acta **967**, 12–32.
129 Gika, H. G., Theodoridis, G. A. and Wilson, I. D. (2008) Hydrophilic interaction and reversed-phase ultra-performance liquid chromatography TOF-MS for metabonomic analysis of Zucker rat urine. J. Sep. Sci. **31**, 1598–1608.
130 Yang, S., Sadilek, M., Synovec, R. E. and Lidstrom, M. E. (2009) Liquid chromatography - tandem quadrupole mass spectrometry and comprehensive two-dimensional gas chromatography - time-of-flight mass spectrometry measurement of targeted metabolites of Methylobacterium extorquens AM1 grown on two different carbon sources. J. Chromatogr. A **1216**, 3280–3289.
131 Goutier, W., Spaans, P. A., van der Neut, M. A. W., McCreary, A. C. and Reinders, J. H. (2010) Development and application of an LC–MS/MS method for measuring the effect of (partial) agonists on cAMP accumulation in vitro. J. Neurosci. Methods **188**, 24–31.
132 HILIC | SIELC.
133 Clarke, W. (2017) Mass spectrometry in the clinical laboratory: determining the need and avoiding pitfalls. In Mass Spectrometry for the Clinical Laboratory, pp 1–15, Elsevier.
134 Marshall, A. G. and Hendrickson, C. L. (2008) High-Resolution Mass Spectrometers. Annu. Rev. Anal. Chem. **1**, 579–599.
135 Macherone, A. and Hopkins, J. (2013) Resolving Power and Mass Resolution Technical Overview.
136 Wang, J., Lin, T., Lai, J., Cai, Z. and Yang, M. S. (2009) Analysis of adenosine phosphates in HepG-2 cell by a HPLC–ESI-MS system with porous graphitic carbon as stationary phase. J. Chromatogr. B **877**, 2019–2024.
137 Han, X. and Gross, R. W. (2005) Shotgun lipidomics: Electrospray ionization mass spectrometric analysis and quantitation of cellular lipidomes directly from crude extracts of biological samples. Mass Spectrom. Rev. **24**, 367–412.

138 Pulfer, M. and Murphy, R. C. (2003) Electrospray mass spectrometry of phospholipids. Mass Spectrom. Rev. **22**, 332–364.
139 Griffiths, W. J. (2003) Tandem mass spectrometry in the study of fatty acids, bile acids, and steroids. Mass Spectrom. Rev. **22**, 81–152.
140 Murphy, R. C., Fiedler, J. and Hevko, J. (2001) Analysis of Nonvolatile Lipids by Mass Spectrometry. Chem. Rev. **101**, 479–526.
141 Kilár, A., Dörnyei, Á. and Kocsis, B. (2013) Structural characterization of bacterial lipopolysaccharides with mass spectrometry and on- and off-line separation techniques. Mass Spectrom. Rev. **32**, 90–117.
142 Tam, V. C., Quehenberger, O., Oshansky, C. M., Suen, R., Armando, A. M., Treuting, P. M., Thomas, P. G., Dennis, E. A. and Aderem, A. (2013) Lipidomic Profiling of Influenza Infection Identifies Mediators that Induce and Resolve Inflammation. Cell **154**, 213–227.
143 Divito, E. B., Davic, A. P., Johnson, M. E. and Cascio, M. (2012) Electrospray Ionization and Collision Induced Dissociation Mass Spectrometry of Primary Fatty Acid Amides. Anal. Chem. **84**, 2388–2394.
144 Brügger, B. (2014) Lipidomics: Analysis of the Lipid Composition of Cells and Subcellular Organelles by Electrospray Ionization Mass Spectrometry. Annu. Rev. Biochem. **83**, 79–98.
145 Cajka, T. and Fiehn, O. (2014) Comprehensive analysis of lipids in biological systems by liquid chromatography-mass spectrometry. TrAC Trends Anal. Chem. **61**, 192–206.
146 Han, X. and Gross, R. W. (2005) Shotgun lipidomics: multidimensional MS analysis of cellular lipidomes. Expert Rev. Proteomics **2**, 253–264.
147 Wang, M., Hayakawa, J., Yang, K. and Han, X. (2014) Characterization and Quantification of Diacylglycerol Species in Biological Extracts after One-Step Derivatization: A Shotgun Lipidomics Approach. Anal. Chem. **86**, 2146–2155.
148 Wang, M., Han, R. H. and Han, X. (2013) Fatty Acidomics: Global Analysis of Lipid Species Containing a Carboxyl Group with a Charge-Remote Fragmentation-Assisted Approach. Anal. Chem. **85**, 9312–9320.
149 Ståhlman, M., Ejsing, C. S., Tarasov, K., Perman, J., Borén, J. and Ekroos, K. (2009) High-throughput shotgun lipidomics by quadrupole time-of-flight mass spectrometry. J. Chromatogr. B **877**, 2664–2672.
150 Boja, E., Rivers, R., Kinsinger, C., Mesri, M., Hiltke, T., Rahbar, A. and Rodriguez, H. (2010) Restructuring proteomics through verification. Biomark. Med. **4**, 799–803.
151 QTRAP 5500 LC-MS/MS System.
152 Preinerstorfer, B., Schiesel, S., Lämmerhofer, M. and Lindner, W. (2010) Metabolic profiling of intracellular metabolites in fermentation broths from β-lactam antibiotics production by liquid chromatography–tandem mass spectrometry methods. J. Chromatogr. A **1217**, 312–328.
153 Graves, P. R. and Haystead, T. A. J. (2002) Molecular Biologist's Guide to Proteomics. Microbiol. Mol. Biol. Rev. **66**, 39–63.
154 Eilertsen, H., Huseby, S., Degerlund, M., Eriksen, G., Ingebrigtsen, R. and Hansen, E. (2014) The Effect of Freeze/Thaw Cycles on Reproducibility of Metabolic Profiling of Marine Microalgal Extracts Using Direct Infusion High-Resolution Mass Spectrometry (HR-MS). Molecules **19**, 16373–16380.
155 Miller, J. H., Poston, P. A. and Karnes, H. T. (2012) A quantitative method for acylcarnitines and amino acids using high resolution chromatography and tandem mass spectrometry in newborn screening dried blood spot analysis. J. Chromatogr. B **903**, 142–149.

156 Oe, T., Ackermann, B. L., Inoue, K., Berna, M. J., Garner, C. O., Gelfanova, V., Dean, R. A., Siemers, E. R., Holtzman, D. M., Farlow, M. R., et al. (2006) Quantitative analysis of amyloidβ peptides in cerebrospinal fluid of Alzheimer's disease patients by immunoaffinity purification and stable isotope dilution liquid chromatography/negative electrospray ionization tandem mass spectrometry. Rapid Commun. Mass Spectrom. **20**, 3723–3735.
157 Bajad, S. U., Lu, W., Kimball, E. H., Yuan, J., Peterson, C. and Rabinowitz, J. D. (2006) Separation and quantitation of water soluble cellular metabolites by hydrophilic interaction chromatography-tandem mass spectrometry. J. Chromatogr. A **1125**, 76–88.
158 Yuan, M., Breitkopf, S. B., Yang, X. and Asara, J. M. (2012) A positive/negative ion–switching, targeted mass spectrometry–based metabolomics platform for bodily fluids, cells, and fresh and fixed tissue. Nat. Protoc. **7**, 872–881.
159 Dumlao, D. S., Buczynski, M. W., Norris, P. C., Harkewicz, R. and Dennis, E. A. (2011) High-throughput lipidomic analysis of fatty acid derived eicosanoids and N-acylethanolamines. Biochim. Biophys. Acta BBA - Mol. Cell Biol. Lipids **1811**, 724–736.
160 Peng, M., Liu, L., Jiang, M., Liang, C., Zhao, X., Cai, Y., Sheng, H., Ou, Z. and Luo, H. (2013) Measurement of free carnitine and acylcarnitines in plasma by HILIC-ESI-MS/MS without derivatization. J. Chromatogr. B **932**, 12–18.
161 Paul, J. H. and Myers, B. (1982) Fluorometric determination of DNA in aquatic microorganisms by use of Hoechst 33258. Deep Sea Res. Part B Oceanogr. Lit. Rev. **29**, 795.
162 Zhang, Q.-Q., Hu, X.-W., Liu, Y.-L., Ye, Z.-J., Gui, Y.-H., Zhou, D.-L., Qi, C.-L., He, X.-D., Wang, H. and Wang, L.-J. (2015) CD11b deficiency suppresses intestinal tumor growth by reducing myeloid cell recruitment. Sci. Rep. **5**.
163 Neises, B. and Steglich, W. (1978) Simple Method for the Esterification of Carboxylic Acids. Angew. Chem. Int. Ed. Engl. **17**, 522–524.
164 Fan, G. and Yan, D. (2015) Positional isomers of cyanostilbene: two-component molecular assembly and multiple-stimuli responsive luminescence. Sci. Rep. **4**.
165 Aalberg, L., Clark, C. R. and DeRuiter, J. (2004) Chromatographic and mass spectral studies on isobaric and isomeric substances related to 3, 4-methylenedioxymethamphetamine. J. Chromatogr. Sci. **42**, 464–469.
166 Pubchem. Malonylcarnitine.
167 Hydroxybutyrylcarnitine | C11H21NO5 - PubChem.
168 Pomar, C. A., Kuda, O., Kopecky, J., Rombaldova, M., Castro, H., Picó, C., Sánchez, J. and Palou, A. (2019) Alterations in plasma acylcarnitine and amino acid profiles may indicate poor nutrition during the suckling period due to maternal intake of an unbalanced diet and may predict later metabolic dysfunction. FASEB J. **33**, 796–807.
169 Ibrahim, M. M. (2010) Subcutaneous and visceral adipose tissue: structural and functional differences. Obes. Rev. **11**, 11–18.
170 Cildir, G., Akıncılar, S. C. and Tergaonkar, V. (2013) Chronic adipose tissue inflammation: all immune cells on the stage. Trends Mol. Med. **19**, 487–500.
171 Rath, M., MÃ¼ller, I., Kropf, P., Closs, E. I. and Munder, M. (2014) Metabolism via Arginase or Nitric Oxide Synthase: Two Competing Arginine Pathways in Macrophages. Front. Immunol. **5**.
172 Arner, P. and Langin, D. (2014) Lipolysis in lipid turnover, cancer cachexia, and obesity-induced insulin resistance. Trends Endocrinol. Metab. **25**, 255–262.
173 Tchoukalova, Y. D., Sarr, M. G. and Jensen, M. D. (2004) Measuring committed preadipocytes in human adipose tissue from severely obese patients by using adipocyte

fatty acid binding protein. Am. J. Physiol.-Regul. Integr. Comp. Physiol. **287**, R1132–R1140.
174 Rossmeisl, M., Macek Jilkova, Z., Kuda, O., Jelenik, T., Medrikova, D., Stankova, B., Kristinsson, B., Haraldsson, G. G., Svensen, H., Stoknes, I., et al. (2012) Metabolic Effects of n-3 PUFA as Phospholipids Are Superior to Triglycerides in Mice Fed a High-Fat Diet: Possible Role of Endocannabinoids. PLoS ONE (Schunck, W.-H., ed.) **7**, e38834.
175 Březinová, B. M. CÍLENÁ ANALÝZA VĚTVENÝCH ESTERŮ MASTNÝCH KYSELIN POMOCÍ LC/MS 56.
176 Suh, J. H., Kim, R. Y. and Lee, D. S. (2012) A new metabolomic assay to examine inflammation and redox pathways following LPS challenge. J. Inflamm. **9**, 37.
177 Becker, K., Schroecksnadel, S., Gostner, J., Zaknun, C., Schennach, H., Überall, F. and Fuchs, D. (2014) Comparison of in vitro tests for antioxidant and immunomodulatory capacities of compounds. Phytomedicine **21**, 164–171.
178 Mohammad, M. A., Sunehag, A. L. and Haymond, M. W. (2014) De novo synthesis of milk triglycerides in humans. Am. J. Physiol.-Endocrinol. Metab. **306**, E838–E847.
179 Brezinova, M., Kuda, O., Hansikova, J., Rombaldova, M., Balas, L., Bardova, K., Durand, T., Rossmeisl, M., Cerna, M., Stranak, Z., et al. (2018) Levels of palmitic acid ester of hydroxystearic acid (PAHSA) are reduced in the breast milk of obese mothers. Biochim. Biophys. Acta BBA - Mol. Cell Biol. Lipids **1863**, 126–131.
180 Lee, J., Moraes-Vieira, P. M., Castoldi, A., Aryal, P., Yee, E. U., Vickers, C., Parnas, O., Donaldson, C. J., Saghatelian, A. and Kahn, B. B. (2016) Branched Fatty Acid Esters of Hydroxy Fatty Acids (FAHFAs) Protect against Colitis by Regulating Gut Innate and Adaptive Immune Responses. J. Biol. Chem. **291**, 22207–22217.

6. LIST OF PUBLICATIONS AND MY CONTRIBUTION TO THEM

I.

Olga Horakova, Jana Hansikova, Kristina Bardova, Alzbeta Gardlo, Martina Rombaldova, Ondrej Kuda, Martin Rossmeisl, Jan Kopecky. *Plasma Acylcarnitines and Amino Acid Levels As an Early Complex Biomarker of Propensity to High-Fat Diet-Induced Obesity in Mice.* PLOS ONE Volume 11, Issue 5, 2016.

IF (2016): 2,806
Times Cited:5
Participation: 20%

I participated in mice dissection and collecting of plasma samples. I optimized several UPLC-MS/MS methods. Finally, I extracted the samples and analysed them by UPLC-MS/MS methodology.

II.

Catalina A. Pomar, Ondrej Kuda, Jan Kopecky, Martina Rombaldova, Heriberto Castro, Catalina Picó, Juana Sánchez, Andreu Palou. *Alterations in plasma acylcarnitine and amino acid profiles may indicate poor nutrition during the suckling period due to maternal intake of an unbalanced diet and may predict later metabolic dysfunction.* FASEB Journal Vol. 33, No. 1, 2019

IF (2017): 5,595
Times Cited:0
Participation: 10%

I collaborated in extraction of metabolomic samples. I carried out the liquid chromatography coupled to mass spectrometry analyses.

III.

Martina Rombaldova, Petra Janovska, Jan Kopecky, Ondrej Kuda. *Omega-3 fatty acids promote fatty acid utilization and production of pro-resolving lipid mediators in alternatively activated adipose tissue macrophages.* Biochemical and Biophysical Research Communications Volume 490, Issue 3, 26 August 2017, Pages 1080-1085.

IF (2017): 2,559
Times Cited:6
Participation: 90%

I assisted with design the attempts. I sacrificed mice and prepared the macrophages from cell lines and mice tibias. I performed all the co-culture experiments. Then I processed the samples, i.e. I performed the LLE and SPE extraction as well as extraction of metabolomic samples. Also, I made ready the internal standards or combined them. Later, I accomplished the UPLC-MS/MS analyses. I participated in interpretation of data and statistical analyses and I partook of writing the paper.

IV.

Ondrej Kuda, Martina Rombaldova, Petra Janovska, Pavel Flachs, Jan Kopecky. *Cell type specific modulation of lipid mediator's formation in murine adipose tissue by omega-3 fatty acids.* Biochemical and Biophysical Research Communications 469 (2016) 731e736

IF (2016): 2,466
Times Cited:13
Participation: 70%

I was involved in planning of the experiments. I contributed to mice dissection and processed their tissue as well as I cultivated macrophages. Then I carried out the co-culture experiments. I extracted the metabolomic samples by solvents and lipidomic samples by liquid liquid and solid phase extraction methods. I combined the internal standards added to samples. I analysed the samples by liquid chromatography coupled to mass spectrometry.

V.

Ondrej Kuda, Marie Brezinova, Martina Rombaldova, Barbora Slavikova, Martin Posta, Petr Beier, Petra Janovska, Jiri Veleba, Jan Kopecky Jr., Eva Kudova, Terezie Pelikanova, Jan Kopecky. *Docosahexaenoic Acid–Derived Fatty Acid Esters of Hydroxy Fatty Acids (FAHFAs) With Anti-inflammatory Properties*. Diabetes 2016;65:2580–2590.

IF (2016):8,684
Times Cited:27
Participation: 30%

I partook in sacrification of mice and gaining the animal samples. I participated in extraction of samples by LLE and SPE methods. Also, I contributed to analyses of samples by UPLC-MS/MS and MS identification of DHAHLA. I cultivated macrophages and adipocytes and I performed all the cell lines experiments. I did polymerase chain reaction analyses.

VI.

Marie Brezinova, Ondrej Kuda, Jana Hansikova, Martina Rombaldova, Laurence Balas, Kristina Bardova, Thierry Durand, Martin Rossmeisl, Marcela Cerna, Zbynek Stranak, Jan Kopecky. *Levels of palmitic acid ester of hydroxystearic acid (PAHSA) are reduced in the breast milk of obese mothers.* BBA - Molecular and Cell Biology of Lipids 1863 (2018) 126-131.

IF (2018): 4,966
Times Cited:6
Participation: 20%

I prepared the protocol for collecting human milk samples. I contributed to extraction of milk samples by liquid liquid and solid phase extraction platforms. Later, I orally gavaged mice by 5-PAHSA and carried out the mice experiment. I participated in UPLC-MS/MS analyses of human milk samples and mice plasma samples.

As a representative of the co-authors I declare that Martina Rombaldová, M.Sc. participated in the publications listed above.

……

RNDr. Ondřej Kuda, Ph.D.